

---

Masters Theses

Student Theses and Dissertations

---

Summer 2024

## Metal-Ion Doped Borate Bioactive Glasses- a Novel Direction in Minimizing Nosocomial Infections and Antibiotic Resistance

Sarah Fakher

*Missouri University of Science and Technology*

Follow this and additional works at: [https://scholarsmine.mst.edu/masters\\_theses](https://scholarsmine.mst.edu/masters_theses)



Part of the [Microbiology Commons](#)

Department:

---

### Recommended Citation

Fakher, Sarah, "Metal-Ion Doped Borate Bioactive Glasses- a Novel Direction in Minimizing Nosocomial Infections and Antibiotic Resistance" (2024). *Masters Theses*. 8210.

[https://scholarsmine.mst.edu/masters\\_theses/8210](https://scholarsmine.mst.edu/masters_theses/8210)

This thesis is brought to you by Scholars' Mine, a service of the Missouri S&T Library and Learning Resources. This work is protected by U. S. Copyright Law. Unauthorized use including reproduction for redistribution requires the permission of the copyright holder. For more information, please contact [scholarsmine@mst.edu](mailto:scholarsmine@mst.edu).

METAL-ION DOPED BORATE BIOACTIVE GLASSES- A NOVEL DIRECTION  
IN MINIMIZING NOSOCOMIAL INFECTIONS AND ANTIBIOTIC RESISTANCE

by

SARAH FAKHER

A THESIS

Presented to the Graduate Faculty of the

MISSOURI UNIVERSITY OF SCIENCE AND TECHNOLOGY

In Partial Fulfillment of the Requirements for the Degree

MASTER OF SCIENCE IN APPLIED AND ENVIRONMENTAL BIOLOGY

2024

Approved by:

David Westenberg, Advisor

Julie Semon

Anthony Convertine

© 2024

Sarah Fagher

All Rights Reserved

## **PUBLICATION THESIS OPTION**

This thesis consists of the following four articles, which will be submitted for publication and have been formatted in the style used by Missouri University of Science and Technology:

Paper I, “Metal-ion Doped Borate Bioactive Glasses: Antimicrobial Mechanisms and Biomedical Applications”, found on pages 7-73, has been submitted to the Journal of Acta Biomaterialia.

Paper II, “Evaluation of the Antibacterial Properties of Four Bioactive Wound Repair Compositions”, found on pages 74-103, and is intended for submission to the Journal of American Society for Microbiology.

Paper III, “The Antibiofilm Efficacy of Metal-ion Doped Borate Bioactive Glasses: A Comprehensive Predictive Modeling Approach for Infection Control in Healthcare Settings”, found on pages 104-142, and is intended for submission to the Journal of American Society for Microbiology.

Paper IV, “In Vitro Assessment of the Anti-biofilm Effectiveness of Copper and Zinc Enhanced Borate Bioactive Glasses Using Processed Microscopic Images”, found on pages 143-175, and is intended for submission.

## ABSTRACT

Nosocomial infections represent a formidable challenge and induce a substantial burden on patients and healthcare systems. These infections result from the interaction of numerous pathogenic microorganisms, particularly bacteria, and lead to increased morbidity, mortality, and healthcare costs. Extensive research has been carried out to devise innovative solutions, mainly focusing on antimicrobial natural and synthetic substances. However, the proclivity of bacterial strains to form biofilms complicates treatment and elevates antibiotic resistance, prompting research into pioneering more effective and versatile antibacterial strategies. Borate bioactive glasses (BBGs) are the latest, remarkable classes of biomaterials with a wide array of medical applications, owing to their superior bioactive properties, antibacterial capabilities, and biodegradability. This research aims to provide an *in vitro* comprehensive modeling to investigate the antibacterial properties of copper and zinc-doped BBGs and endeavors to establish their prospective mechanisms in inhibiting/preventing biofilm formation and reducing bacterial species commonly implicated in HAI incidences: *Staphylococcus epidermidis*, *Escherichia coli*, and *Pseudomonas aeruginosa*. Results demonstrate a significant reduction in bacterial growth within 2 days and 3 days for direct and indirect application of copper and zinc-doped BBGs respectively, and findings were consistent among all the bacterial species. The amalgamation of Molecular Microbiology and Materials Science within this research paves the way for future endeavors to optimize the application of enhanced BBGs in medical settings to combat the pervasive, ceaseless threats of nosocomial infections.

## ACKNOWLEDGMENTS

I start by thanking God, from whom all blessings flow, for providing me with strength and assurance through every phase of this journey.

I turn with immense appreciation toward my family, whose unwavering love, encouragement, and support have been my constant source of strength and inspiration. With a heart brimming and gratitude, I would like to especially thank my beloved Mom and acknowledge her influence and endless love in directing me toward my dreams and ambitions; without her, the achievements I celebrate today and the successes I aim for tomorrow would remain beyond my grasp.

I extend my profound gratitude to my advisor, Dr. Westenberg, whose guidance has been pivotal in my academic journey. He has indelibly influenced both my academic pursuits and personal growth, and I'm forever thankful to him. I extend my heartfelt thanks to my committee members, Dr. Semon and Dr. Convertine. Their insightful feedback and expertise have been invaluable to the fruition of my research.

I'd like to thank the Mo-Sci Corporation for providing the research biomaterials. I'd also like to thank Dr. Bai and Dr. Shannon for training me on the microscopy equipment as well as Dr. Yang and Lei for their help with the ICP-MS. I'm thankful for the support of the Biological Sciences Department for providing me with an assistantship that made it possible to pursue my master's degree.

Lastly, I would like to thank myself for the dedication, hard work, and persistence that brought me to this milestone. It's in acknowledging the significance of hardships, more than the smooth passages, that I have found profound growth and learning.

## TABLE OF CONTENTS

	Page
PUBLICATION THESIS OPTION.....	iii
ABSTRACT.....	iv
ACKNOWLEDGMENTS.....	v
LIST OF ILLUSTRATIONS.....	x
LIST OF TABLES.....	xii
NOMENCLATURE.....	xiii
 SECTION	
1. INTRODUCTION.....	1
 PAPER	
I. METAL-ION DOPED BORATED BASED BIOACTIVE GLASSES: ANTIMICROBIAL MECHANISMS AND BIOMEDICAL APPLICATIONS.....	7
ABSTRACT.....	7
1. INTRODUCTION.....	8
2. BORATE BIOACTIVE GLASSES.....	11
2.1. OVERVIEW.....	11
2.2. MANUFACTURING AND CHARACTERISTICS.....	12
2.3. CLINICAL TRIALS.....	15
3. NOSOCOMIAL INFECTIONS.....	17
3.1. BIOFILM FORMATION.....	19
3.2. MEDICAL INSTRUMENTS.....	20

4. ANTIBACTERIAL MECHANISMS OF BORATE GLASSES .....	23
4.1. CHANGES IN THE LOCAL PHYSIOLOGICAL ENVIRONMENT .....	23
4.2. ENHANCED BORATE BIOACTIVE GLASSES .....	23
4.2.1 Zinc.....	25
4.2.2. Copper .....	26
4.2.3. Silver .....	27
4.2.4. Cerium.....	29
4.2.5. Tellurium.....	30
4.2.6. Gallium.....	31
4.2.7. Strontium.....	33
4.2.8. Iodine.....	34
4.2.9. Titanium .....	34
4.3. BIOACTIVE GLASS IN CONJUNCTION WITH ANTIBIOTICS .....	35
5. BIOMEDICAL APPLICATIONS .....	36
5.1. WOUND HEALING .....	36
5.2. BONE GRAFTS .....	42
5.3. SCAFFOLDS.....	43
5.4. OSTEOMYELITIS.....	45
5.5. NERVE REGENERATION .....	46
5.6. DRUG DELIVERY .....	47
6. CONCLUSION .....	50
REFERENCES .....	51
II. THE ANTIBACTERIAL PROPERTIES OF FOUR BIOACTIVE CHRONIC WOUND REPAIR COMPOSITIONS .....	74



ABSTRACT .....	74
1. INTRODUCTION.....	75
2. RESULTS.....	80
2.1. ANTIBACTERIAL EFFECTIVENES.....	80
2.2. TIME-COURSE STUDY .....	80
2.3. BIOFILM EFFECTIVENESS .....	81
2.4. ELEMENT RELEASE .....	84
3. DISCUSSION .....	88
4. MATERIALS AND METHODS .....	97
REFERENCES .....	100
III. THE ANTIBIOFILM EFFICACY OF METAL-ION DOPED BORATE BIOACTIVE GLASS: A COMPREHENSIVE PREDICTIVE MODELING APPROACH FOR INFECTION CONTROL IN HEALTHCARE SETTINGS.....	104
ABSTRACT .....	104
1. INTRODUCTION.....	105
2. RESULTS.....	110
2.1. STATIC BIOFILM GROWTH .....	110
2.2. BBG DIRETCT/INDIRECT APPLICATION ON STATIC BIOFILMS.....	111
2.3. SCANNING ELECTRON MICROSCOPY (SEM).....	114
2.4. BIOFILM DYNAMIC GROWTH .....	116
2.5. BBG DIRECT/INDIRECT APPLICATION ON DYNAMIC BIOFILMS .....	117
2.6. SCANNING ELECTRON MICROSCOPY (SEM).....	121

3. DISCUSSION .....	122
4. MATERIALS AND METHODS .....	134
REFERENCES .....	138
IV. IN VITRO ASSESMENT OF THE ANTI-BIOFILM EFFECTIVENESS OF COPPER AND ZINC ENHANCED BORATE BIOACTIVE GLASS USING PROCESSED MICROSCOPIC IMAGES .....	143
ABSTRACT .....	143
1. INTRODUCTION.....	144
2. RESULTS.....	147
2.1. ANTIBIOFILM EFFECTIVENESS .....	147
2.2. SEM.....	149
2.3. CLSM .....	151
2.4. BIOFILM STRUCTURAL PARAMETERETERS.....	156
3. DISCUSSION .....	160
4. MATERIALS AND METHODS .....	170
REFERENCES .....	172
SECTION	
2. MULTI-SPECIES BIOFILMS.....	176
2.1. STATIC BIOFILMS.....	177
2.2. DYNAMIC BIOFILMS.....	177
3. CONCLUSIONS .....	179
BIBLIOGRAHY .....	181
VITA .....	184

## LIST OF ILLUSTRATIONS

	Page
PAPER I	
Figure 1. Bioactive glass degradation.....	15
Figure 2. Bioactive Glasses timeline .....	17
Figure 3. Biofilm formation diagram.....	21
Figure 4. Antibacterial and biological properties of metal-ion dopant.....	26
Figure 5. Biomedical applications of borate bioactive glasses .....	37
PAPER II	
Figure 1. Antibacterial effectiveness of the biomaterials after 24 hours of contact with the bacterial species. ....	82
Figure 2. Time course study of the antibacterial effectiveness of the biomaterials.....	83
Figure 3. Antibiofilm effectiveness of the biomaterials after 24 and 48 hours of contact. ....	85
Figure 4. Element release profile from the biomaterials over four days .....	86
Figure 5. Correlation Between Element-Induced Biofilm Log Reduction and Element Release .....	87
Figure 6. Schematic of the four stages of normal and chronically infected wound healing proces .....	90
Figure 7. Prevalence of Common Healthcare-Acquired Infections.....	91
PAPER III	
Figure 1. Static biofilm development of <i>S. epidermidis</i> , <i>E. coli</i> , and <i>P. aeruginosa</i> . ....	112
Figure 2. Borate bioactive glass direct and indirect application on severely pre-formed static biofilms.....	113
Figure 3. SEM.....	118

Figure 4. Dynamic biofilm development of <i>S. epidermidis</i> , <i>E. coli</i> , and <i>P. aeruginosa</i> .....	119
Figure 5. Borate bioactive glass direct and indirect application on severely pre-formed static biofilms.....	123
Figure 6. SEM.....	124
Figure 7. Summary of the clinical scenarios represented by the direct/indirect BBG application of static/dynamic biofilm modes.....	131
PAPER IV	
Figure 1. SEM.....	150
Figure 2. Mean % of remaining biofilms from segmented images after 48 hours of bioactive glass treatment.....	151
Figure 3. CLSM .....	153
Figure 4. CLSM .....	154
Figure 5. CLSM .....	155
Figure 6. Biofilm structural parameter.....	157
Figure 7. Biofilm structural parameter.....	158
Figure 8. Biofilm structural parameters .....	159
Figure 9. Antiseptic's Biofilm eradication% values of Mirragen and GL1605 on <i>S. epidermidis</i> , <i>E. coli</i> , and <i>P. aeruginosa</i> biofilms.....	160

**LIST OF TABLES**

	Page
PAPER I	
Table 1. Summary of reviewed literature on the antibacterial mechanisms and effectiveness of metal-ion doped borate-based bioactive glasses.....	39
Table 2. A summary of reviewed literature on metal-ion doped borate-based bioactive glasses for biomedical applications. ....	49
PAPER II	
Table 1. Commercially available wound healing biomaterials assessed in this study.....	98
PAPER IV	
Table 1. Log reduction of biofilms after 24 hours and 48 hours of exposure to the bioactive glasses .....	148

**NOMENCLATURE**

Symbol	Description
BGs	Bioactive glasses
BBGS	Borate bioactive glasses
HAP	Hydroxycarbonate apatite
ROS	Reactive oxygen species
EPS	Extracellular polymeric substance
VEGF	Vascular endothelial growth factor
SBF	Stimulated body fluid
HAIs	Healthcare acquire infections
OD	Optical density
SEM	Scanning electron microscopy
ATCC	American type culture collection
CSTR	Continous flow stirred tank reactor
CLSM	Confocal laser scanning microscopy
PIA	Polysaccharide intercellular adhesin
ABE	Antiseptic's biofilm eradication

## 1. INTRODUCTION

Nosocomial infections pose a significant global health concern, imposing a severe burden on healthcare systems. These infections, often caused by highly adaptable pathogenic microorganisms, are responsible for substantial morbidity and mortality rates, leading to increased healthcare costs [1, 2]. Nosocomial infections affect hundreds of millions of patients worldwide each year, with the CDC estimating that on any given day, about one in 31 hospital patients has at least one infection [3, 4]. The ability of bacteria to form biofilms, complex communities that are inherently resistant to antibiotics, exacerbates the challenge of treatment and elevates antibiotic resistance [5].

Borate bioactive glasses (BBGs) are a class of bioactive materials that were first introduced in the late 1990s and early 2000s as alternatives to silicate-based bioactive glasses, which were pioneered by Larry Hench in the late 1960s [6]. BBGs were developed to enhance the bioactivity and degradation rate thereby offering improved performance for certain biomedical applications [7, 8]. BBGs have been explored for a wide range of medical applications due to their unique combination of bioactivity, biodegradability, and antibacterial properties. Some of their prominent applications include [7-11]:

1. Bone Regeneration: BBGs have been used in orthopedics and dentistry for bone tissue engineering due to their ability to bond to bone and stimulate osteogenesis.
2. Wound Healing: They have been studied for wound healing applications because of their ability to release therapeutic ions that can enhance healing.
3. Drug Delivery Systems: BBGs have been used as vehicles for controlled drug delivery, especially for localized treatment at the site of implantation or injury.

4. Tissue Scaffolds: Their solubility and bioactivity make them suitable for scaffolding, helping to support and guide the growth of new tissue.
5. Antimicrobial Applications: Due to their ability to release therapeutic ions, BBGs have been investigated for their potential to prevent or treat infections, particularly in scenarios where bacterial biofilms are a concern.
6. Bioactive Coatings: BBGs can be used to coat metal implants to improve their integration with bone and to reduce the risk of post-surgical infections.
7. Cancer Treatment: Research is investigating the incorporation of therapeutic ions or drugs into BBGs for localized cancer therapy, exploiting their bioactive properties to target tumor sites.
8. Enzyme Immobilization: The porous structure of BBGs can be advantageous for immobilizing enzymes in biosensors or bioreactors, which have applications in diagnostics and industry.
9. Nerve Regeneration: There is interest in using BBGs in nerve repair and regeneration due to their ability to support the growth of nerve cells and tissues.
10. Soft Tissue Engineering: BBGs are also being tailored for soft tissue applications by modifying their degradation rates and mechanical properties to match those of soft tissues.
11. Ocular Applications: Due to their biocompatibility and transparency when processed appropriately, BBGs have potential uses in ocular implants or in the delivery of ocular drugs.
12. Vascularization: BBGs doped with specific ions can promote blood vessel formation, which is critical for the success of any tissue-engineered implant.



13. Anti-inflammatory Applications: Certain compositions of BBGs can exert an anti-inflammatory effect, making them suitable for treating chronic inflammatory diseases.

14. Scaffold for Cartilage Repair: The ionic dissolution products from BBGs can stimulate chondrocytes, making them suitable for cartilage tissue engineering scaffolds.

15. Gene Delivery: Modifying BBGs to serve as vectors for gene delivery is a novel area that could facilitate the treatment of genetic diseases or tissue regeneration through gene therapy.

16. Detoxification: BBGs with specific compositions can adsorb and neutralize toxins in the body or in the environment, which could be used in applications for detoxification.

17. Radiopacity: BBGs can be designed to be radiopaque, which is beneficial for real-time monitoring of the behavior and degradation of implants within the body using non-invasive imaging techniques.

18. Stem Cell Carriers: BBGs can serve as carriers for stem cells, providing a supportive matrix that can be used to repair or regenerate diseased tissues and organs.

19. Dental Regeneration: BBGs are being studied for their potential in dentin regeneration, root repair, and as components in dental fillings due to their ability to support the mineralization of tooth structures.

The wide range of applications for BBGs demonstrate to their versatility and potential to revolutionize various aspects of healthcare. As research continues to advance, new and more varied uses for BBGs will be likely discovered.

Metal-ion doped BBGs emerge as potent biomaterials for their potential application in mitigating nosocomial infections. Since BBGs are highly biodegradable, they allow for a faster, controlled dissolution and localized therapeutic effects [7]. Copper-doped BBGs

exhibit potent antimicrobial activity, which has been attributed to the oligodynamic effect of copper ions [12, 13]. Copper can disrupt bacterial cell membranes and induce oxidative stress within microbial cells, leading to cell death. Besides, zinc plays a pivotal role in numerous biological processes, including enzyme function, protein synthesis, and cell signaling [14]. Zinc-doped BBGs release zinc ions in a controlled manner, which can promote osteogenesis by stimulating bone-forming cells and enhancing bone tissue regeneration. Zinc ions have also been shown to exhibit antibacterial properties, although typically less potent than copper [15]. The release of zinc ions at concentrations of around 0.5 to 2.0 weight percent from BBGs has been demonstrated to inhibit bacterial colonization and biofilm formation [7, 16]. When combined, copper and zinc ions can provide a broad spectrum of antibacterial effects while also supporting cellular functions essential for tissue regeneration.

This study aims to unravel the potential of copper and zinc doped BBGs to inhibit severe biofilms in various of clinically relevant scenarios through a comprehensive predictive modeling approach, considering various factors such as bacterial growth kinetics, biofilm formation propensity, and material dissolution rates, to assess the antibacterial effectiveness of these innovative materials. Severe biofilms, often associated with chronic infections and high treatment failure rates, were selected for rigorous testing in this research. The BBGs were applied either directly onto the biofilm structures or indirectly, utilizing their dissolution products to understand the full scope of their antibacterial potential. To assess the efficacy of BBGs against the biofilms, several analytical techniques were employed. Scanning Electron Microscopy (SEM) provided detailed morphological insights into biofilm disruption, while Confocal Laser Scanning

Microscopy (CLSM) offered a three-dimensional visualization of biofilm architecture and viability. Moreover, machine learning algorithms were utilized for quantitative analysis, enhancing the objectivity and reproducibility of biofilm assessment.

*S. epidermidis*, *E. coli*, and *P. aeruginosa* are three bacterial species that are notably implicated in nosocomial infections, presenting significant challenges in clinical settings due to their prevalence, virulence, and resistance profiles [17]. *S. epidermidis* is a gram-positive bacterium that has emerged as a major nosocomial pathogen, particularly associated with infections related to indwelling medical devices such as catheters and prostheses. The ability of *S. epidermidis* to persist on surfaces and within biofilms makes it a formidable cause of nosocomial infections [18]. *E. coli* is a gram-negative bacterium commonly found in the human gut. While many strains are harmless, many are pathogenic, causing illnesses ranging from urinary tract infections (UTIs) to neonatal meningitis and gastroenteritis [19]. Moreover, *P. aeruginosa* is a gram-negative, opportunistic pathogen characterized by its intrinsic resistance to many antibiotics and disinfectants. It is particularly notorious in hospital settings for causing chronic respiratory infections in cystic fibrosis patients, burn wound infections, and keratitis [20]. *P. aeruginosa* biofilms are highly resistant to both immune responses and antimicrobials due to their complex architecture and reduced metabolic rate. This bacterium's ability to thrive in moist environments, such as respiratory equipment and indwelling catheters, coupled with its formidable defense mechanisms, makes it a leading cause of nosocomial infections.

This study represents a multidisciplinary approach among microbiology, chemistry, and materials science to introduce a novel treatment modality to minimize nosocomial

infections and the clinical emergence of antibiotic-resistant genes. Nosocomial infections and antibiotic resistance are intertwined issues that drive up the cost of healthcare significantly. Therefore, this research could have profound implications for healthcare costs by reducing the frequency of these infections, the need for prolonged antibiotic treatments, and the incidence of antibiotic-resistant infections. The application of copper and zinc doped BBGs could represent a paradigm shift in infection control within clinical, biomedical, and medical settings. Successful implementation of the proposed biomaterial can significantly reduce unnecessary morbidity and mortality, the economic burden associated with nosocomial infections and antibiotic resistance, and create more resilient healthcare systems.

## PAPER

### I. METAL-ION DOPED BORATED BASED BIOACTIVE GLASSES: ANTIMICROBIAL MECHANISMS AND BIOMEDICAL APPLICATIONS

Sarah Fakher and David Westenberg

#### ABSTRACT

Bioactive glasses (BGs) are physiologically reactive surface biomaterials widely used in biomedical applications and various treatments. Borate bioactive glasses (BBGs) are third-generation BGs, and they exhibit superior biodegradable, bioactive, osteoconductive, antibacterial, and biocompatible properties compared to other types of BGs. Certain concentrations of dopant ions have been incorporated into the chemical structure of BBGs to enhance their biological functionalities and antimicrobial properties. It was demonstrated that those ions play a crucial role in the biological responsiveness *in vitro* and *in vivo* once in contact with a physiological environment. The dissolution products of ion-doped BBGs were noted in their ability to stimulate gene expression related to cell differentiation and proliferation, promote angiogenesis, display anti-inflammatory effects, and inhibit bacterial growth within a few hours. Thus, metal-ion-doped BBGs address several limitations encountered by biomedical, tissue engineering, and infection control applications. Considering the research studies on BBGs to date, this review aims to analyze metal-ion-doped BBGs based on their primary antibacterial mechanisms and biomedical properties.

## 1. INTRODUCTION

BGs have been widely used during the last 50 years to regenerate, replace, and repair living tissues. The first silicate-based BG, trade named 45S5 Bioglass® (wt. %: 45SiO<sub>2</sub>, 24.5Na<sub>2</sub>O, 24.5CaO, 6P<sub>2</sub>O<sub>5</sub>), was produced by Larry Hench in 1969, and it was subsequently approved by the US Food and Drug Administration (FDA) [1] [2]. Because the 45S5 glass structure encompassed various elements and maintained several basic characteristics, it was used for bone replacement, orthopedic, and dental applications. Since then, novel BG compositions have been developed for biomedical applications, and efforts have been concentrated on developing BGs with enhanced properties, such as those that can enhance cellular proliferation and influence gene expression.

BGs are considered “bioactive” based on their ability to form an apatite layer after contact with body fluids and upon their degradation and dissolution of biologically active ions. The degradation of BGs occurs through several stages [1] [2]. As the BG gets in contact with body fluids, an ion exchange occurs, and the pH increases as a result. The phosphate ions present in the medium react with the calcium ions that disintegrated from the glass. This reaction forms an amorphous calcium phosphate layer (ACP) on the BG’s surface. The ACP continues to form and grow as ions continue to disintegrate. After the calcium-phosphate layer grows on the surface of the BG, it crystallizes to form a hydroxycarbonate apatite (HAP), which is the main mechanism beyond bone-BG bonding. The ion disintegration is associated with enhanced osteogenic functions, and the HAP is critical in bond formations between the soft tissue and/or the bond between the implant and the bone. The bioactivity of the glass is assessed by how fast it is integrated and the rate by which the HAP layer forms. Depending on the type, composition,

porosity, and manufacturing method, each form of BGs has a distinctive degradation kinetic, which can take from hours to months.

The most common BGs used in biomedical applications are 45S5 S53P4 (silicate-based BGs) and 13-93B3 (borate-based BGs). In the past 20 years, research has introduced BBGs, which were proven to be advantageous over all other types of BGs. *In vitro* and *in vivo* studies elucidated the potency of borate-based BGs in biomedical and regenerative applications such as chronic wound healing. According to research studies, the conversion of calcium phosphate in silicate-based BGs is partially complete. Due to the high heat treatment required for silicate-based BGs, silicate glasses become non-crystallized and difficult to produce in various forms. The degradation and conversion of BBGs into HAP is similar to that of silicate-based BGs [3] [4]; however, BBGs do not involve the formation of a silica-rich layer, demonstrating the faster surface reaction of BBGs and their complete conversion into a HAP (Figure. 1). Moreover, the rapid degradation rate of the glass supports cell proliferation *in vivo*. The therapeutic potential of silicate BGs is limited by incomplete degradation *in vitro*; unlike silicate glasses, borate glasses fully degrade and convert into a HAP layer [5]-[7]. Some studies have observed the conversion of BBGs in SBF after 7 days through scanning electron microscopy (SEM) and x-ray diffraction (XDR) analysis [8]. According to other studies, BBGs displayed complete degradation in as less as 4 days, converting ultimately into a HAP layer [9]. This phenomenon has been imputed to the combination of the trigonal and tetrahedral reduced network connectivity in BBGs [10] [11]. It was further observed that borate also fully degraded in the body fluids, leaving no remaining degradation products [12].

BBGs come in different forms such as granules for regenerative purposes, fibers for wound healing, composites for fillings, and powder for biomedical device coatings. Another potential application is BBGs loaded with antibiotics for treating local infections. For the aforementioned reasons, BBGs have gained considerable attention recently in wound healing applications and tissue engineering. Most forms of borate glasses were approved by the US FDA and are currently commercially available [13] [14]. Metallic ions are essential components of BGs. Besides metallic ions, biologically active ions have been incorporated into BGs to enhance their antibacterial and biological activity. Those ions include silver (Ag), copper (Cu), gallium (Ga), titanium (Ti), strontium (Sr), Iodine (I), zinc (Zn), cerium (Ce), and tellurium (Te) [15]-[18]. According to the literature, those elements have been particularly documented to play a role in promoting the antibacterial and biological activity of BBGs [19]-[21].

Infections are one of the most serious risks that accompany surgical procedures and most biomedical applications. For instance, about 2.5% of hip and knee replacement surgeries and 10% of joint replacement surgeries get complicated due to bacterial infections [22]. BGs have been modified to overcome the risk of infection and failure of implants. Incorporating metal ions into BGs has been demonstrated to help prevent bacterial colonization and minimize infections [23]. The ion disintegration of BGs increases the pH and causes an acid-base imbalance, leading to osmotic pressure in the surrounding medium, creating a hostile environment for the bacteria, and inhibiting bacterial growth. However, a very high increase in pH that exceeds the level of critical concentration can also have a cytotoxic effect on the surrounding cells, altering the gene expression of cells [24]. Moreover, biocidal ions can prevent bacterial attachment and



disrupt the bacterial replication processes by damaging their DNA and RNA in different ways such as decreasing the bacterial iron uptake, generating reactive oxygen species (ROS), and altering the bacterial metabolic and functional pathways. Despite all studies performed to elucidate the antibacterial effect of BGs, the main mechanism beyond the antibacterial properties of BGs has not yet been fully investigated.

## **2. BORATE BIOACTIVE GLASSES**

### **2.1. OVERVIEW**

Boron affects some metabolic pathways and is an essential element for humans, making boron-containing BGs beneficial in biomedical applications. BBGs have gained considerable attention for their potential application in soft tissues and bone grafts due to their low chemical durability and high solubility compared to other types of BGs [8][25]. The faster dissolution rate of BBGS is ascribed to the boron content of the glass. Moreover, boric acid renders BBGs antiseptic. The antibacterial activity and the faster degradation rate of BBGs make them promising in wound healing and other biomedical applications [26]. Given their ability to fully and rapidly transform into bone-like apatite crystals, BBGs provide a potent alternative to other types of BGs. The high bioactivity and biodegradability of BBGs open multifarious possibilities for their application in the biomedical and tissue engineering fields. Numerous studies have highlighted the ability of BBGs to promote wound healing as well as cell differentiation and proliferation [27]-[29]. Furthermore, potential uses of BBGs include the treatment of chronic osteomyelitis by acting as important carriers of antibiotics and other therapeutic substances [32].

According to studies, borate glasses are effectively used as scaffolds, in terms of their promising composition and morphology [33]. BBGs degrade and convert into scaffolds through the disintegration of  $B_2O_3$ ,  $Na_2O$ , and  $K_2O$ . The dissolution of these components results in the formation of  $(BO_3)^3$ ,  $Na^+$ , and  $K^+$ , and as the  $Ca^{+2}$  from the glass interacts with the  $PO_3^{-4}$  from the solution, HAP is formed [8] [34].

The chemical durability of the glass can be enhanced by adding some metal to it such as gallium to stabilize the glass's network [35]. The main component of BBGs is  $B_2O_3$ , and the composition of the glass consists of different alkali metals (lithium, sodium, and potassium), alkaline-earth metals (calcium, magnesium, and strontium), and transitional metals such as copper and zinc. When doped with certain metal ions, the BBGs exhibited higher angiogenesis and antibacterial properties. Borate glasses do not form a borate-rich layer upon contact with body fluids; instead, a HAP layer is formed directly [36]. This helps maintain the dissolution kinetics of the glass [12].

## **2.2. MANUFACTURING AND CHARACTERISTICS**

BBGs can be produced via two routes: the traditional melt-quenching method or the modern sol-gel method [37]. The melt-quenching method requires temperatures higher than  $1000^\circ C$ . BGs obtained through this route often lack porosity. In contrast, in the sol-gel method, metal hydroxides, alkoxides, or organic salts are achieved through the processes of hydrolyzation and polymerization. The first sol gel-derived BGs were introduced in the 1990s and required a temperature between  $600^\circ C$  and  $700^\circ C$  [38]. Sol-gel methods eliminate the need for elevated temperatures. Besides, the structural properties of the glass can be modulated, obtaining controlled glass structures with

different pore types- nano, macro, or meso pores [39]. Due to their potent resorption and degradation, glasses produced through the sol-gel method exhibit higher HAP formation compared to those produced through melt-quenching. Moreover, surfactants can be introduced into the sol-gel processes [40]. Given their supramolecular chemical characteristics, surfactants result in the formation of mesoporous bioactive glasses (MBGs) with increased porosity and bioactivity. The mesoporous structure of BGs has a greater potential for incorporating antimicrobial agents such as antibiotics, thereby acting as an effective therapy for bacterial infections [41]. Additionally, sol-gel methods are the main processes by which three-dimensional scaffolds are produced; scaffolds are needed for tissue engineering and biomedical applications [42].

The melt-and-quench method is most commonly used to synthesize BBGs. This method was first used by Hench in 1969 at a temperature between 1300°C and 1450°C. After melting, the glass is allowed to anneal to minimize the internal stress caused by a high thermal expansion of the glass. Due to the low melting point of B<sub>2</sub>O<sub>3</sub>, the melting temperature used to manufacture the BBGs is lower compared to that used in developing other types of BGs [43]. Moreover, B<sub>2</sub>O<sub>3</sub> influences the stability and formability of the glass, allowing the glass to be processed into different forms such as coating and fibers. The fiber form of BBGS is effective in most biomedical applications particularly in soft tissue engineering as it mimics the tissue's fibrous morphology as well as allows the diffusion of nutrients and wastes throughout the scaffolds [4] [44]. Besides, glass fibers structurally support the scaffold and proliferation/attachment of cells. BBG fibers have been documented to effectively treat chronic wounds and repair soft tissue [45]. Boron-containing BGs can also be used as a potential coating on implants, which cannot bond to

host tissues. Coating implant aids in ameliorating the stability and bonding between the host tissue and the implant and prevents corrosion of the metallic implants [33].

The surface area of the glass relies on the particle size of the glass. Several studies have pointed out the correlation between the particle size of the glass and its anti-biofilm activity, emphasizing that the smaller the particle size, the higher the antibacterial activity. The anti-biofilm activity of smaller particle sizes was observed against a wide variety of clinically relevant pathogens including *P. aeruginosa*, *S. aureus*, and *S. epidermidis* [46] [47]. A smaller particle size strongly influences the pH and the dissolution rate of the glass; smaller particles tend to degrade at a faster rate compared to larger ones and slightly increase the pH. The composition of BBGs can be tailored by a lower transition temperature ( $T_g$ ) compared to silicate-based BGs [48] [49]. This property is achieved by adding specific oxides and allows the borate glass to release ions at a more biologically controlled rate. One study [50] used FTIR to corroborate the corrosion activity and conversion of BBGs into HAP in an aqueous environment.

The degradation of silicate-based and borate bioactive glasses occurs through a series of steps. The lower chemical durability of borate-based bioactive glasses allows them to degrade faster than silicate glasses. The degradation and conversion into a HAP of borate glasses start at the surface, whereas silicate glasses involve the formation of a silicate gel layer on the surface, which takes a longer time to convert into a HAP.

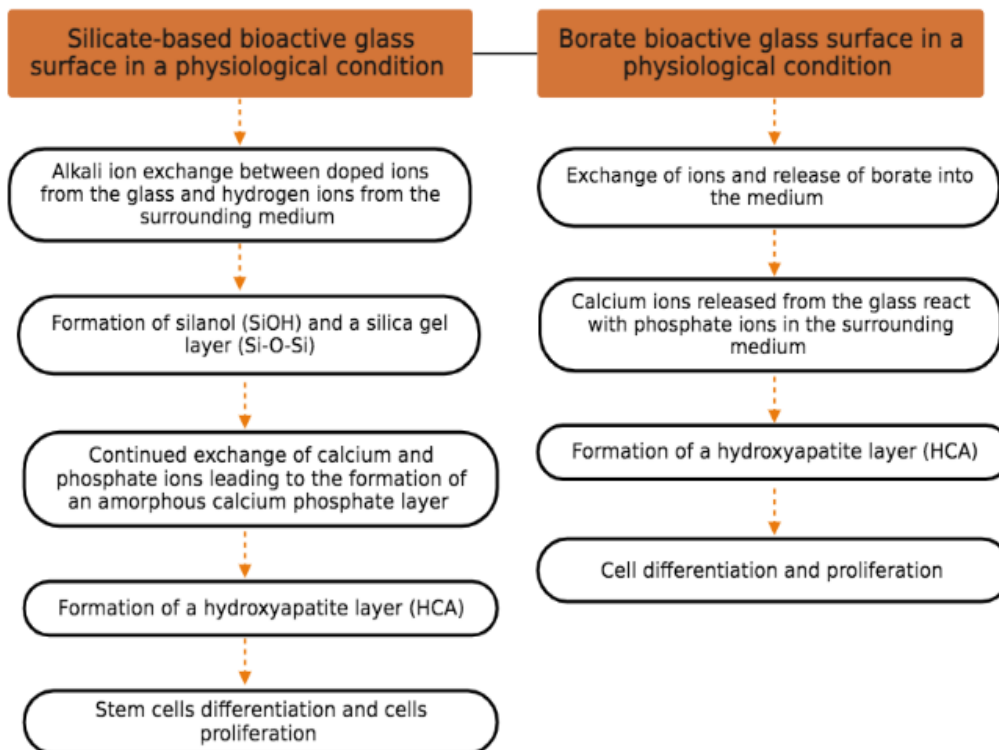


Figure 1. Bioactive glass degradation

### 2.3. CLINICAL TRIALS

The faster reactivity of BBGs promotes faster healing, which is favorable for clinical applications. Some studies have documented the toxicity of high boron levels ( $>0.65\text{mM}$ ) in static conditions, owing to their lower degradation rate. A study performed by Ospina *et al.* [51] evaluated the dissolution of BBGs in both static and dynamic conditions, and it was observed that the glass disintegrated faster under dynamic conditions. Borate-based BG materials such as MIRRAGEN have been approved by the US FDA after their disintegration rate and release of ions were observed. These materials were shown to promote angiogenesis, accelerate the healing process, and reduce bacterial growth in randomized clinical trials. More research is being carried out to better assess the clinical

outcome of BBGs, with a focus on reconstructive/regenerative medicine and infection treatments.

In 2017, the US FDA approved the use of cotton candy-like 13-93B3 glass microfibers, commercially known as MIRRAGEN, in skin wound healing [52]-[55]. MIRRAGEN microfibers in clinical trials were shown to treat diabetic foot ulcers as well as bedsores in as little as 10 weeks [56]-[58]. The nanofiber forms of borate glasses are preferred as they are easy to handle and take the shape/form of wounds [57]. Even though this product has yielded promising results in healing wounds, further studies are needed to investigate the cytotoxicity and mechanism of borate-based BGs in treating wounds.

In a research study by Rahaman *et al.* [59], BBGs in micro and nanofibers were shown to mimic the fibrin clot's microstructure and prompted accelerated wound closure *in vivo* in both animal models and diabetic patients who did not respond initially to conventional therapy. The therapeutic potential of the BBG fibers was ascribed to their ability to generate angiogenesis, epidermal cell migration, and skin generation [60]. The BBG's "cotton candy" structure was approved by the FDA, and it has been there since 2016 and used commercially for veterinarian medicine under the name ReadiHeal.

BBG nanofibers, trade-named DermaFuse, were developed by a company that specializes in precision glass technology called Mo-Sci. The composition of the glass is as follows: 51.5, 53 %  $B_2O_3$ , 4 %  $P_2O_5$ , 20 %  $CaO$ , 6 %  $Na_2O$ , 12 %  $K_2O$ , 5 %, 0–1 %  $ZnO$   $MgO$ , and 0–0.4 %  $CuO$  (in wt%). This product aims to treat recalcitrant wounds such as diabetic ulcers and bedsores. In clinical trials involving more than 60 patients, this product displayed successful healing capabilities. It is hypothesized that the calcium content of the glass is essential in the healing process as it helps in the migration of

epidermal cells. It is also assumed that the nanofiber creates an antibacterial environment as well as easily forms the clot-like structure for wound healing [59]-[62]. Moreover, silver-doped borate glasses with the composition 40–80 %  $B_2O_3$ , 0–70 %  $P_2O_5$ , 0–30 %  $Al_2O_3$ , 0–12 %  $Li_2O$ ,  $Na_2O$ ,  $K_2O$ , and 1–30 %  $Ag_2O$  (wt%), also developed by Mo-Sci, is very promising in biomedical applications due to their high antibacterial properties [62]. The antibacterial effectiveness of this glass is ascribed to the silver ions incorporated in the glass which get disintegrated in body fluids at a controlled rate. The rate by which the glass dissolves is generally maintained by the composition and particle size of the glass. A timeline summary of BG applications [63] [64] and several commercially available BBGs [65]-[70] is shown in Figure 2.

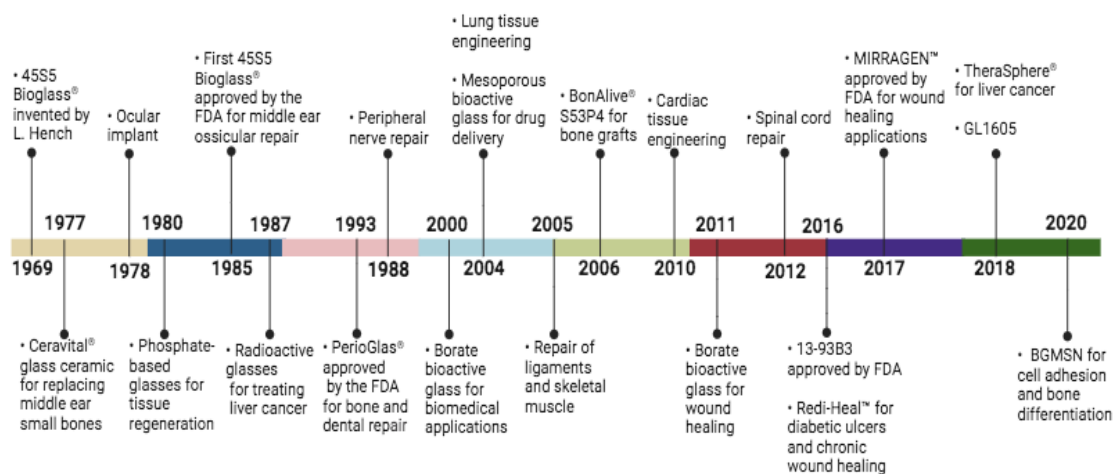


Figure 2. Bioactive Glasses timeline

### 3. NOSOCOMIAL INFECTIONS

Nosocomial infections, also known as hospital-acquired infections, are caused by pathogenic microorganisms and are associated with high morbidity and mortality rates.

Bacteria account for about 90% of nosocomial infections, and the most common clinically relevant bacteria include *P. aeruginosa*, *S. aureus*, and *E. coli* [71]. Excessive and misuse of antibiotics and remarkably increasing antibiotic resistance and accelerating nosocomial infections [72]. Attention has been given to biomaterials in the past few years, and among biomaterials, BGGs have shown promising antimicrobial properties. BGGs display antimicrobial activity against a wide variety of bacteria both gram-positive and gram-negative in planktonic and sessile forms. The antimicrobial activity of BGGs is ascribed to an increase in the pH and osmotic pressure as ions diffuse out of the glass in the surrounding medium upon contact with fluids [73]. In particular, the high antibacterial properties of metal-ion-doped BGGs against bacteria -without documented resistance- make them effective in dealing with nosocomial infections and improving public health [15].

The main etiological agent of nosocomial infections is biofilm adherence to medical devices. Of greater concern to the medical community is the attachment of biofilms to medical instruments and devices [74]-[76]. Medical devices can be classified into non-invasive and invasive medical devices. Non-invasive devices, such as bandages, hospital beds, and waste-collection body devices, are those that come in contact with the skin and are used only as mechanical barriers. Whereas, invasive devices include those that are administered in and penetrate the body such as catheters, tracheal tubes, needles, and examination gloves [77]. Both non-invasive and invasive medical devices are most commonly associated with biofilm formation [78], with the latter being more common, posing a major problem in the public health sector. Infections associated with medical surgeries, such as an orthopedic implant, can take from 3 to 24 months to occur,



depending on how virulent the bacteria are [79] [80]. These infections lead to increased hospitalization rates accompanied by increased morbidity and mortality. Properly managing this phenomenon has prompted the escalation of researching novel strategies to prevent and minimize nosocomial infections.

### **3.1. BIOFILM FORMATION**

Biofilm is a complex aggregation of microbial cells encapsulated in an extracellular polymeric substance (EPS), which is the main component by which microbial cells exchange genetic information and quorum sensing. Biofilms are highly resistant to the host's immune system and antimicrobial agents. About 80% of nosocomial infections are caused by biofilm-containing microbial cells. After 3 to 5 days of primary colonization of microbial cells, microbial co-aggregation occurs using adhesins and causes an irreversible biofilm adherence to surfaces. Following adherence, microbial cells form a well-organized biofilm structure and continue to mature within 2 to 3 weeks [81]-[84]. Compared to planktonic forms of bacteria, biofilms are more than one thousand times more resistant to therapeutic agents [81] [84].

About 99% of microorganisms exist in a sessile form, or biofilms [85]. A critical step in biofilm formation and microbial pathogenicity is the adherence to a substrate, which can be a natural substrate such as skin, or an artificial substrate such as medical devices and implants. Biofilm formation occurs through three main steps [86]: (1) transport; (2) initial reversible bonding; (3) irreversible binding; and (4) colonization. Once bacteria irreversibly bind to a substrate, they form colonies- of the same or different bacterial species- and a multilayered growth, which results in an irreversible, complex

biofilm. In some cases, the formation of a multilayered biofilm creates an anoxic condition to the deep layers of the biofilm and causes the biofilm to detach from the substrate; however, once biofilms detach, they can immediately attach to different substrates and form new colonies (Figure 3).

One of the main reasons for surgical procedures is nosocomial infections associated with biofilm formation [87] [88]. Strengthened by a biofilm, bacterial infections are not easily eradicated by antibiotics. High doses and long-term treatment by antibiotics are generally used, leading to the prevalence of antibiotic resistance. One method considered ideal for impeding implant-associated bacterial infections is local prophylaxis [89]. However, this method achieves a local sustained release of antibiotics for a prolonged time, aimed at minimizing the emergence of antibiotic-resistant bacterial strains. Bacteria do not adhere readily to BGs [90]. BBGs display superior antibacterial properties and therefore, they would be ideal as coatings for medical instruments.

### **3.2. MEDICAL INSTRUMENTS**

Bacterial infections associated with medical devices and instruments are one of the major causes of surgical procedure failure [91] [92]. Medical devices-internal or invasive- are used in almost all medical procedures, both diagnostic and therapeutic. It was reported that nosocomial infections associated with medical devices account for about 45-60% of hospitalized patients [93]. Biofilm formation on medical instruments occurs as bacteria adhere to the surface of the device, proliferate, and form multiple, complex layers of bacterial cells that are encapsulated in the EPS matrix, which plays a pivotal role in the irreversible attachment of the bacterial cells and protection against

external factors [94]. When an injured skin comes in contact with a biofilm-associated medical device, serious bacterial infections occur. The most common methods used to address this issue are using non-adherent medical materials or medical devices modified with antimicrobial properties. However, to date, there is no 100% effective material known to inhibit bacterial adhesion to medical devices.

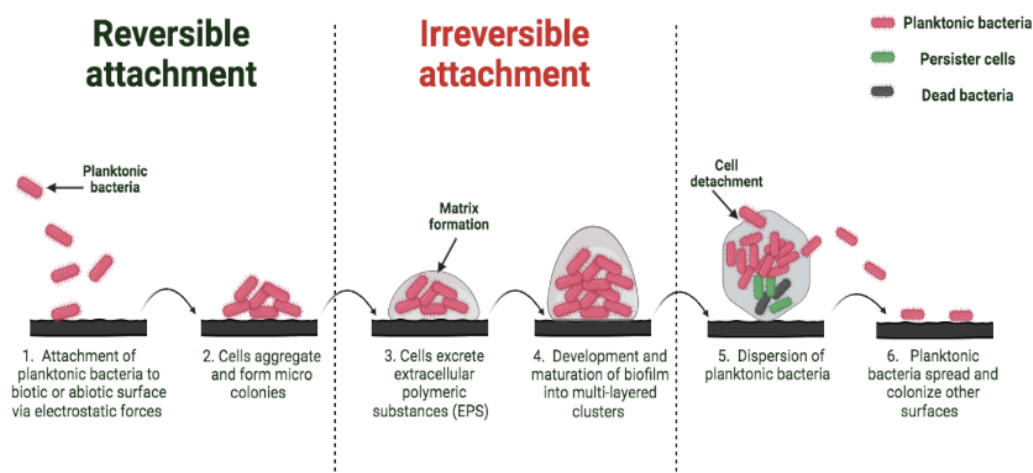


Figure 3. Biofilm formation diagram

Biofilms can also attach to medical devices through several other routes, including contamination, blood, and adjacent paths [92] [95]. Bacteria are negatively charged in general and have hydrophobic surfaces, like the surfaces of most medical devices [96]. Even though this similarity creates repulsive forces, van der Waals forces can counteract this repulsion once the bacteria encounter the surface of the medical device, and initiate bacterial attachment. Upon initial attachment, hydrophobic forces combined with electrostatic repulsion lead to an irreversible bacterial adhesion [97]. To

inhibit biofilm formation after medical procedures, high doses of antibiotic treatments are needed, which can form severe side effects and increase the prevalence of the clinical emergence of antibiotic resistance [98] [99]. A method used to inhibit implants associated with infection is local antibacterial prophylaxis, which involves using adequate concentrations of antibiotics for an extended time [90]. Another method is modifying the implant's surface by using broad-spectrum antibacterial ions such as silver ions [100] [101]. Even though silver can be incorporated directly into implants, BBGs act as potent materials for the incorporation of silver to minimize silver cytotoxicity and control the release of silver. Silver-doped BBGs in powder form can be used as coatings on medical devices to inhibit the growth of biofilms [102] [103], further reducing the risk of antibiotic resistance and nosocomial infections. BBGs can therefore be used as an alternative to minimize the incidence of infections in medical procedures given their enhanced biodegradability and antibacterial properties.

Nosocomial infections can stem from medical surgeries including orthopedic surgeries, hip replacement, cardiovascular implants, and ophthalmic implants [104] [105]. For instance, every year, about 1 million joint and hip replacement surgeries are being done worldwide [106], with the most serious complications associated with prosthetic implants being imputed to the occurrence of biofilm-associated infections [107] [108]. Conventional antibiotic therapies fail to cure those recalcitrant types of infections. During medical surgeries, a patient's immune system is compromised, increasing the risk of biofilm formation at the surgical site and ultimately causing infection. Infections in this case are ascribed to opportunistic pathogens that are circulating the wound or to pathogens from adjacent infections. Because these biofilm-

associated infections are not easily treatable, most of the time the medical surgery becomes unsuccessful, and the patients undergo subsequent medical surgery to treat the infection [109] [110]. Using metal-ion-doped BBGs, however, can help mitigate nosocomial infections, hence a high percentage of morbidity and mortality.

#### **4. ANTIBACTERIAL MECHANISMS OF BORATE GLASSES**

The antibacterial activity of BBGs is achieved through three main ways: (1) using a specific glass formulation that can highly alter the local physiology [111] [112] (2) doping the BG during the manufacturing process with biocidal metals (3) applying the BG in conjunction with antibiotics [113].

##### **4.1. CHANGES IN THE LOCAL PHYSIOLOGICAL ENVIRONMENT**

The general mechanism beyond the antibacterial activity of BGs is ascribed to the local change in pH and the osmotic pressure that occurs as the glass is converted into HAP [19] [114] [115]. The pH of the surrounding medium can increase up to 12 within the first few hours and can remain high for more than two days. A main concern is the effect of the high pH (associated with calcium sulfate dissolution) on the host's tissues and cells.

##### **4.2. ENHANCED BORATE BIOACTIVE GLASSES**

Bacteria have high tendencies to develop resistance against antibiotics through several processes, expressly selection and mutation. Using biocidal metal ions is one potent

alternative to treat bacterial infections due to the low bacterial resistance to those ions. Considering the concentration of dopant ions is imperative as low ion concentration might not produce the desired antibacterial effect, while high concentrations can produce cytotoxic effects. The antibacterial effect of most ions has been imputed to the production of ROS as well as the ion interaction with the bacterial cell membrane [116] [117]. Several characteristics of metal-ion doped glasses such as the surface, composition, oxidation status, and shape play a key role in ROS generation [118]. Upon contact with body fluids, the metal ions get released from the BG and interact with the bacterial cell through electrostatic forces. This results in the inability of the bacterial cells to assimilate nutrients; thus, they lose their cellular functions.

ROS production is mediated by the type of metal dopant as well as the metal uptake by the bacterial cell. ROS are composed of singlet oxygen, superoxide, hydroxyl, and hydrogen peroxide, which are highly unstable O<sub>2</sub> radicals [119]. Due to the contact of metal ions with the bacterial cell wall, ROS is generated extracellularly and intracellularly through reduction and oxidation reactions. High levels of ROS disrupt the bacterial cell wall, causing the cells to leak their cellular contents. Moreover, ROS induces oxidative stress that hinders the electron transport chain of cells and inhibits their proton motive force, interfering with nucleic acid components of the cells and disrupting their functions and cellular metabolism. As ROS accumulate in the bacterial cell, the functions of the bacteria are altered, ultimately leading to bacterial death [120].

Ameliorating the inherent properties of BBGs is a critical approach used to enhance a versatile therapeutic application of BBGS, particularly infection management. When

considering potential BGs for disintegrating therapeutic ions, BBGs are ideal due to their high degradability and accelerated ion release rate.

The antibacterial effectiveness as well as the *in vitro* and *in vivo* performance of BBGS is enhanced by the incorporation of several biocidal ions. Metal ions - Ag, Ce, Ga, Cu, Sr, Zn, I, Te, and Ti - have been investigated by numerous researchers in their ability to promote antibacterial activity against a broad spectrum of clinically relevant bacteria and enhance several biological functions (Figure 4). Most results and observations from SEM, XDR, and FTIR analysis demonstrated the prominent characteristics and functionalities of metal-ion doped BBG.

**4.2.1 Zinc.** Zinc plays a role in DNA replication and is considered a multifarious therapeutic ion. It is involved in bone formation and displays anti-biofilm activity [121] [122]. As zinc disintegrates from a zinc-doped BG, it promotes oxidative stress intracellularly and damages the bacterial cell membrane [123]. When introduced into BBGs, zinc ions display a trivial amelioration in the antibacterial activity of the glass. Most of the studies demonstrated that zinc-doped BBGs had a bacteriostatic effect on a few clinically relevant bacterial species, suggesting a minor antibacterial effect of zinc-doped BBGs. The proposed mechanism of action of zinc ions is ascribed to their ability to interfere with and inhibit the acid production, translocation of membrane proton, and glycolytic processes of the bacteria. [124]-[126]. The disintegration of zinc ions is highly linked to the pH of the surrounding medium. As the bacteria grow, they create an acidic environment which aids in the release of the zinc ions from the glass. As the zinc ions diffuse, the growth of the bacteria is reduced.

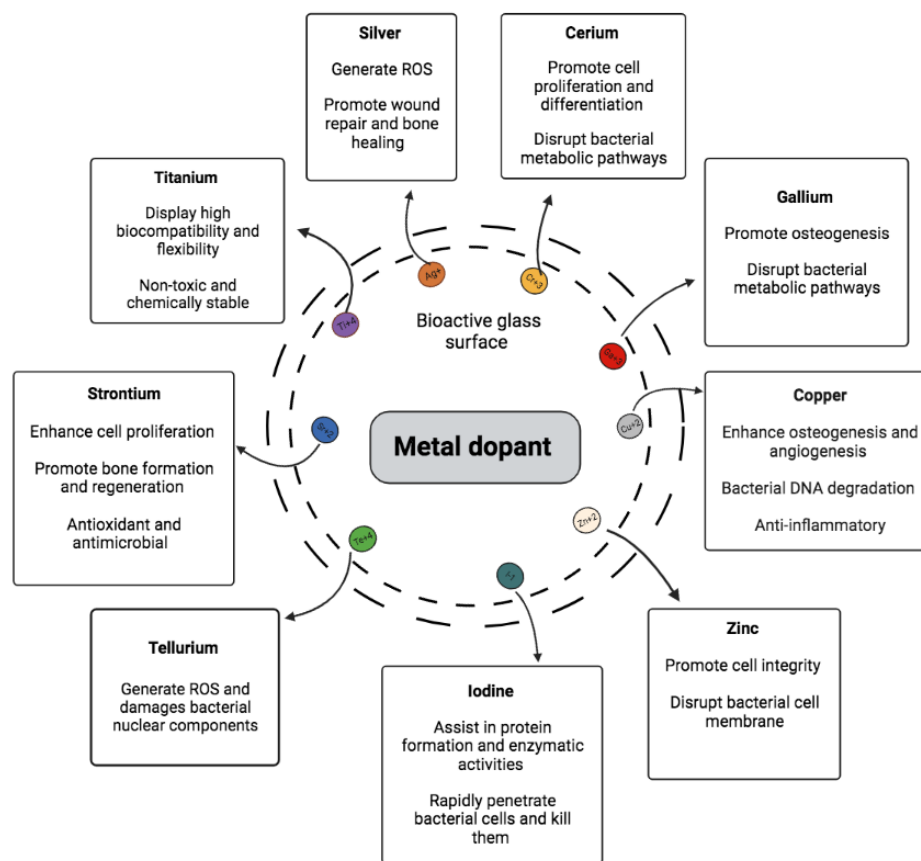


Figure 4. Antibacterial and biological properties of metal-ion dopants. Based on research studies, this figure provides a summary of the most critical antibacterial and biological features of metal ions.

Two *in vitro* evaluations of zinc-doped BBGs have displayed an antibiofilm activity of the glass against the following bacteria after 48 hours: *S. aureus*, *A. baumannii*, *P. aeruginosa*, and *C. albicans* [19] [20]. The authors observed that the addition of zinc slightly enhanced the antibacterial activity of the borate glasses. The antibacterial activity of the glass was ascribed to an increased pH as well as the boron and ion release from the glass.

**4.2.2. Copper.** In 2008, the US Environmental Protection Agency (USEPA) identified copper as the first metallic antimicrobial agent [127]. Since then, copper has



sparked interest in antibacterial applications. The antibacterial effect of copper-doped BBGs is mainly ascribed to the release of copper ions, which cause oxidative damage to the membrane phospholipid of the bacteria and disrupt the integrity of the bacterial cell membrane [127]. As the copper ions penetrate the bacteria, they form oxidative damage and lead to DNA degradation.

Copper displays a low cytotoxicity effect on human cells and high antibacterial activity against a wide range of gram-positive and negative bacteria [128]. It also plays a role in bone formation, promoting angiogenesis and osteogenesis. Moreover, studies have demonstrated the antibacterial efficacy of copper against the growth and development of bacterial biofilms, displaying their effectiveness over conventional antibiotic systemic therapies [129] [130]. It was observed that incorporating copper into BBGs enhanced the antibacterial efficiency of the glass, compared to several other types of metals. Furthermore, due to the inherent antibacterial activity of borate, the concentration of copper doping used in the glass is lower compared to that used in other types of glasses. A minimal concentration of the metal dopant is needed as it has been shown that using high amounts of antibacterial modifiers can alter the reaction and dissolution rate of the glass [73].

**4.2.3. Silver.** Silver displays potent antibacterial activity and its ability to prevent bacterial colonization in biomaterial infections has been exploited in many studies. The addition of silver to BGs was shown to broaden the bactericidal activity of glasses. According to most literature, the propensity of bacteria to develop resistance against silver is very minimal due to the bactericidal effect of silver produced in small concentrations [131]-[133]. The toxicity of silver is further reduced when it is

incorporated into a BG. Therefore, it is imperative to consider using a BG with inherent antibacterial properties to minimize the concentration of silver dopant and meantime achieve a high antibacterial activity. As the silver-doped BG disintegrates, the silver is released from the glass matrix at a rate considered clinically acceptable. Luo *et al.* [134] conducted a study on silver-doped BBG and observed that silver ions were released from the borate glass over seven days, demonstrating a controlled release of silver over a short period. Other studies pointed out the bactericidal effect against gram-positive and gram-negative bacteria achieved with BBGs doped with minimal concentrations of silver as low as 1% [135].

Compared to other silver-doped BGs, silver-containing BBGs display a greater capacity to inhibit bacterial growth. The antibacterial efficiency of silver-doped BBGs is synergetic with the degradation rate of the glass as well as the concentration of the metal incorporated. The release of metal ions creates a balance between the BG's biocompatibility and antibacterial effect. Even though high doses of silver can eradicate bacterial infections, they are also associated with a cytotoxicity risk and adverse effects on cells and tissues [136]. When used in a specific dose, silver is not highly toxic and does not produce adverse effects on human cells [137]-[139].

Using silver for surgically treating wounds has long been documented. Silver has been directly applied to metal alloys and ceramics; however, BGs are more effective materials for the incorporation of silver ions. Studies have shown the promising approach of using silver-doped BBGs as coatings for surgical instruments. Recurrent infections usually take place within the first two weeks of a surgical procedure [140] [141]. BBGs controlled the release kinetics of silver, inhibiting bacterial formation at a gradual rate. A

rapid release of silver was observed during the first 48 hours and continued to release gradually at a longer time [134].

Silver interacts with the surface proteins of the cell wall bacteria with the S-S and the -SH groups, inhibiting the electron transfer process. The proton motive force gets inhibited, and the protons leak out of the bacterial cell membrane. Additionally, silver promotes ROS production, leading to bacterial death. [142]-[145] The antibacterial effect of silver has been observed against many bacterial species as well as antibiotic-resistant strains [18] [146] [147] [148]. Silver-doped BBGs are highly considered in clinical applications as potent alternatives to antibiotics to eliminate bacterial infections [149] [150]. A recent publication by Naseri *et al.* [151] elucidated the antibacterial activity of silver-doped BBGs against *P. aeruginosa* in biofilms. It was observed that the bacterial cell count was reduced by 99.7%. It is assumed that a silver concentration of more the 10  $\mu\text{g/mL}$  is cytotoxic [152] [153]. Silver is preferred to other metal dopants due to their ability to achieve the same antibacterial activity as other metals at lower concentrations [154].

**4.2.4. Cerium.** The antibacterial properties of cerium can be described as the ability of cerium ions to undergo the reversible oxidation conversion from Ce (III) to Ce (IV) [155], disrupting the outer membrane of bacteria and dissociating it from the cytoplasmic component. The negatively charged bacterial cell membrane interacts with cerium ions via electrostatic interactions, persisting on the bacterial surface and changing the viscosity of the cell membrane. As a result, the ion pumps get disrupted, and the bacterial growth is disturbed as the transport exchanges are inhibited [156]. Furthermore, after attaching to the cell membrane, cerium can also attack the proteins on the outer

membrane of the bacteria and alter their electron flow and respiration by reacting with thiol groups. Oxidative stress is another important antibacterial property of cerium. The ability of cerium to cycle between oxidation states from Ce (III) to Ce (IV) generates ROS which leads to bacterial death [155].

As observed in several studies, cerium-doped BGs exhibited antibacterial effectiveness against gram-positive and gram-negative bacteria including *S. aureus* and *E. coli* [157]. Few studies have investigated the antibacterial effectiveness of cerium-doped BBGs. A notable decrease in the OD was observed after 4 hours only, suggesting a fast inhibitory effect of cerium glasses on bacterial growth [159]. Cerium-doped BBGs were shown to achieve a bacteriostatic effect and promote cell differentiation, and the cytotoxicity of the cerium-doped glass has not been documented [158].

**4.2.5. Tellurium.** Classified as chalcogens, tellurium displays different oxidation states, making it not of very high interest in biological and biomolecular applications. Nevertheless, tellurium has recently gained consideration in its biological applications due to its antibacterial characteristics [160] [161] [162]. It was shown that tellurium achieved high antibacterial activity against bacteria such as *E. coli* at low concentrations [163]. The antibacterial activity of tellurium is ascribed to different mechanisms as described by Turner *et al.* [164]. Due to changes in the environmental pH in the outer membrane of the bacterial cell, tellurium can induce adverse effects on the cell membrane of a bacteria. Moreover, tellurium plays a role in the superoxide dismutase activity, which counteracts the negative effects formed by ROS generated by cells [165]. A study performed by Zhong *et al.* [166] noted the antibacterial activity of tellurium dioxide nanoparticles against some types of gram-positive bacteria.

Few studies have been carried out on tellurium-doped BBGs. However, a recent study was performed using tellurium-doped silica-based BG against *S. aureus* and *S. epidermidis*, and a significant biofilm reduction was observed [167]. This study demonstrates the possibility of developing and studying BGs containing tellurium in terms of their toxicity and antimicrobial activity. In a comparative study [168], the antibacterial activity of tellurium and titanium-doped BBGs was assessed against MRSA, and complete inhibition of the bacteria was observed after 24 hours using the good agar diffusion method. High concentrations of the glass dopant displayed higher antibacterial activity. Compared to the other biocidal elements, tellurium is a non-essential trace element, and its toxicity is highly dose-dependent. Further studies are needed to assess the antibacterial effectiveness of tellurium-doped BBGs.

**4.2.6. Gallium.** Gallium is primarily known for tissue metabolism and distribution in medical imaging as well as for its therapeutic properties in treating multiple disorders such as cancer and autoimmune diseases [169]-[171]. After the antibacterial properties of gallium were exploited, gallium sparked interest in its potential application as an antibacterial agent in treating infectious diseases. Widely used as a therapeutic ion, gallium is well-known for its broad-spectrum antimicrobial activity and high potential to replace antibiotics. The main antibacterial mechanism of gallium is imputed to its ability to disrupt the metabolic pathways of bacteria. Gallium alters the iron metabolism of the bacteria, acting as a “Trojan horse” [172]. Iron and Gallium have the same ionic radii; therefore, it is difficult for biological systems to distinguish between them.

The presence of iron in the intracellular environment of bacteria is essential since bacteria need iron for many of their protein processes. Iron is involved in the DNA synthesis, response to oxidative stress, and metabolism of bacteria. However, iron is poorly soluble in neutral aqueous environments and not readily available for bacteria [173]. Due to limited iron availability, bacteria evolved methods such as the production of siderophores, xenosiderophores, and hemophores to actively acquire iron [174] [175]. Given that iron is scarcely present in mammalian hosts in free forms, inducing mutations in specific iron-uptake strategies can reduce the ability of bacteria to cause infections. Bacteria utilize iron by obtaining  $\text{Fe}^{3+}$  and reducing it into  $\text{Fe}^{2+}$ . Due to gallium's similarity to iron, when the bacteria encounter gallium, they immediately uptake it, replacing it with iron. However,  $\text{Ga}^{3+}$  cannot be reduced to  $\text{Ga}^{2+}$ , inactivating the bacterial proteins [176].

Therefore, disrupting bacterial iron metabolism has been suggested as a potent target for developing novel antibacterial drugs [177]-[179]. Strategies using iron cheaters and inhibiting the bacterial iron-uptake pathways have been considered. However, most of these strategies were found to be limited. It was observed that iron cheaters can promote the growth of the bacteria rather than inhibit it under iron-limiting conditions [180]. Therefore, studies have focused on using iron mimetics, expressly gallium, to disrupt the bacteria's iron metabolism and to reduce the possibility of bacteria developing resistance. Unlike iron, gallium cannot undergo redox cycles in physiological conditions and has detrimental effects on the bacteria, interfering with the bacteria's ability to transport oxygen. Bacteria exposed to gallium have reduced iron-containing enzyme activities, indicating a lower probability of bacteria developing resistance against gallium

toxicity [172]. Therefore, developing gallium-based therapies can be pivotal in dealing with bacterial infections and other diseases. The antibacterial effectiveness of gallium has been demonstrated *in vitro* and *in vivo* against bacteria in planktonic and sessile forms [171].

The antibacterial activity of gallium-doped BGs has been widely considered [181] [182]. Studies have emphasized the antibacterial efficacy of BBGs doped with gallium ions and their enhanced antibacterial and antibiofilm activity; the reduction of clinically relevant bacteria such as *P. aeruginosa*, *S. aureus*, and *MRSA*, and *S. epidermidis* has been observed in many studies. In a study by Yazdi *et al.* [183], gallium-doped BBGs were shown to exhibit bacteriostatic effects against *P. aeruginosa*. Ions were observed to release at a gradual rate over 28 days. Gallium-doped BBGs produced inhibitory effects against some gram-negative and positive bacterial strains [181]. Some studies have pointed out that gram-positive bacteria were more sensitive to gallium-doped borate glasses compared to gram-negative bacteria [184]. This property can be ascribed to the lipopolysaccharide layer on the gram-negative bacterial cell wall that makes them less susceptible to antimicrobials.

**4.2.7. Strontium.** Strontium has a high atomic weight and is effective in controlling the degradation rate of BBGs. Sinouh *et al.* [185] observed that strontium increased the polymerization rate of BBGs and enhanced their degradation capacity. Like calcium, strontium plays a pivotal role in stabilizing and promoting bone structure by maintaining the upregulation and downregulation of osteoblasts and osteoclasts. Strontium, however, is needed in very high doses. Li *et al.* [186] demonstrated that high strontium concentrations incorporated into BBGs decelerated the dissolution rate of the

glass. The antibacterial activity of strontium ions stems from their ability to impede bacterial cell division through interference with bacterial metabolism and genetic components. However, the antibacterial property of strontium is very poor compared to other bivalent cations, and high concentrations of strontium are required to reduce bacterial cells.

**4.2.8. Iodine.** Iodine exhibits broad-spectrum antimicrobial properties and has been used for disinfection purposes [187]. High concentrations of iodine (>300mg/ml) have been used in catheter angiograms with no cytotoxic effects reported, pointing out iodine's cytocompatibility in large amounts [188]. Iodine is not commonly used as a BG dopant. One study assessed the antibacterial effectiveness of iodine-doped BBG, and the study reported a bacteriostatic effect of the glass against clinically relevant pathogens, both gram-positive and gram-negative [19]. Findings from this study indicate that iodine can potentially be used to enhance the antibacterial properties of BBGs.

**4.2.9. Titanium.** Titanium is commonly used in implant materials due to its noted ability to promote bone growth through osteointegration [189][190]. Few studies have focused on assessing the antibacterial properties of titanium. Titanium-doped BBGs, however, were noted in their ability to minimize the growth of gram-positive bacteria. Rodriguez *et al.* [191] observed inhibition zones for *S. epidermidis* after 7 days of contact with titanium-doped BBG. No zone of inhibition was observed for *E. coli*, indicating the ineffectiveness of the glass against gram-negative bacteria. Similar results were demonstrated by other studies [168].



### 4.3. BIOACTIVE GLASS IN CONJUNCTION WITH ANTIBIOTICS

To treat surgical infections with antibiotics, BGs are mainly used either as mesoporous antibiotic carriers [192] or antibiotic-loaded biodegradable composites [193] [194]. The mesoporous glass structure is sol-gel derived, which is accompanied by several limitations. Sol-gel-derived BGs possess a low ability to release antibiotics in a controlled manner. This can be attributed to the fact that some BGs produced through the sol-gel route display high surface area, yet lower strength compared to glasses produced by the conventional melting/casting method. As shown by Domingues *et al.* [192], a sol-gel BG loaded with tetracycline showed a 12% release of tetracycline in contact with SBF during the first 8 hours, and very few amounts of antibiotics were released over a 3 months duration (about 20-25% of the initial amount of tetracycline loaded in the glass). In contrast, antibiotic-loaded biodegradable composites show a very rapid release of antibiotics. More than 85% of the amount loaded in the composite is released in the first 10 days upon immersion in SBF [32]. The release of antibiotics was shown to stop after about 21 days [195].

Some studies have demonstrated a significant reduction in the bacteria using only BBG composites, particles, or powder. Borate glasses have shown promising results in eradicating several nosocomial infections and diseases such as osteomyelitis while being non-toxic to cells [59]. However, using BBGs loaded with antibiotics most often requires glasses with high boron concentration, which can induce toxicity to cells [196]. The porosity and surface area of the BBG form used are very critical in determining the antibiotic loading capacity of the glass. Because most forms of the glass- particles in particular- are dense, scaffolds would be best as antibiotic delivery systems. Given their

faster, controlled degradation rate, BBGs are ideal for their versatility in terms of sustained drug delivery.

## 5. BIOMEDICAL APPLICATIONS

The biomedical research field shows an increasing interest in bioactive biomaterials, particularly BGs. Due to their high biocompatibility, biodegradability, angiogenic and osteogenic, and antibacterial properties, BBGs are used in a multitude of biomedical applications. BBGs help overcome several limitations associated with other BGs such as lower mechanical strength and biodegradability. Moreover, enhanced BBGs combine antibacterial and bioactive properties; this synergetic effect minimizes the chance of infections in medical applications. BBGs can be used in different forms and compositions, indicating their broad spectrum uses. Incorporating cations into BBGs ameliorates angiogenesis, mineralization, tissue formation, and bone metabolism. Additionally, *in vivo* and *in vitro* studies demonstrated the effective performance of metal-ion-doped BBGs in cell differentiation and proliferation, highlighting their unique ability to promote wound healing. Overall, the mechanical and surface characteristics of metal-ion-doped BBGs render them favorable in a multitude of biomedical applications (Figure 5).

### 5.1. WOUND HEALING

The epidermis is the outermost layer of skin and is composed of epithelial tissues that cover the entire body and act as protection against foreign substances and pathogens. The

epidermis is constantly subjected to damage and plays a key role in complex wound-healing processes that can result from injuries and burns [203].

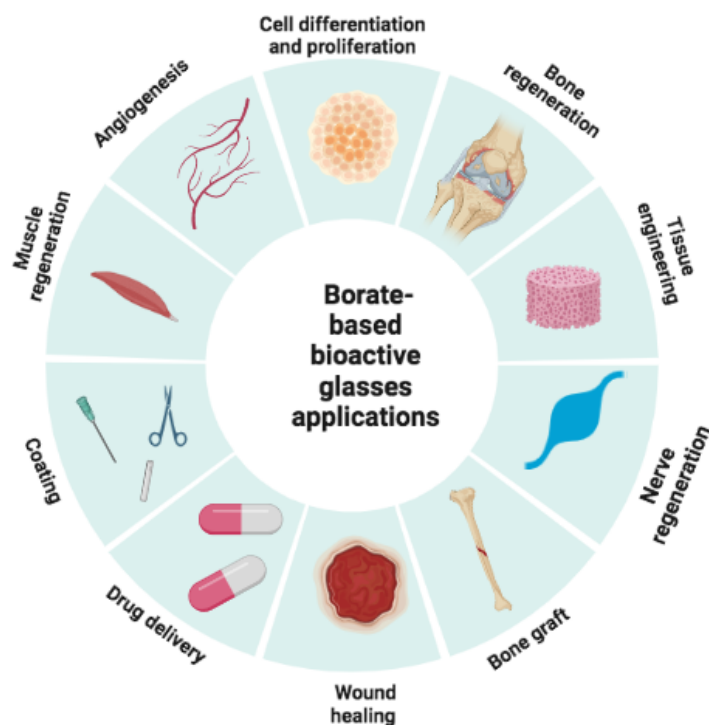


Figure 5. Biomedical applications of borate bioactive glasses

Therefore, various treatments such as wound dressings and matrices were developed for epithelial tissues [204]. Besides their application in regenerative medicine, BGs created new hopes in healing soft tissues, proliferating epithelial cells, and reducing inflammation. It has been documented that the therapeutic ions released from BGs have a potent regenerative capacity while reducing microbial contamination and ameliorating the process of wound healing [205]. As described by Naseri *et al.* [153], BGs promote

Table 1. Summary of reviewed literature on the antibacterial mechanisms and effectiveness of metal-ion doped borate-based bioactive glasses

Borate bioactive glass composition in mol%	Synthesis method	Metal dopant	Proposed mechanism of action of the metal dopant	Antibacterial effectiveness	Form and particle size	Application	Ref.
1. (5.5 Na <sub>2</sub> O, 11.1 K <sub>2</sub> O, 4.6 MgO, 18.5 CaO, 56.6 B <sub>2</sub> O <sub>3</sub> , 3.7 P <sub>2</sub> O <sub>5</sub> )	Melt-derived route	1. Cu (3%)	DNA degradation	1. <i>S. aureus</i> and <i>E. coli</i>	1. Powder (5-20µm)	1. Wound healing	[197]
2. (48 SiO <sub>2</sub> , 26 Na <sub>2</sub> O, 22 CaO, 3 P <sub>2</sub> O <sub>5</sub> , 0.43 B <sub>2</sub> O <sub>3</sub> , 0.57 Al <sub>2</sub> O <sub>3</sub> )		2. Cu (10%)	Disrupts the bacterial cell membrane integrity and the transport protein activity	2. <i>S. epidermidis</i>	2. Powder (<20µm)	2. Nosocomial infections	[198]
3. (45 B <sub>2</sub> O <sub>3</sub> , 24.5 CaO, 24.5 Na <sub>2</sub> O, 6 P <sub>2</sub> O <sub>5</sub> )		3. Cu (1%)		3. <i>S. epidermidis</i> , <i>E. coli</i> , and <i>S. aureus</i>	3. Powder NA	3. General applications	[199]
(54.6 B <sub>2</sub> O <sub>3</sub> , 22.1 CaO, 6.1 Na <sub>2</sub> O, 7.6 MgO, 7.9 K <sub>2</sub> O, 1.7 P <sub>2</sub> O <sub>5</sub> )	Sol-gel route	Ag (7.5%)	Promotes ROS production	<i>E. coli</i> , <i>S. aureus</i> , <i>P. aeruginosa</i> , and <i>B. cereus</i>	Powder (0.05-0.1µm)	Wound healing	[26]
1. (6 Na <sub>2</sub> O, 8 K <sub>2</sub> O, 8 MgO, 16 CaO, 2 P <sub>2</sub> O <sub>5</sub> , 6 SrO, 36 B <sub>2</sub> O <sub>3</sub> , 18 SiO <sub>2</sub> )	Melt-derived route	1. Ag (1%)	Promotes ROS production	1. MRSA	1. Powder coating NA	1. Infection control in fracture fixation	[200]
2. (6 Na <sub>2</sub> O, 12 K <sub>2</sub> O, 5 MgO, 20 CaO, 4 P <sub>2</sub> O <sub>5</sub> , 52 B <sub>2</sub> O <sub>3</sub> )		2. Ag (1%)		2. <i>E. coli</i> , <i>V. natriegens</i> , <i>S. sonnei</i> , <i>S. marsecens</i> , and <i>S. epidermidis</i>	2. Powder (>45µm)	2. Nosocomial infections	[19]
3. (5 Na <sub>2</sub> O, 43.5 B <sub>2</sub> O <sub>3</sub> , 6.5 Li <sub>2</sub> O, 44 SiO <sub>2</sub> )		3. Ag (1%)		3. <i>E. coli</i> , <i>S. aureus</i> , and <i>P. aeruginosa</i>	3. Powder coating (>45µm)	3. Medical applications	[103]
4. (59.5 B <sub>2</sub> O <sub>3</sub> , 2 P <sub>2</sub> O <sub>5</sub> , 9.5 CaO, 9 CaF <sub>2</sub> )		4. Ag (0.75%)		4. <i>E. coli</i> , <i>S. aureus</i> , and <i>P. aeruginosa</i>	4. Powder coating (>45µm)	4. General applications	[201]
1. (6 Na <sub>2</sub> O, 12 K <sub>2</sub> O, 5 MgO, 20 CaO, 4 P <sub>2</sub> O <sub>5</sub> , 52 B <sub>2</sub> O <sub>3</sub> )	Melt-derived route	1. Ga (2%)	Competes with the iron Fe <sup>3+</sup> uptake	1. MRSA, <i>S. epidermidis</i> , <i>V. natriegens</i> , and <i>S. marsecens</i>	1. Powder (>45µm)	1. Nosocomial infections	[19]
2. (14 Na <sub>2</sub> O, 12 CaO, 6 P <sub>2</sub> O <sub>5</sub> , 37 B <sub>2</sub> O <sub>3</sub> , 16 ZnO)		2. Ga (15%)	Inhibits the bacterial biological reactions and metabolic pathways	2. <i>S. epidermidis</i> and <i>P. aeruginosa</i>	2. Powder (90–710 µm)	2. Tissue engineering	[183]

Table 1. Summary of reviewed literature on the antibacterial mechanisms and effectiveness of metal-ion doped borate-based bioactive glasses (cont.)

(6 Na <sub>2</sub> O, 12 K <sub>2</sub> O, 5 MgO, 20 CaO, 4 P <sub>2</sub> O <sub>5</sub> , 52 B <sub>2</sub> O <sub>3</sub> )	Melt-derived route	I (1%)	Inhibits bacterial cell membrane and protein synthesis	MRSA, <i>S. marcescens</i> , <i>S. epidermidis</i> , <i>E. coli</i> , and <i>M. catarrhalis</i>	Powder (>45µm)	Nosocomial infections	[19]
1. (14 Na <sub>2</sub> O, 12 CaO, 6 P <sub>2</sub> O <sub>5</sub> , 32 B <sub>2</sub> O <sub>3</sub> , 16 ZnO) 2. (45 B <sub>2</sub> O <sub>3</sub> , 24.5 CaO, 24.5 Na <sub>2</sub> O, 6 P <sub>2</sub> O <sub>5</sub> )	Melt-quenching	1. Ti (20%) 2. Ti (2%)	NA	1. <i>S. epidermidis</i> , <i>E. coli</i> , and <i>S. aureus</i> 2. MRSA	1. Scaffolds containing 42% powder (≤20 µm) 2. Powder NA	1. Bone loss 2. Osteomyelitis	[202] [168]
(45 B <sub>2</sub> O <sub>3</sub> , 24.5 CaO, 24.5 Na <sub>2</sub> O, 6 P <sub>2</sub> O <sub>5</sub> )	Melt-quenching	Te (2%)	Increases the levels of ROS	MRSA	Powder NA	Osteomyelitis	[168]
1. (6 Na <sub>2</sub> O, 7.9 K <sub>2</sub> O, 7.7 MgO, 22.1 CaO, 1.7 P <sub>2</sub> O <sub>5</sub> , 54.6 B <sub>2</sub> O <sub>3</sub> ) 2. (32 B <sub>2</sub> O <sub>3</sub> , 12 CaO, 14 Na <sub>2</sub> O, 6 P <sub>2</sub> O <sub>5</sub> ) 3. (5.5 Na <sub>2</sub> O, 11.1 K <sub>2</sub> O, 4.6 MgO, 17.5 CaO, 56.6 B <sub>2</sub> O <sub>3</sub> , 3.7 P <sub>2</sub> O <sub>5</sub> )	Melt-quenching	1. Zn (6%) 2. Zn (14%) 3. Zn (1%)	Stimulates the production of ROS Destabilizes the bacterial cell membrane	1. <i>S. aureus</i> and <i>E. coli</i> 2. <i>S. epidermidis</i> , <i>E. coli</i> , and <i>S. aureus</i> 3. <i>S. aureus</i> and <i>E. coli</i>	1. Powder (224–500 µm) 2. Scaffolds containing 42% powder (≤20 µm) 3. Powder (300–500 µm)	1. Biomedical applications 2. Bone loss 3. Wound healing	[201] [202] [196]
(45 B <sub>2</sub> O <sub>3</sub> , 24.5 CaO, 24.5 Na <sub>2</sub> O, 6 P <sub>2</sub> O <sub>5</sub> )	Melt-quenching	Ce (2%)	Generates ROS Disrupts the metabolic pathways, cellular respiration, and O <sub>2</sub> uptake in the cell	MRSA	Powder NA	Osteomyelitis	[168]
(20 B <sub>2</sub> O <sub>3</sub> , 10 CaO, 20 Na <sub>2</sub> O, 50 P <sub>2</sub> O <sub>5</sub> )	Melt-quenching	Sr (2%)	Hinders the bacterial metabolism and replication processes	<i>B. subtilis</i> , <i>E. coli</i> , and <i>S. aureus</i>	Powder NA	General applications	[199]

wound healing as follows: (1) enhancing cell proliferation (2) decreasing inflammation (3) improving angiogenesis (4) exerting antibacterial effects.

The fast degradation of BBGs and their properties make them potent for wound healing applications, and the boric acid that disintegrates from BBGs is effectively

considered in wound healing. In addition, the calcium component of the glass is essential for the migration of epidermal cells and bone growth. Borate glasses, particularly the 13-93B3 fabricated in fibers with very small diameter sizes, sparked interest in soft and hard tissue regeneration and in managing chronic wounds [206] [207]. Moreover, the rapid degradation rate of borate glasses allows them to be rapidly converted into a HAP layer, thus reducing toxicity associated with the  $(\text{BO}_3)^{3-}$  ions [208].

Wound healing occurs as a result of blood vessel formation at the wound area. Due to thick, complex tissues, it is difficult for some growth factors to get stimulated and prompt the formation of blood vessels. BBGs, however, take a major part in promoting angiogenesis due to the boron content of the glass which promotes collagen and protein secretion as well as the formation of extracellular matrix [209] [210]. BBG microfibrillar scaffolds exhibit high degradation rates and slow crystallization into HAP. As documented by several studies, boron helps stimulate the MAPK signal pathway as well as enhance the proliferation and migration of HUVEC and keratinocytes [27] [115]. Besides, boron helps upregulate the vascular endothelial growth factor (VEGF), which plays a critical role in blood vessel formation. [211]. All these mechanisms are associated with triggered wound-healing processes at different stages. Moreover, the dissolution of borate glasses produces high calcium ions in body fluids as compared to other types of BGs [208]. Calcium ions are very critical for the wound healing cascade, particularly for the migration and regeneration of epidermal cells. Studies performed by Line *et al.* [60] and Zhou *et al.* [212] corroborated the ability of BBG microfibers to promote microvascular density and their effectiveness in treating Sprague-Dawley rats with full-thick dermal wounds. Moreover, a very remarkable feature of BBGs lies in their ability to

form hollow cavities that living tissue can use for directional growth. This feature is expressly beneficial for highly vascularized tissues such as bones as hollow cavities can help stimulate the healing process in connective tissues. BBGs were shown to form hollow cavities *in vivo* where blood vessels with red blood cells were observed to grow inside the soft tissue.

Incorporating biocidal ions in the glass structure has been demonstrated to enhance the angiogenesis and the antibacterial activity of BBGs, further optimizing the process of wound healing. In *vitro* and *in vivo*, enhanced borate glasses increase the pH and enhance cell/tissue proliferation. It was found that copper ions increased endothelial cell proliferation *in vitro* studies [29]. In a study performed by Zhao *et al.* [28], it was shown that the release of copper ions from copper-doped BBG in a microfiber form highly stimulated angiogenesis compared to the undoped borate glass. The copper ions stimulated VEGF by mimicking hypoxia conditions [213]. The researchers used microfiber 19-93B3 doped with 3% copper in rodents with full-thickness skin wounds, and they observed that blood vessels formed, and the skin healed after 14 days as shown by computed tomography. Results from this study were confirmed by Chen *et al.* [214]. Furthermore, doping borate glasses with different dopants such as silver, gallium, and copper enhanced the antimicrobial properties of the scaffold for soft tissue repair [33] [135]. In a study by Naseri *et al.* [153], the antibacterial effect of silver doped BBG was assessed on *P. aeruginosa*; a reduction of bacteria was observed on day 4, and it was further shown that fibroblasts and keratinocyte cell viability increased, promoting wound healing.

If inappropriately treated, wounds will get exposed to and colonized by bacteria and form chronic wounds. It has been demonstrated that metal-ion-doped BBGs can inhibit the colonization of numerous types of gram-positive and gram-negative bacteria through different well-defined mechanisms. The mechanisms most commonly described in the literature are a local increase in pH and the generation of ROS that damages bacterial DNA and RNA. Besides inhibiting bacterial infections, the potent biological properties of metal-ion-doped BBGs aid in an accelerated wound-healing process.

## 5.2. BONE GRAFTS

Treating bone defects is constantly a great challenge for surgeons and orthopedists due to the limitations accompanied by both autologous and allogenic bone grafts, which can trigger immunological reactions and infection transmission. Bone tissue engineering has broadened the possibilities of regenerating bone defects mainly through the development of scaffolds, which allow seeded cells to attach to the defective surface and form new bones through a series of biological and biochemical reactions [215] [216].

Due to their flexibility and potent ability to promote an effective bonding between the surface of the material and the bone tissue, BG scaffolds were given considerable attention. BBGs have been considered for regeneration applications after Jung *et al.* [59] demonstrated their high capacity in wound healing. The disintegration of boron at controlled rates can help stimulate osteogenesis and bone formation through efficient cell, nutrients, and growth factors transportation. Besides, the calcium content of the borate glass is imperative in activating osteogenic gene expression [217]-[219]. The bioactivity of borate glasses in bone regeneration is ascribed to the fast conversion of borate glasses



into HAP, indicating faster healing [220] [221]. Xie *et al.* [32] showed through radiographic images that new bone was highly replaced by BBG scaffolds. The complete degradation of the glass enhanced the differentiation and proliferation of mesenchymal stem cells, further supporting bone growth. Besides, it was observed that BBG scaffolds were completely converted into HAP 12 weeks after being implanted in rats with calvarial defects [222]. Additionally, it was demonstrated that 13-93B3 promoted the secretion of CX43 and IG-1, indicating the potential use of BBGs in muscle regeneration and healing [223].

Vascularization is an essential component for the survival of bone cells and the regeneration of bones. Administering growth factors, which is a very expensive procedure, is therefore critical to promote vascularization in bone grafts [224]. Silicate-based BGs are known for their ability to form a HAP layer that aids in bone formation; however, their ability to promote angiogenesis or new blood vessels, is lower compared to that of BBGS. The angiogenesis properties of borate glasses can be regulated by doping the glass with metals such as copper. BBGs are also preferred in bone grafts due to their slow release of ions over a long period. The cytotoxicity of borate glasses was not observed by studies performed on bone regeneration [225]-[227].

### **5.3. SCAFFOLDS**

Designing biomaterial scaffolds by harvesting living tissues is the key approach to tissue engineering and biomedical application. Scaffolds are vastly needed for tissue engineering applications; therefore, the structure of scaffolds should maintain mechanical strength and potent integrity to support tissue formation. The degradation capacity is a

key component of scaffolds, with higher degradation rates being optimal. Liu *et al.* [228] demonstrated that BBG scaffolds degraded altogether after being in contact with SBF for 1 week and formed a HAP layer. Furthermore, other studies have indicated the release of 35% of boron ions 13-93B3 scaffolds in only 1 day following contact with SBF and 80-90% boron release after 1 week [8]. It was documented that increasing the boron concentration increased the degradation rate of the borate glass, nevertheless, it decreased osteogenic cell proliferation. It was observed that after being in contact with SBF for 3 days, elevated levels of calcium were released from the glass microfibers, and after 2 weeks, the borate glass microfibers completely degraded and slowly formed HAP [222]. However, it was further indicated by other studies that the partial conversion of scaffolds into HAP was more effective for cell proliferation [5]. This alludes to the point that the slow crystallization rate of borate glasses can help ameliorate the scaffold's biocompatibility.

Moreover, the particle size of BBGs was shown to influence the pH and the dissolution rate of the scaffolds. A study performed by Deliormanli *et al.* [229] studied BBG scaffolds for 3D printing and observed that the borate glass scaffolds with smaller particle sizes (130  $\mu\text{m}$ ) degraded faster and completely compared to those with larger particle sizes (300  $\mu\text{m}$ ). Besides, as Zhang *et al.* [230] demonstrated, smaller particle sizes increased the pH during the degradation of BBG scaffolds. These studies indicate that the partial conversion of borate glasses into HAP can minimize cell toxicity, and a moderate boron ion dissolution can help enhance cell proliferation.

#### 5.4. OSTEOMYELITIS

Osteomyelitis is a complicated bone infection that is very difficult to treat and involves a surgical debridement of the infected area followed by a long antibiotic therapy [231]. However, antibiotic therapy is not very efficient, and high doses are required over an extended period. Even though silicate glasses were approved for treating bone infections in 2006, BBGs are more advantageous due to their faster conversion into HAP [232]. Besides, BBGs can be effectively loaded with antibiotics that are highly released at the infected site, as shown by Liu *et al.* [228].

Local delivery of antibiotics is the common method of treating osteomyelitis as it allows high doses of antibiotics to diffuse into avascular sites that cannot be accessed by systemic antibiotics. Polymethylmethacrylate (PMMA) antibiotic-loaded beads are used to locally treat infected bones. However, about 90% of the loaded antibiotics remain trapped inside the beads and are not delivered, and the beads have to be removed by another surgical procedure as they are non-biodegradable [233]. Moreover, PMMA beads have poor osteoconductivity and transient cytotoxicity and act as good substrates for biofilm formation, exacerbating the infection [234]. Other materials such as biodegradable polymers including collagen are considered antibiotic carriers. Even though those carriers are biodegradable, they do not promote osteoconductive ingrowth of bone and do not maintain a regulated release of antibiotics [233]. Injectable biomaterials such as calcium sulfate (CS) loaded with antibiotics are also commonly used methods in dealing with osteomyelitis. CS fills irregular-shaped bone defects, allowing no room for bacterial survival; however, CS displays slow-releasing antibiotic rates and

poor mechanical strength [235]-[237]. To overcome these limitations, BBGs are considered.

Metal-ion-doped borate-based BGs have a regulated degradation rate, bioactivity, and biocompatibility, and promote the growth and differentiation of mesenchymal stem cells [36] [196] [219] [238]. Previous studies have demonstrated the effectiveness of vancomycin-loaded BBGs against MRSA in rabbit models with bone infection [32] [239]. Another study has shown the ability of gentamicin-loaded BBG pellets to treat *S. aureus* causing osteomyelitis in rabbit models [240]. In a similar study by Xie *et al.* [32], BBGs loaded with vancomycin reduced chronic osteomyelitis in rabbits, indicating the efficiency of borate glasses as antibiotic carriers in treating bone infections as compared to the convention non-biodegradable biomaterials. The researchers observed that the borate glass powder displays hydrophilicity which allows for an enhanced loading procedure of the antibiotic. They further examined the release of the antibiotic *in vitro* using high-performance liquid chromatography (HPLS) and observed an 85-94% antibiotic release at day 22. Furthermore, they induced osteomyelitis in rabbits by injecting their medullar cavity with MRSA, and after 3 weeks, they treated one group with debridement, a second group with plain borate glass pellets, and a third group with vancomycin-loaded BBG pellets. They observed that the loaded glass ameliorated the effects of osteomyelitis, reducing MRSA.

## **5.5. NERVE REGENERATION**

Peripheral nerve damage is a very challenging problem, and it is estimated that about 200,000 surgeries are performed annually to repair nerves. Only a few percent of those

surgeries are altogether successful [241] [2]. Nerve regeneration surgeries rely on material that connects damaged nerves to severed ones. BGs were shown to provide neuroprotective cues and deliver growth factors [11] [242]. BGs, when fabricated in glass fibers, can be effectively applied in soft tissue engineering such as nerve repair [243]. Even though studies performed on the role of BBGs on nerve regeneration are very few, the effectiveness of BBGs in neural tissue engineering applications was demonstrated by those studies. The physical and chemical formulations of BBGs can be altered to produce several forms of glass including powder, beads, composites, rods, and fibers [244] [245]. Moreover, the functionalities of the borate glasses can be ameliorated without inducing toxicity by doping the glass with a certain concentration of metal ions (Table 2). As shown by Gupta *et al.* [246], 13-93B3 incorporated into fibrin microfibers increased the cell viability in embryonic dorsal root ganglia (DRG). PCL fibers enhanced with 50% 13-93B3 stimulated DRG growth and doping the borate glass with metal ions significantly resulted in neurite outgrowth. Besides, Marquardt *et al.* [247] demonstrated the cytocompatibility of borate glass microfibers (53B<sub>2</sub>O<sub>3</sub>, 6Na<sub>2</sub>O, 20CaO, 12K<sub>2</sub>O, 5MgO, and 4P<sub>2</sub>O wt.%) with neural cells.

## 5.6. DRUG DELIVERY

Enzymes and chemical reactions in the body can inactivate biomolecules during systemic drug delivery, and as a result, high doses of the drug would be needed. Another drawback to systemic drug delivery is that the drug does not efficiently reach the targeted site. Therefore, local drug delivery systems are prominently needed. In the context of tissue engineering, specialized scaffolds that act as carriers for local drug delivery are

greatly considered. The drug mode of action can be optimized through local delivery as the amount of drug can be increased while reducing the excretion of the drug and other protein and growth factors by renal filtration, a phenomenon known as sustained release systems [248] [249]. To be effective, drug carriers/biomaterials should be biodegradable, biocompatible, bioresorbable, and osteoconductive with flexible mechanical properties [250] [251]. BGs fulfill the aforementioned requirements and act as suitable candidates for drug delivery. When used as drug-loaded scaffolds, BBGs combine the glass's therapeutic properties and the loaded drug's enhanced effect.

Several different therapeutic substances, including antibiotics, can reduce pathogens and minimize infection and inflammation. Other substances include growth factors, hormones, peptides, and a combination of several bioactive molecules. The procedure of loading the drug into the BG can be achieved during the manufacturing process. Because the conventional glass melt process involves very high temperatures, the sol-gel technology is preferred as it allows incorporating drugs into the glass while preserving the drug's functionality. To further control the release rate of drugs, BGs can be combined with chitosan, a biodegradable and biocompatible natural, nontoxic polymer used for drug delivery systems. Jia *et al.* [195] combined teicoplanin-loaded BBGs of the composition 54B<sub>2</sub>O<sub>3</sub>, 6Na<sub>2</sub>O, 8K<sub>2</sub>O, 22CaO, 8MgO, and 2P<sub>2</sub>O<sub>5</sub> in mol% with chitosan using the melt-derived method and measured the drug release over time using HPLC. A total of 78-83% drug release was observed. Once implanted the drug can take a few weeks to penetrate the surrounding tissue.

Table 2. A summary of reviewed literature on metal-ion doped borate-based bioactive glasses for biomedical applications.

Borate bioactive glass composition in mol%	Synthesis method	Metal dopant	Mechanism of action of the metal dopant	Form	Application	Ref.
(52B <sub>2</sub> O <sub>3</sub> , 12CaO, 6P <sub>2</sub> O <sub>5</sub> , 14Na <sub>2</sub> O, 16ZnO)	Melt-quenching	Ti (5-20%)	Stabilizes the BBG degradation rate	Scaffold	Cell adhesion and proliferation Degradation of scaffold	[202]
1. (52.6B <sub>2</sub> O <sub>3</sub> , 6Na <sub>2</sub> O, 12K <sub>2</sub> O MgO, 5CaO, 20P <sub>2</sub> O <sub>5</sub> ) 2. (6Na <sub>2</sub> O, 12 K <sub>2</sub> O, 5 MgO, 20 CaO, 4 P <sub>2</sub> O <sub>5</sub> , 53 B <sub>2</sub> O <sub>3</sub> )	Melt-quenching	1. Cu (4%)	Promotes bone formation	1. Scaffold	Healing chronic soft tissues wounds	[211]
2. Cu (0.4%)		Enhances osteogenesis and angiogenesis	2. Microfibers	[252]		
3. (6Na <sub>2</sub> O, 8K <sub>2</sub> O, 8MgO, 22CaO, 54B <sub>2</sub> O <sub>3</sub> , 2P <sub>2</sub> O <sub>5</sub> )		3. Cu (0.4%)	Induces dermal tissue regeneration	3. Microfiber	Healing full-thickness skin wounds	[28]
4. (6Na <sub>2</sub> O, 8K <sub>2</sub> O-8MgO, 22CaO, 18SiO <sub>2</sub> , 36B <sub>2</sub> O <sub>3</sub> , 2P <sub>2</sub> O <sub>5</sub> , 6SrO)		4. Cu (3%)		4. Fibers		[27]
1. (59.5B <sub>2</sub> O <sub>3</sub> , 2P <sub>2</sub> O <sub>5</sub> , 9.5CaO, 9CaF <sub>2</sub> , 20Na <sub>2</sub> O) 2. (6Na <sub>2</sub> O, 8K <sub>2</sub> O, 8MgO, 22CaO, 36B <sub>2</sub> O <sub>3</sub> , 18SiO <sub>2</sub> , 2P <sub>2</sub> O <sub>5</sub> )	Melt-quenching	1. Ag (0.25-0.75%) 2. Ag (0.05-1%)	Improves bioactivity	1. Powder 2. Scaffold	Bone regeneration	[201] [135]
1. (45B <sub>2</sub> O <sub>3</sub> , 24.5CaO, 24.5Na <sub>2</sub> O, 6P <sub>2</sub> O <sub>5</sub> ) 2. (56.6B <sub>2</sub> O <sub>3</sub> , 18.5CaO, 3.7P <sub>2</sub> O <sub>5</sub> , 5.5Na <sub>2</sub> O, 11.1K <sub>2</sub> O, 4.6 MgO)	Melt-quenching	1. Ce (2%) 2. Ce (5%)	Displays oxygen buffering capacity Promotes proliferation, differentiation and mineralization of osteoblasts	1. Powder 2. Scaffold	Bone regeneration	[168] [157]

Table 2. A summary of reviewed literature on metal-ion doped borate-based bioactive glasses for biomedical applications. (cont.)

(6.0 Na <sub>2</sub> O, 7.9 K <sub>2</sub> O, 7.7 MgO, 22.1 CaO, 54.6 B <sub>2</sub> O <sub>3</sub> , 1.7 P <sub>2</sub> O <sub>5</sub> )	Melt-quenching	Zn (3, and 6%)	Enhances haemostatic ability  Maintains cell wall stability, DNA, RNA and protein synthesis	Powder	Enhancing the viability of MG-63 osteoblast-like cells	[181]
1. (6.0 Na <sub>2</sub> O, 7.9 K <sub>2</sub> O, 7.7 MgO, 22.1 CaO, 4.6 B <sub>2</sub> O <sub>3</sub> , 1.7 P <sub>2</sub> O <sub>5</sub> )  2. (56.6B <sub>2</sub> O <sub>3</sub> , 18.5CaO, 3.7P <sub>2</sub> O <sub>5</sub> , 5.5Na <sub>2</sub> O, 11.1K <sub>2</sub> O, 4.6 MgO)	Melt-quenching	1. Ga (3, and 6%)  2. Ga (5%)	Promotes osteogenesis	1. Powder  2. Scaffold	Enhancing the viability of MG-63 osteoblast-like cells  Bone regeneration	[181]  [157]
(6Na <sub>2</sub> O, 8K <sub>2</sub> O, 8MgO, 22CaO, 54B <sub>2</sub> O <sub>3</sub> , 2P <sub>2</sub> O <sub>5</sub> )	Melt-quenching	Sr (9%)	Enhances the proliferation and differentiation of mesenchymal stem cells  Promotes the formation of extracellular matrix	Cement paste	Bone repair	[253]

## 6. CONCLUSION

BGs are widely studied for clinical applications. Among BGs, BBGs are preferred owing to their desirable properties and faster degradation rate. Furthermore, BBGs are promising biomaterials in medical applications and tissue engineering research due to their antibiofilm capabilities, high degradability, and regenerative potential. Bacterial biofilms pose a major burden in medicine; they display unique and complicated defense mechanisms that make them resistant to antimicrobial agents and a host's immune defenses. The potential use of BBGs in most biomedical applications lies in the glass's accelerated capability to convert into a HAP, promoting bone/tissue bonding. Despite their



intrinsic properties, BBGs can be specifically manufactured to have enhanced antibacterial and biomedical applications. A comprehensive review of studies indicates that metal-ion dopants vastly enhance the antimicrobial and biological functions of BBGs *in vivo* and *in vitro*. Besides metallic ions, the chemical composition, form, and particle size play a crucial role in the dissolution and functionalities of BBGs. The most common manufacturing method of metal-ion doped BBGs is melt-quenching; however, the sol-gel method could lead to better, controlled performance. Even though BBGs were discovered more than 20 years ago, they continue to spark research interests and are considered promising future biomaterials.

## REFERENCES

- [1] L. L. Hench, "The story of Bioglass," *J. Mater. Sci. Mater. Med.*, vol. 17, no. 11, pp. 967–978, 2006.
- [2] J. R. Jones, "Review of bioactive glass: from Hench to hybrids," *Acta Biomater.*, vol. 9, no. 1, pp. 4457–4486, 2013.
- [3] M. M. Pereira, A. E. Clark, and L. L. Hench, "Calcium phosphate formation on sol-gel-derived bioactive glasses *in vitro*," *J. Biomed. Mater. Res.*, vol. 28, no. 6, pp. 693–698, 1994.
- [4] J. A. Sanz-Herrera and A. R. Boccaccini, "Modelling bioactivity and degradation of bioactive glass-based tissue engineering scaffolds," *Int. J. Solids Struct.*, vol. 48, no. 2, pp. 257–268, 2011.
- [5] Q. Fu, M. N. Rahaman, H. Fu, and X. Liu, "Silicate, borosilicate, and borate bioactive glass scaffolds with controllable degradation rate for bone tissue engineering applications. I. Preparation and *in vitro* degradation," *J. Biomed. Mater. Res. A*, vol. 95, no. 1, pp. 164–171, 2010.

- [6] W. Huang, D. E. Day, K. Kittiratanapiboon, and M. N. Rahaman, "Kinetics and mechanisms of the conversion of silicate (45S5), borate, and borosilicate glasses to hydroxyapatite in dilute phosphate solutions," *J. Mater. Sci. Mater. Med.*, vol. 17, no. 7, pp. 583–596, 2006.
- [7] W. Huang, M. N. Rahaman, D. E. Day, and Y. Li, "Mechanisms for converting bioactive silicate, borate, and borosilicate glasses to hydroxyapatite in dilute phosphate solution," *Phys. Chem. Glasses Eur. J. Glass Sci. Technol. B*, vol. 47, no. 6, pp. 647–658, 2006.
- [8] W. Liang, M. N. Rahaman, D. E. Day, N. W. Marion, G. C. Riley, and J. J. Mao, "Bioactive borate glass scaffold for bone tissue engineering," *J. Non Cryst. Solids*, vol. 354, no. 15–16, pp. 1690–1696, 2008.
- [9] D. E. Day, J. E. White, R. F. Brown, and K. D. McMennamin, "Transformation of borate glasses into biologically useful materials," *Glass Technol.*, vol. 44, no. 2, pp. 75–81, 2003.
- [10] K. A. Cole, G. A. Funk, M. N. Rahaman, and T. E. McIff, "Mechanical and degradation properties of poly(methyl methacrylate) cement/borate bioactive glass composites," *J. Biomed. Mater. Res. B Appl. Biomater.*, vol. 108, no. 7, pp. 2765–2775, 2020.
- [11] K. A. Cole, G. A. Funk, M. N. Rahaman, and T. E. McIff, "Characterization of the conversion of bone cement and borate bioactive glass composites," *J. Biomed. Mater. Res. B Appl. Biomater.*, vol. 108, no. 4, pp. 1580–1591, 2020.
- [12] A. A. Gorustovich, T. Steimetz, F. H. Nielsen, and M. B. Guglielmotti, "A histomorphometric study of alveolar bone modelling and remodelling in mice fed a boron-deficient diet," *Arch. Oral Biol.*, vol. 53, no. 7, pp. 677–682, 2008.
- [13] Q. Yang, S. Chen, H. Shi, H. Xiao, and Y. Ma, "In vitro study of improved wound-healing effect of bioactive borate-based glass nano-/micro-fibers," *Mater. Sci. Eng. C Mater. Biol. Appl.*, vol. 55, pp. 105–117, 2015.
- [14] S. Kargozar, F. Baino, S. Hamzehlou, R. G. Hill, and M. Mozafari, "Bioactive glasses: Sprouting angiogenesis in tissue engineering," *Trends Biotechnol.*, vol. 36, no. 4, pp. 430–444, 2018.
- [15] M. B. Taye, "Biomedical applications of ion-doped bioactive glass: a review," *Appl. Nanosci.*, vol. 12, no. 12, pp. 3797–3812, 2022.
- [16] A. R. Zorzi and J. B. de Miranda, *Advanced techniques in bone regeneration*. London, England: InTech, 2016.

- [17] I. Cacciotti, “Bivalent cationic ions doped bioactive glasses: the influence of magnesium, zinc, strontium and copper on the physical and biological properties,” *J. Mater. Sci.*, vol. 52, no. 15, pp. 8812–8831, 2017.
- [18] H. Palza, B. Escobar, J. Bejarano, D. Bravo, M. Diaz-Dosque, and J. Perez, “Designing antimicrobial bioactive glass materials with embedded metal ions synthesized by the sol-gel method,” *Mater. Sci. Eng. C Mater. Biol. Appl.*, vol. 33, no. 7, pp. 3795–3801, 2013.
- [19] M. Ottomeyer, A. Mohammadkhan, D. Day, and D. Westenberg, “Broad-spectrum antibacterial characteristics of four novel borate-based bioactive glasses,” *Adv. Microbiol.*, vol. 06, no. 10, pp. 776–787, 2016.
- [20] S. Jung, T. Day, T. Boone, B. Buziak, and A. Omar, “Anti-biofilm activity of two novel, borate based, bioactive glass wound dressings,” *Biomed. Glasses*, vol. 5, no. 1, pp. 67–75, 2019.
- [21] K. Schuhladen, X. Wang, L. Hupa, and A. R. Boccaccini, “Dissolution of borate and borosilicate bioactive glasses and the influence of ion (Zn, Cu) doping in different solutions,” *J. Non Cryst. Solids*, vol. 502, pp. 22–34, 2018.
- [22] X. Qu, H. Yang, B. Jia, Z. Yu, Y. Zheng, and K. Dai, “Biodegradable Zn-Cu alloys show antibacterial activity against MRSA bone infection by inhibiting pathogen adhesion and biofilm formation,” *Acta Biomater.*, vol. 117, pp. 400–417, 2020.
- [23] C. Tao, “Antimicrobial activity and toxicity of gold nanoparticles: research progress, challenges and prospects,” *Lett. Appl. Microbiol.*, vol. 67, no. 6, pp. 537–543, 2018.
- [24] F. E. Ciraldo, E. Boccardi, V. Melli, F. Westhauser, and A. R. Boccaccini, “Tackling bioactive glass excessive in vitro bioreactivity: Preconditioning approaches for cell culture tests,” *Acta Biomater.*, vol. 75, pp. 3–10, 2018.
- [25] Y. Li, M. N. Rahaman, Q. Fu, B. S. Bal, A. Yao, and D. E. Day, “Conversion of bioactive borosilicate glass to multilayered hydroxyapatite in dilute phosphate solution,” *J. Am. Ceram. Soc.*, 2007.
- [26] F. Kermani *et al.*, “Modified sol-gel synthesis of mesoporous borate bioactive glasses for potential use in wound healing,” *Bioengineering (Basel)*, vol. 9, no. 9, p. 442, 2022.
- [27] H. Hu *et al.*, “Angiogenesis and full-thickness wound healing efficiency of a copper-doped borate bioactive glass/poly(lactic- co-glycolic acid) dressing loaded with vitamin E in vivo and in vitro,” *ACS Appl. Mater. Interfaces*, vol. 10, no. 27, pp. 22939–22950, 2018.

- [28] S. Zhao *et al.*, “Wound dressings composed of copper-doped borate bioactive glass microfibers stimulate angiogenesis and heal full-thickness skin defects in a rodent model,” *Biomaterials*, vol. 53, pp. 379–391, 2015.
- [29] O. D. Abodunrin, K. El Mabrouk, and M. Bricha, “A review on borate bioactive glasses (BBG): effect of doping elements, degradation, and applications,” *J. Mater. Chem. B Mater. Biol. Med.*, vol. 11, no. 5, pp. 955–973, 2023.
- [30] Y. Gu, W. Xiao, L. Lu, W. Huang, M. N. Rahaman, and D. Wang, “Kinetics and mechanisms of converting bioactive borate glasses to hydroxyapatite in aqueous phosphate solution,” *J. Mater. Sci.*, vol. 46, no. 1, pp. 47–54, 2011.
- [31] S. S. Hakki, B. S. Bozkurt, and E. E. Hakki, “Boron regulates mineralized tissue-associated proteins in osteoblasts (MC3T3-E1),” *J. Trace Elem. Med. Biol.*, vol. 24, no. 4, pp. 243–250, 2010.
- [32] Z. Xie, X. Liu, W. Jia, C. Zhang, W. Huang, and J. Wang, “Treatment of osteomyelitis and repair of bone defect by degradable bioactive borate glass releasing vancomycin,” *J. Control. Release*, vol. 139, no. 2, pp. 118–126, 2009.
- [33] L. Peddi, R. K. Brow, and R. F. Brown, “Bioactive borate glass coatings for titanium alloys,” *J. Mater. Sci. Mater. Med.*, vol. 19, no. 9, pp. 3145–3152, 2008.
- [34] H. Fu *et al.*, “In vitro evaluation of borate-based bioactive glass scaffolds prepared by a polymer foam replication method,” *Mater. Sci. Eng. C Mater. Biol. Appl.*, vol. 29, no. 7, pp. 2275–2281, 2009.
- [35] M. Franchini, G. Lusvardi, G. Malavasi, and L. Menabue, “Gallium-containing phospho-silicate glasses: synthesis and in vitro bioactivity,” *Mater. Sci. Eng. C Mater. Biol. Appl.*, vol. 32, no. 6, pp. 1401–1406, 2012.
- [36] N. W. Marion *et al.*, “Borate glass supports the in vitro osteogenic differentiation of human mesenchymal stem cells,” *Mech. Adv. Mater. Struct.*, vol. 12, no. 3, pp. 239–246, 2005.
- [37] A. R. Boccaccini, M. Erol, W. J. Stark, D. Mohn, Z. Hong, and J. F. Mano, “Polymer/bioactive glass nanocomposites for biomedical applications: A review,” *Compos. Sci. Technol.*, vol. 70, no. 13, pp. 1764–1776, 2010.
- [38] R. Li, A. E. Clark, and L. L. Hench, “An investigation of bioactive glass powders by sol-gel processing,” *J. Appl. Biomater.*, vol. 2, no. 4, pp. 231–239, Winter 1991.
- [39] F. Baino, S. Fiorilli, and C. Vitale-Brovarone, “Bioactive glass-based materials with hierarchical porosity for medical applications: Review of recent advances,” *Acta Biomater.*, vol. 42, pp. 18–32, 2016.

- [40] C. Wu and J. Chang, "Multifunctional mesoporous bioactive glasses for effective delivery of therapeutic ions and drug/growth factors," *J. Control. Release*, vol. 193, pp. 282–295, 2014.
- [41] K. Zheng and A. R. Boccaccini, "Sol-gel processing of bioactive glass nanoparticles: A review," *Adv. Colloid Interface Sci.*, vol. 249, pp. 363–373, 2017.
- [42] A. Lucas-Girot, F. Z. Mezahi, M. Mami, H. Oudadesse, A. Harabi, and M. Le Floch, "Sol-gel synthesis of a new composition of bioactive glass in the quaternary system  $\text{SiO}_2\text{-CaO-Na}_2\text{O-P}_2\text{O}_5$ ," *J. Non Cryst. Solids*, vol. 357, no. 18, pp. 3322–3327, 2011.
- [43] S. Plimpton, "Fast parallel algorithms for short-range molecular dynamics," *J. Comput. Phys.*, vol. 117, no. 1, pp. 1–19, 1995.
- [44] E. A. Abou Neel, D. M. Pickup, S. P. Valappil, R. J. Newport, and J. C. Knowles, "Bioactive functional materials: a perspective on phosphate-based glasses," *J. Mater. Chem.*, vol. 19, no. 6, pp. 690–701, 2009.
- [45] nS. B. Jung, "Treatment of non-healing diabetic venous stasis ulcers with bioactive glass nanofibers," vol. 19, MALDEN 02148, MA USA: WILEY-BLACKWELL, 2011.
- [46] M. Bortolin, E. De Vecchi, C. L. Romanò, M. Toscano, R. Mattina, and L. Drago, "Antibiofilm agents against MDR bacterial strains: is bioactive glass BAG-S53P4 also effective?," *J. Antimicrob. Chemother.*, vol. 71, no. 1, pp. 123–127, 2016.
- [47] D. C. Coraça-Huber, M. Fille, J. Hausdorfer, D. Putzer, and M. Nogler, "Efficacy of antibacterial bioactive glass S53P4 against *S. aureus* biofilms grown on titanium discs in vitro: BAG-S53P4 AGAINST BIOFILMS," *J. Orthop. Res.*, vol. 32, no. 1, pp. 175–177, 2014.
- [48] P. Balasubramanian, T. Büttner, V. Miguez Pacheco, and A. R. Boccaccini, "Boron-containing bioactive glasses in bone and soft tissue engineering," *J. Eur. Ceram. Soc.*, vol. 38, no. 3, pp. 855–869, 2018.
- [49] E. Mancuso, O. Bretcanu, M. Marshall, and K. W. Dalgarno, "Sensitivity of novel silicate and borate-based glass structures on in vitro bioactivity and degradation behaviour," *Ceram. Int.*, vol. 43, no. 15, pp. 12651–12657, 2017.
- [50] A. M. Abdelghany, "Novel method for early investigation of bioactivity in different borate bio-glasses," *Spectrochim. Acta A Mol. Biomol. Spectrosc.*, vol. 100, pp. 120–126, 2013.

- [51] M. Arango-Ospina, L. Hupa, and A. R. Boccaccini, “Bioactivity and dissolution behavior of boron-containing bioactive glasses under static and dynamic conditions in different media,” *Biomed. Glasses*, vol. 5, no. 1, pp. 124–139, 2019.
- [52] D. L. Wheeler, K. E. Stokes, R. G. Hoellrich, D. L. Chamberland, and S. W. McLoughlin, “Effect of bioactive glass particle size on osseous regeneration of cancellous defects,” *J. Biomed. Mater. Res.*, vol. 41, no. 4, pp. 527–533, 1998.
- [53] S. Kargozar, R. K. Singh, H.-W. Kim, and F. Baino, “‘Hard’ ceramics for ‘Soft’ tissue engineering: Paradox or opportunity?,” *Acta Biomater.*, vol. 115, pp. 1–28, 2020.
- [54] S. Banijamali, M. Heydari, and M. Mozafari, “Cellular response to bioactive glasses and glass–ceramics,” in *Handbook of Biomaterials Biocompatibility*, M. Mozafari, Ed. Elsevier, pp. 395–421, 2020.
- [55] S. B. Jung, “Bioactive Borate Glasses,” in *Bio-Glasses*, Chichester, UK: John Wiley & Sons, Ltd, pp. 75–95., 2012
- [56] D. G. Armstrong *et al.*, “A multi-centre, single-blinded randomised controlled clinical trial evaluating the effect of resorbable glass fibre matrix in the treatment of diabetic foot ulcers,” *Int. Wound J.*, vol. 19, no. 4, pp. 791–801, 2022.
- [57] D. W. Buck 2nd, “Innovative bioactive glass fiber technology accelerates wound healing and minimizes costs: A case series,” *Adv. Skin Wound Care*, vol. 33, no. 8, pp. 1–6, 2020.
- [58] M. Bengisu, “Borate glasses for scientific and industrial applications: a review,” *J. Mater. Sci.*, vol. 51, no. 5, pp. 2199–2242, 2016.
- [59] M. N. Rahaman *et al.*, “Bioactive glass in tissue engineering,” *Acta Biomater.*, vol. 7, no. 6, pp. 2355–2373, 2011.
- [60] Y. Lin, R. F. Brown, S. B. Jung, and D. E. Day, “Angiogenic effects of borate glass microfibers in a rodent model: Use of Bioactive Borate-Based Glass Microfibers for Angiogenesis,” *J. Biomed. Mater. Res. A*, vol. 102, no. 12, pp. 4491–4499, 2014.
- [61] P. Wray, “Wound healing: An update on Mo-Sci’s novel borate glass fibers,” *Am Ceram Bull*, vol. 92, pp. 30–35, 2013.
- [62] “Bioactive glass,” *Mo-Sci*, 17-Feb-2020. [Online]. Available: <https://mo-sci.com/products/bioactive-glass/>. [Accessed: 25-Feb-2023].
- [63] G. E. Merwin, “Bioglass middle ear prosthesis: preliminary report,” *Ann. Otol. Rhinol. Laryngol.*, vol. 95, no. 1 Pt 1, pp. 78–82, 1986.

- [64] F. Bahmad Jr and S. N. Merchant, "Histopathology of ossicular grafts and implants in chronic otitis media," *Ann. Otol. Rhinol. Laryngol.*, vol. 116, no. 3, pp. 181–191, 2007.
- [65] R. Reck, S. Störkel, and A. Meyer, "Bioactive glass-ceramics in middle ear surgery. An 8-year review," *Ann. N. Y. Acad. Sci.*, vol. 523, no. 1 Bioceramics, pp. 100–106, 1988.
- [66] I. Kinnunen, K. Aitasalo, M. Pöllönen, and M. Varpula, "Reconstruction of orbital floor fractures using bioactive glass," *J. Craniomaxillofac. Surg.*, vol. 28, no. 4, pp. 229–234, 2000.
- [67] B. Ilharreborde *et al.*, "Bioactive glass as a bone substitute for spinal fusion in adolescent idiopathic scoliosis: a comparative study with iliac crest autograft," *J. Pediatr. Orthop.*, vol. 28, no. 3, pp. 347–351, 2008.
- [68] E. S. Tadjoeidin, G. L. de Lange, D. M. Lyaruu, L. Kuiper, and E. H. Burger, "High concentrations of bioactive glass material (BioGran) vs. autogenous bone for sinus floor elevation," *Clin. Oral Implants Res.*, vol. 13, no. 4, pp. 428–436, 2002.
- [69] Q. Z. Chen, I. D. Thompson, and A. R. Boccaccini, "45S5 Bioglass-derived glass-ceramic scaffolds for bone tissue engineering," *Biomaterials*, vol. 27, no. 11, pp. 2414–2425, 2006.
- [70] R. Sergi, D. Bellucci, R. Salvatori, A. Anesi, and V. Cannillo, "A novel bioactive glass containing therapeutic ions with enhanced biocompatibility," *Materials (Basel)*, vol. 13, no. 20, p. 4600, 2020.
- [71] H. A. Khan, A. Ahmad, and R. Mehboob, "Nosocomial infections and their control strategies," *Asian Pac. J. Trop. Biomed.*, vol. 5, no. 7, pp. 509–514, 2015.
- [72] T. C. Horan, M. Andrus, and M. A. Dudeck, "CDC/NHSN surveillance definition of health care-associated infection and criteria for specific types of infections in the acute care setting," *Am. J. Infect. Control*, vol. 36, no. 5, pp. 309–332, 2008.
- [73] L. Drago, M. Toscano, and M. Bottagisio, "Recent evidence on bioactive glass antimicrobial and antibiofilm activity: A mini-review," *Materials (Basel)*, vol. 11, no. 2, p. 326, 2018.
- [74] C. Desrousseaux, V. Sautou, S. Descamps, and O. Traoré, "Modification of the surfaces of medical devices to prevent microbial adhesion and biofilm formation," *J. Hosp. Infect.*, vol. 85, no. 2, pp. 87–93, 2013.
- [75] I. Francolini and G. Donelli, "Prevention and control of biofilm-based medical-device-related infections," *FEMS Immunol. Med. Microbiol.*, vol. 59, no. 3, pp. 227–238, 2010.

- [76] P. S. Stewart and T. Bjarnsholt, "Risk factors for chronic biofilm-related infection associated with implanted medical devices," *Clin. Microbiol. Infect.*, vol. 26, no. 8, pp. 1034–1038, 2020.
- [77] S. A. Pullano *et al.*, "Medical devices for pediatric apnea monitoring and therapy: Past and new trends," *IEEE Rev. Biomed. Eng.*, vol. 10, pp. 199–212, 2017.
- [78] J. D. Bryers, "Medical biofilms," *Biotechnol. Bioeng.*, vol. 100, no. 1, pp. 1–18, 2008.
- [79] W. Zimmerli, "Clinical presentation and treatment of orthopaedic implant-associated infection," *J. Intern. Med.*, vol. 276, no. 2, pp. 111–119, 2014.
- [80] W. Zimmerli, A. Trampuz, and P. E. Ochsner, "Prosthetic-joint infections," *N. Engl. J. Med.*, vol. 351, no. 16, pp. 1645–1654, 2004.
- [81] D. Davies, "Understanding biofilm resistance to antibacterial agents," *Nat. Rev. Drug Discov.*, vol. 2, no. 2, pp. 114–122, 2003.
- [82] A. Dongari-Bagtzoglou, "Pathogenesis of mucosal biofilm infections: challenges and progress," *Expert Rev. Anti. Infect. Ther.*, vol. 6, no. 2, pp. 201–208, 2008.
- [83] M. E. Olson, H. Ceri, D. W. Morck, A. G. Buret, and R. R. Read, "Biofilm bacteria: formation and comparative susceptibility to antibiotics," *Can. J. Vet. Res.*, vol. 66, no. 2, pp. 86–92, 2002.
- [84] M. E. Davey and G. A. O'toole, "Microbial biofilms: from ecology to molecular genetics," *Microbiol. Mol. Biol. Rev.*, vol. 64, no. 4, pp. 847–867, 2000.
- [85] T. R. Garrett, M. Bhakoo, and Z. Zhang, "Bacterial adhesion and biofilms on surfaces," *Prog. Nat. Sci.*, vol. 18, no. 9, pp. 1049–1056, 2008.
- [86] K. Sauer *et al.*, "The biofilm life cycle: expanding the conceptual model of biofilm formation," *Nat. Rev. Microbiol.*, vol. 20, no. 10, pp. 608–620, 2022.
- [87] J. A. Johnson, "Nosocomial Infections," in *Critical Care*, 1st Edition., New York: Routledge, 2021, pp. 82–83.
- [88] P. S. Barie and S. R. Eachempati, "Surgical site infections," *Surg. Clin. North Am.*, vol. 85, no. 6, pp. 1115–35, viii–ix, 2005.
- [89] P. Wu and D. W. Grainger, "Drug/device combinations for local drug therapies and infection prophylaxis," *Biomaterials*, vol. 27, no. 11, pp. 2450–2467, 2006.
- [90] R. M. Donlan, "Biofilms: microbial life on surfaces," *Emerg. Infect. Dis.*, vol. 8, no. 9, pp. 881–890, 2002.



- [91] M. Esposito<sup>1</sup>, J. -Michaé, U. Lekholm<sup>3</sup>, and P. Thomsen<sup>1</sup>, “oral implants University, Goteborg, Sweden,” *Cloudfront.net*, 1998. [Online]. Accessed: 25-Feb-2023].
- [92] S. L. Percival, L. Suleman, C. Vuotto, and G. Donelli, “Healthcare-associated infections, medical devices and biofilms: risk, tolerance and control,” *J. Med. Microbiol.*, vol. 64, no. Pt 4, pp. 323–334, 2015.
- [93] J. M. Schierholz and J. Beuth, “Implant infections: a haven for opportunistic bacteria,” *J. Hosp. Infect.*, vol. 49, no. 2, pp. 87–93, 2001.
- [94] B. Vu, M. Chen, R. J. Crawford, and E. P. Ivanova, “Bacterial extracellular polysaccharides involved in biofilm formation,” *Molecules*, vol. 14, no. 7, pp. 2535–2554, 2009.
- [95] Z. Khatoun, C. D. McTiernan, E. J. Suuronen, T.-F. Mah, and E. I. Alarcon, “Bacterial biofilm formation on implantable devices and approaches to its treatment and prevention,” *Heliyon*, vol. 4, no. 12, p. e01067, 2018.
- [96] F. Song, H. Koo, and D. Ren, “Effects of material properties on bacterial adhesion and biofilm formation,” *J. Dent. Res.*, vol. 94, no. 8, pp. 1027–1034, 2015.
- [97] V. Carniello, B. W. Peterson, H. C. van der Mei, and H. J. Busscher, “Physico-chemistry from initial bacterial adhesion to surface-programmed biofilm growth,” *Adv. Colloid Interface Sci.*, vol. 261, pp. 1–14, 2018.
- [98] O. Ciofu, E. Rojo-Molinero, M. D. Macià, and A. Oliver, “Antibiotic treatment of biofilm infections,” *APMIS*, vol. 125, no. 4, pp. 304–319, 2017.
- [99] H. Wu, C. Moser, H.-Z. Wang, N. Høiby, and Z.-J. Song, “Strategies for combating bacterial biofilm infections,” *Int. J. Oral Sci.*, vol. 7, no. 1, pp. 1–7, 2015.
- [100] H. Cao and X. Liu, “Silver nanoparticles-modified films versus biomedical device-associated infections: Ag NPs-modified films versus BDIs,” *Wiley Interdiscip. Rev. Nanomed. Nanobiotechnol.*, vol. 2, no. 6, pp. 670–684, 2010.
- [101] M. Rizwan, R. Alias, U. Z. Zaidi, R. Mahmoodian, and M. Hamdi, “Surface modification of valve metals using plasma electrolytic oxidation for antibacterial applications: A review,” *J. Biomed. Mater. Res. A*, vol. 106, no. 2, pp. 590–605, 2017.
- [102] V. M. Schatkoski *et al.*, “Current advances concerning the most cited metal ions doped bioceramics and silicate-based bioactive glasses for bone tissue engineering,” *Ceram. Int.*, vol. 47, no. 3, pp. 2999–3012, 2021.

- [103] D. Westenberg, R. Viswanathan, D. L. Kadyk, S. Hibbs, J. Kopel, and D. Day, "Evaluation of three borate-bioactive glass compositions for antibacterial applications," *Adv. Microbiol.*, vol. 11, no. 11, pp. 646–656, 2021.
- [104] S. B. Levy, "Antibiotic and antiseptic resistance: impact on public health," *Pediatr. Infect. Dis. J.*, vol. 19, no. Supplement, pp. S120–S122, 2000.
- [105] A. Shander and H. L. Corwin, "A narrative review on hospital-acquired anemia: Keeping blood where it belongs," *Transfus. Med. Rev.*, vol. 34, no. 3, pp. 195–199, 2020.
- [106] R. J. Ferguson, A. Palmer Jr, A. Taylor, M. L. Porter, H. Malchau, and S. Glyn-Jones, "Hip replacement," *Lancet*, vol. 392, no. 10158, pp. 1662–1671, 2018.
- [107] M. N. Rahaman, B. S. Bal, and W. Huang, "Review: emerging developments in the use of bioactive glasses for treating infected prosthetic joints," *Mater. Sci. Eng. C Mater. Biol. Appl.*, vol. 41, pp. 224–231, 2014.
- [108] J. E. Phillips, T. P. Crane, M. Noy, T. S. J. Elliott, and R. J. Grimer, "The incidence of deep prosthetic infections in a specialist orthopaedic hospital: a 15-year prospective survey: A 15-YEAR PROSPECTIVE SURVEY," *J. Bone Joint Surg. Br.*, vol. 88, no. 7, pp. 943–948, 2006.
- [109] L. Hall-Stoodley *et al.*, "Towards diagnostic guidelines for biofilm-associated infections," *FEMS Immunol. Med. Microbiol.*, vol. 65, no. 2, pp. 127–145, 2012.
- [110] J.-H. Ch'ng, K. K. L. Chong, L. N. Lam, J. J. Wong, and K. A. Kline, "Biofilm-associated infection by enterococci," *Nat. Rev. Microbiol.*, vol. 17, no. 2, pp. 82–94, 2019.
- [111] P. Stoor, E. Sderling, and R. Grnman, "Bioactive glass S53P4 in repair of septal perforations and its interactions with the respiratory infection-associated microorganisms *Haemophilus influenzae* and *Streptococcus pneumoniae*," *J. Biomed. Mater. Res.*, vol. 58, no. 1, pp. 113–120, 2001.
- [112] O. Leppäranta *et al.*, "Antibacterial effect of bioactive glasses on clinically important anaerobic bacteria in vitro," *J. Mater. Sci. Mater. Med.*, vol. 19, no. 2, pp. 547–551, 2008.
- [113] L. Meseguer-Olmo *et al.*, "Biocompatibility and in vivo gentamicin release from bioactive sol-gel glass implants: Gentamicin Release in Sol-Gel Implants," *J. Biomed. Mater. Res.*, vol. 61, no. 3, pp. 458–465, 2002.
- [114] G. Kaur, O. P. Pandey, K. Singh, D. Homa, B. Scott, and G. Pickrell, "A review of bioactive glasses: Their structure, properties, fabrication and apatite formation," *J. Biomed. Mater. Res. A*, vol. 102, no. 1, pp. 254–274, 2014.

- [115] T. Mehrabi, A. S. Mesgar, and Z. Mohammadi, "Bioactive glasses: A promising therapeutic ion release strategy for enhancing wound healing," *ACS Biomater. Sci. Eng.*, vol. 6, no. 10, pp. 5399–5430, 2020.
- [116] H.-C. Flemming *et al.*, "Who put the film in a biofilm? The migration of a term from wastewater engineering to medicine and beyond," *NPJ Biofilms Microbiomes*, vol. 7, no. 1, p. 10, 2021.
- [117] A. Sirelkhatim *et al.*, "Review on zinc oxide nanoparticles: Antibacterial activity and toxicity mechanism," *Nanomicro Lett.*, vol. 7, no. 3, pp. 219–242, 2015.
- [118] M. Godoy-Gallardo *et al.*, "Antibacterial approaches in tissue engineering using metal ions and nanoparticles: From mechanisms to applications," *Bioact. Mater.*, vol. 6, no. 12, pp. 4470–4490, 2021.
- [119] L. Bergendi, L. Beneš, Z. Ďuračková, and M. Ferencik, "Chemistry, physiology and pathology of free radicals," *Life Sci.*, vol. 65, no. 18–19, pp. 1865–1874, 1999.
- [120] K. Nakai and D. Tsuruta, "What are reactive oxygen species, free radicals, and oxidative stress in skin diseases?," *Int. J. Mol. Sci.*, vol. 22, no. 19, p. 10799, 2021.
- [121] C. Hutchings, S. K. Rajasekharan, R. Reifen, and M. Shemesh, "Mitigating milk-associated bacteria through inducing zinc ions antibiofilm activity," *Foods*, vol. 9, no. 8, p. 1094, 2020.
- [122] C. Wu, J. Labrie, Y. D. N. Tremblay, D. Haine, M. Mourez, and M. Jacques, "Zinc as an agent for the prevention of biofilm formation by pathogenic bacteria," *J. Appl. Microbiol.*, vol. 115, no. 1, pp. 30–40, 2013.
- [123] S. Shruti *et al.*, "Curcumin release from cerium, gallium and zinc containing mesoporous bioactive glasses," *Microporous Mesoporous Mater.*, vol. 180, pp. 92–101, 2013.
- [124] J. Pasquet, Y. Chevalier, J. Pelletier, E. Couval, D. Bouvier, and M.-A. Bolzinger, "The contribution of zinc ions to the antimicrobial activity of zinc oxide," *Colloids Surf. A Physicochem. Eng. Asp.*, vol. 457, pp. 263–274, 2014.
- [125] T.-N. Phan, T. Buckner, J. Sheng, J. D. Baldeck, and R. E. Marquis, "Physiologic actions of zinc related to inhibition of acid and alkali production by oral streptococci in suspensions and biofilms," *Oral Microbiol. Immunol.*, vol. 19, no. 1, pp. 31–38, 2004.
- [126] A. Wajda, W. H. Goldmann, R. Detsch, A. R. Boccaccini, and M. Sitarz, "Influence of zinc ions on structure, bioactivity, biocompatibility and antibacterial potential of melt-derived and gel-derived glasses from CaO-SiO<sub>2</sub> system," *J. Non Cryst. Solids*, vol. 511, pp. 86–99, 2019.

- [127] M. Vincent, R. E. Duval, P. Hartemann, and M. Engels-Deutsch, "Contact killing and antimicrobial properties of copper," *J. Appl. Microbiol.*, vol. 124, no. 5, pp. 1032–1046, 2018.
- [128] S. Gomes *et al.*, "Cu-doping of calcium phosphate bioceramics: From mechanism to the control of cytotoxicity," *Acta Biomater.*, vol. 65, pp. 462–474, 2018.
- [129] M. S. Sbarra *et al.*, "The photodynamic effect of tetra-substituted N-methylpyridyl-porphine combined with the action of vancomycin or host defense mechanisms disrupts *Staphylococcus epidermidis* biofilms," *Int. J. Artif. Organs*, vol. 32, no. 9, pp. 574–583, 2009.
- [130] I. Atkinson, "Antibiofilm activity of biocide metal ions containing bioactive glasses (BGs): A mini review," *Bioengineering (Basel)*, vol. 9, no. 10, p. 489, 2022.
- [131] J. L. Clement and P. S. Jarrett, "ANTIBACTERIAL SILVER," *Hindawi.com*. [Online]. Available: <https://downloads.hindawi.com/archive/1994/707103.pdf>. [Accessed: 25-Feb-2023].
- [132] M. Rai, A. Yadav, and A. Gade, "Silver nanoparticles as a new generation of antimicrobials," *Biotechnol. Adv.*, vol. 27, no. 1, pp. 76–83, 2009.
- [133] S. Anees Ahmad *et al.*, "Bactericidal activity of silver nanoparticles: A mechanistic review," *Mater. Sci. Energy Technol.*, vol. 3, pp. 756–769, 2020.
- [134] S.-H. Luo *et al.*, "In vitro evaluation of cytotoxicity of silver-containing borate bioactive glass," *J. Biomed. Mater. Res. B Appl. Biomater.*, vol. 95, no. 2, pp. 441–448, 2010.
- [135] H. Wang *et al.*, "Evaluation of three-dimensional silver-doped borate bioactive glass scaffolds for bone repair: Biodegradability, biocompatibility, and antibacterial activity," *J. Mater. Res.*, vol. 30, no. 18, pp. 2722–2735, 2015.
- [136] P. J. Newby, R. El-Gendy, J. Kirkham, X. B. Yang, I. D. Thompson, and A. R. Boccaccini, "Ag-doped 45S5 Bioglass®-based bone scaffolds by molten salt ion exchange: processing and characterisation," *J. Mater. Sci. Mater. Med.*, vol. 22, no. 3, pp. 557–569, 2011.
- [137] M. A. Hollinger, "Toxicological aspects of topical silver pharmaceuticals," *Crit. Rev. Toxicol.*, vol. 26, no. 3, pp. 255–260, 1996.
- [138] K. Kawata, M. Osawa, and S. Okabe, "In vitro toxicity of silver nanoparticles at noncytotoxic doses to HepG2 human hepatoma cells," *Environ. Sci. Technol.*, vol. 43, no. 15, pp. 6046–6051, 2009.

- [139] M. Ahamed, M. S. Alsalihi, and M. K. J. Siddiqui, "Silver nanoparticle applications and human health," *Clin. Chim. Acta*, vol. 411, no. 23–24, pp. 1841–1848, 2010.
- [140] A. Trampuz and W. Zimmerli, "Diagnosis and treatment of infections associated with fracture-fixation devices," *Injury*, vol. 37 Suppl 2, no. 2, pp. S59–66, 2006.
- [141] R. O. Darouiche, "Treatment of infections associated with surgical implants," *N. Engl. J. Med.*, vol. 350, no. 14, pp. 1422–1429, 2004.
- [142] K. Mijndonckx, N. Leys, J. Mahillon, S. Silver, and R. Van Houdt, "Antimicrobial silver: uses, toxicity and potential for resistance," *Biometals*, vol. 26, no. 4, pp. 609–621, 2013.
- [143] S. Eckhardt, P. S. Brunetto, J. Gagnon, M. Priebe, B. Giese, and K. M. Fromm, "Nanobio silver: its interactions with peptides and bacteria, and its uses in medicine," *Chem. Rev.*, vol. 113, no. 7, pp. 4708–4754, 2013.
- [144] U. Klueh, V. Wagner, S. Kelly, A. Johnson, and J. D. Bryers, "Efficacy of silver-coated fabric to prevent bacterial colonization and subsequent device-based biofilm formation," *J. Biomed. Mater. Res.*, vol. 53, no. 6, pp. 621–631, 2000.
- [145] D. He, A. M. Jones, S. Garg, A. N. Pham, and T. D. Waite, "Silver Nanoparticle–Reactive oxygen species interactions: Application of a Charging–Discharging model," *J. Phys. Chem. C Nanomater. Interfaces*, vol. 115, no. 13, pp. 5461–5468, 2011.
- [146] Z. Kazemian, M. Varzandeh, and S. Labbaf, "A facile synthesis of mono dispersed spherical silver doped bioactive glass nanoparticle," *J. Mater. Sci. Mater. Med.*, vol. 32, no. 3, p. 29, 2021.
- [147] J. P. Ruparelia, A. K. Chatterjee, S. P. Duttagupta, and S. Mukherji, "Strain specificity in antimicrobial activity of silver and copper nanoparticles," *Acta Biomater.*, vol. 4, no. 3, pp. 707–716, 2008.
- [148] A. I. Mekkawy *et al.*, "In vitro and in vivo evaluation of biologically synthesized silver nanoparticles for topical applications: effect of surface coating and loading into hydrogels," *Int. J. Nanomedicine*, vol. 12, pp. 759–777, 2017.
- [149] J. da Silva Buriti *et al.*, "Synthesis and characterization of Ag-doped 45S5 bioglass and chitosan/45S5-Ag biocomposites for biomedical applications," *J. Therm. Anal. Calorim.*, vol. 145, no. 1, pp. 39–50, 2021.
- [150] H. N. Wilkinson, S. Iveson, P. Catherall, and M. J. Hardman, "A novel silver bioactive glass elicits antimicrobial efficacy against *Pseudomonas aeruginosa* and *Staphylococcus aureus* in an ex vivo skin wound biofilm model," *Front. Microbiol.*, vol. 9, p. 1450, 2018.

- [151] S. Naseri, G. Griffanti, W. C. Lepry, V. B. Maisuria, N. Tufenkji, and S. N. Nazhat, "Silver-doped sol-gel borate glasses: Dose-dependent effect on *Pseudomonas aeruginosa* biofilms and keratinocyte function," *J. Am. Ceram. Soc.*, vol. 105, no. 3, pp. 1711–1722, 2022.
- [152] J. Helmlinger *et al.*, "Silver nanoparticles with different size and shape: equal cytotoxicity, but different antibacterial effects," *RSC Adv.*, vol. 6, no. 22, pp. 18490–18501, 2016.
- [153] S. Grade, J. Eberhard, J. Jakobi, A. Winkel, M. Stiesch, and S. Barcikowski, "Alloying colloidal silver nanoparticles with gold disproportionally controls antibacterial and toxic effects," *Gold Bull.*, vol. 47, no. 1–2, pp. 83–93, 2014.
- [154] C. Wu *et al.*, "Copper-containing mesoporous bioactive glass scaffolds with multifunctional properties of angiogenesis capacity, osteostimulation and antibacterial activity," *Biomaterials*, vol. 34, no. 2, pp. 422–433, 2013.
- [155] D. A. Pelletier *et al.*, "Effects of engineered cerium oxide nanoparticles on bacterial growth and viability," *Appl. Environ. Microbiol.*, vol. 76, no. 24, pp. 7981–7989, 2010.
- [156] A. Thill *et al.*, "Cytotoxicity of CeO<sub>2</sub> nanoparticles for *Escherichia coli*. Physico-chemical insight of the cytotoxicity mechanism," *Environ. Sci. Technol.*, vol. 40, no. 19, pp. 6151–6156, 2006.
- [157] Y.-F. Goh, A. Z. Alshemary, M. Akram, M. R. Abdul Kadir, and R. Hussain, "In-vitro characterization of antibacterial bioactive glass containing ceria," *Ceram. Int.*, vol. 40, no. 1, pp. 729–737, 2014.
- [158] A. Łapa *et al.*, "Gallium- and cerium-doped phosphate glasses with antibacterial properties for medical applications," *Adv. Eng. Mater.*, vol. 22, no. 9, p. 1901577, 2020.
- [159] A. M. Deliormanlı, "Synthesis and characterization of cerium- and gallium-containing borate bioactive glass scaffolds for bone tissue engineering," *J. Mater. Sci. Mater. Med.*, vol. 26, no. 2, p. 67, 2015.
- [160] R. K. Matharu, Z. Charani, L. Ciric, U. E. Illangakoon, and M. Edirisinghe, "Antimicrobial activity of tellurium-loaded polymeric fiber meshes," *J. Appl. Polym. Sci.*, vol. 135, no. 25, p. 46368, 2018.
- [161] A. G. Morena, A. Bassegoda, J. Hoyo, and T. Tzanov, "Hybrid tellurium-lignin nanoparticles with enhanced antibacterial properties," *ACS Appl. Mater. Interfaces*, vol. 13, no. 13, pp. 14885–14893, 2021.

- [162] E. Zonaro, S. Lampis, R. J. Turner, S. J. S. Qazi, and G. Vallini, “Biogenic selenium and tellurium nanoparticles synthesized by environmental microbial isolates efficaciously inhibit bacterial planktonic cultures and biofilms,” *Front. Microbiol.*, vol. 6, p. 584, 2015.
- [163] D. E. Taylor, “Bacterial tellurite resistance,” *Trends Microbiol.*, vol. 7, no. 3, pp. 111–115, 1999.
- [164] R. J. Turner, R. Borghese, and D. Zannoni, “Microbial processing of tellurium as a tool in biotechnology,” *Biotechnol. Adv.*, vol. 30, no. 5, pp. 954–963, 2012.
- [165] F. Borsetti, F. Francia, R. J. Turner, and D. Zannoni, “The thiol:disulfide oxidoreductase DsbB mediates the oxidizing effects of the toxic metalloid tellurite (TeO<sub>3</sub><sup>2-</sup>) on the plasma membrane redox system of the facultative phototroph *Rhodobacter capsulatus*,” *J. Bacteriol.*, vol. 189, no. 3, pp. 851–859, 2007.
- [166] C. L. Zhong, B. Y. Qin, X. Y. Xie, and Y. Bai, “Antioxidant and antimicrobial activity of tellurium dioxide nanoparticles sols,” *J. Nano Res.*, vol. 25, pp. 8–15, 2013.
- [167] M. Miola, J. Massera, A. Cochis, A. Kumar, L. Rimondini, and E. Vernè, “Tellurium: A new active element for innovative multifunctional bioactive glasses,” *Mater. Sci. Eng. C Mater. Biol. Appl.*, vol. 123, no. 111957, p. 111957, 2021.
- [168] W. M. Abd-Allah and R. M. Fathy, “Gamma irradiation effectuality on the antibacterial and bioactivity behavior of multicomponent borate glasses against methicillin-resistant *Staphylococcus aureus* (MRSA),” *J. Biol. Inorg. Chem.*, vol. 27, no. 1, pp. 155–173, 2022.
- [169] C. Bonchi, F. Imperi, F. Minandri, P. Visca, and E. Frangipani, “Repurposing of gallium-based drugs for antibacterial therapy: Gallium-Based Antibacterials,” *Biofactors*, vol. 40, no. 3, pp. 303–312, 2014.
- [170] M. Frezza, C. Verani, D. Chen, and Q. P. Dou, “The therapeutic potential of gallium-based complexes in anti-tumor drug design,” *Lett. Drug Des. Discov.*, vol. 4, no. 5, pp. 311–317, 2007.
- [171] F. Minandri, C. Bonchi, E. Frangipani, F. Imperi, and P. Visca, “Promises and failures of gallium as an antibacterial agent,” *Future Microbiol.*, vol. 9, no. 3, pp. 379–397, 2014.
- [172] Y. Kaneko, M. Thoendel, O. Olakanmi, B. E. Britigan, and P. K. Singh, “The transition metal gallium disrupts *Pseudomonas aeruginosa* iron metabolism and has antimicrobial and antibiofilm activity,” *J. Clin. Invest.*, vol. 117, no. 4, pp. 877–888, 4 2007.

- [173] E. D. Weinberg, "Iron availability and infection," *Biochim. Biophys. Acta*, vol. 1790, no. 7, pp. 600–605, 2009.
- [174] M. Miethke and M. A. Marahiel, "Siderophore-based iron acquisition and pathogen control," *Microbiol. Mol. Biol. Rev.*, vol. 71, no. 3, pp. 413–451, 2007.
- [175] C. Wandersman and P. Delepelaire, "Bacterial iron sources: from siderophores to hemophores," *Annu. Rev. Microbiol.*, vol. 58, no. 1, pp. 611–647, 2004.
- [176] C. R. Chitambar and J. Narasimhan, "Targeting iron-dependent DNA synthesis with gallium and transferrin-gallium," *Pathobiology*, vol. 59, no. 1, pp. 3–10, 1991.
- [177] H. Takase, H. Nitani, K. Hoshino, and T. Otani, "Requirement of the *Pseudomonas aeruginosa* tonB gene for high-affinity iron acquisition and infection," *Infect. Immun.*, vol. 68, no. 8, pp. 4498–4504, 2000.
- [178] T. J. Brickman and S. K. Armstrong, "Impact of alcaligin siderophore utilization on in vivo growth of *Bordetella pertussis*," *Infect. Immun.*, vol. 75, no. 11, pp. 5305–5312, 2007.
- [179] R. M. Wells *et al.*, "Discovery of a siderophore export system essential for virulence of *Mycobacterium tuberculosis*," *PLoS Pathog.*, vol. 9, no. 1, p. e1003120, 2013.
- [180] P. Visca, C. Bonchi, F. Minandri, E. Frangipani, and F. Imperi, "The dual personality of iron chelators: growth inhibitors or promoters?," *Antimicrob. Agents Chemother.*, vol. 57, no. 5, pp. 2432–2433, 2013.
- [181] N. Mutlu *et al.*, "Effect of Zn and Ga doping on bioactivity, degradation, and antibacterial properties of borate 1393-B3 bioactive glass," *Ceram. Int.*, vol. 48, no. 11, pp. 16404–16417, 2022.
- [182] A. Rahimnejad Yazdi, L. Torkan, S. D. Waldman, and M. R. Towler, "Development of a novel bioactive glass suitable for osteosarcoma-related bone grafts," *J. Biomed. Mater. Res. B Appl. Biomater.*, vol. 106, no. 3, pp. 1186–1193, 2018.
- [183] A. Rahimnejad Yazdi, L. Torkan, W. Stone, and M. R. Towler, "The impact of gallium content on degradation, bioactivity, and antibacterial potency of zinc borate bioactive glass," *J. Biomed. Mater. Res. B Appl. Biomater.*, vol. 106, no. 1, pp. 367–376, 2018.
- [184] Z. Xu, X. Zhao, X. Chen, Z. Chen, and Z. Xia, "Antimicrobial effect of gallium nitrate against bacteria encountered in burn wound infections," *RSC Adv.*, vol. 7, no. 82, pp. 52266–52273, 2017.



- [185] H. Sinouh *et al.*, “Effect of TiO<sub>2</sub> and SrO additions on some physical properties of 33Na<sub>2</sub>O–xSrO–xTiO<sub>2</sub>–(50 – 2x)B<sub>2</sub>O<sub>3</sub>–17P<sub>2</sub>O<sub>5</sub> glasses,” *J. Therm. Anal. Calorim.*, vol. 111, no. 1, pp. 401–408, 2013.
- [186] H. B. Pan *et al.*, “Strontium borate glass: potential biomaterial for bone regeneration,” *J. R. Soc. Interface*, vol. 7, no. 48, pp. 1025–1031, 2010.
- [187] W. Fleischer and K. Reimer, “Povidone-iodine in antisepsis--state of the art,” *Dermatology*, vol. 195 Suppl 2, no. Suppl. 2, pp. 3–9, 1997.
- [188] M. S. Solbak, M. K. Henning, A. England, A. C. Martinsen, T. M. Aaløkken, and S. Johansen, “Impact of iodine concentration and scan parameters on image quality, contrast enhancement and radiation dose in thoracic CT,” *Eur. Radiol. Exp.*, vol. 4, no. 1, p. 57, 2020.
- [189] R. Brånemark, P. I. Brånemark, B. Rydevik, and R. R. Myers, “Osseointegration in skeletal reconstruction and rehabilitation: a review,” *J. Rehabil. Res. Dev.*, vol. 38, no. 2, pp. 175–181, 2001.
- [190] A. Chaudhari *et al.*, “Bone tissue response to porous and functionalized titanium and silica based coatings,” *PLoS One*, vol. 6, no. 9, p. e24186, 2011.
- [191] O. Rodriguez *et al.*, “Titanium addition influences antibacterial activity of bioactive glass coatings on metallic implants,” *Heliyon*, vol. 3, no. 10, p. e00420, 2017.
- [192] Z. R. Domingues *et al.*, “Bioactive glass as a drug delivery system of tetracycline and tetracycline associated with  $\beta$ -cyclodextrin,” *Biomaterials*, vol. 25, no. 2, pp. 327–333, 2004.
- [193] X. Cui *et al.*, “A novel injectable borate bioactive glass cement for local delivery of vancomycin to cure osteomyelitis and regenerate bone,” *J. Mater. Sci. Mater. Med.*, vol. 25, no. 3, pp. 733–745, 2014.
- [194] H. Ding *et al.*, “A novel injectable borate bioactive glass cement as an antibiotic delivery vehicle for treating osteomyelitis,” *PLoS One*, vol. 9, no. 1, p. e85472, 2014.
- [195] W.-T. Jia *et al.*, “Novel borate glass/chitosan composite as a delivery vehicle for teicoplanin in the treatment of chronic osteomyelitis,” *Acta Biomater.*, vol. 6, no. 3, pp. 812–819, 2010.
- [196] R. F. Brown *et al.*, “Effect of borate glass composition on its conversion to hydroxyapatite and on the proliferation of MC3T3-E1 cells,” *J. Biomed. Mater. Res. A*, vol. 88, no. 2, pp. 392–400, 2009.

- [197] K. Schuhladen, P. Mukoo, L. Liverani, Z. Neščáková, and A. R. Boccaccini, "Manuka honey and bioactive glass impart methylcellulose foams with antibacterial effects for wound-healing applications," *Biomed. Mater.*, vol. 15, no. 6, p. 065002, 2020.
- [198] M. Miola, A. Cochis, A. Kumar, C. R. Arciola, L. Rimondini, and E. Verné, "Copper-doped bioactive glass as filler for PMMA-based bone cements: Morphological, mechanical, reactivity, and preliminary antibacterial characterization," *Materials (Basel)*, vol. 11, no. 6, p. 961, 2018.
- [199] H. A. ElBatal *et al.*, "In vitro bioactivity behavior of some borophosphate glasses containing dopant of ZnO, CuO or SrO together with their glass-ceramic derivatives and their antimicrobial activity," *Silicon*, vol. 11, no. 1, pp. 197–208, 2019.
- [200] W. Xiao *et al.*, "Evaluation of Ti implants coated with Ag-containing borate bioactive glass for simultaneous eradication of infection and fracture fixation in a rabbit tibial model," *J. Mater. Res.*, vol. 27, no. 24, pp. 3147–3156, 2012.
- [201] L. C. A. da Silva *et al.*, "The role of Ag<sub>2</sub>O on antibacterial and bioactive properties of borate glasses," *J. Non Cryst. Solids*, vol. 554, no. 120611, p. 120611, 2021.
- [202] R. Shafaghi *et al.*, "In vitro evaluation of novel titania-containing borate bioactive glass scaffolds," *J. Biomed. Mater. Res. A*, vol. 109, no. 2, pp. 146–158, 2021.
- [203] C. K. Sen *et al.*, "Human skin wounds: a major and snowballing threat to public health and the economy," *Wound Repair Regen.*, vol. 17, no. 6, pp. 763–771, 2009.
- [204] J. S. Boateng, K. H. Matthews, H. N. E. Stevens, and G. M. Eccleston, "Wound healing dressings and drug delivery systems: a review," *J. Pharm. Sci.*, vol. 97, no. 8, pp. 2892–2923, 2008.
- [205] A. Grandjean-Laquerriere *et al.*, "Influence of the zinc concentration of sol-gel derived zinc substituted hydroxyapatite on cytokine production by human monocytes in vitro," *Biomaterials*, vol. 27, no. 17, pp. 3195–3200, 2006.
- [206] H.-W. Kim, H.-E. Kim, and J. C. Knowles, "Production and potential of bioactive glass nanofibers as a next-generation biomaterial," *Adv. Funct. Mater.*, vol. 16, no. 12, pp. 1529–1535, 2006.
- [207] W. Xia, D. Zhang, and J. Chang, "Fabrication and in vitro biomineralization of bioactive glass (BG) nanofibres," *Nanotechnology*, vol. 18, no. 13, p. 135601, 2007.

- [208] X. Liu, M. N. Rahaman, and D. E. Day, "Conversion of melt-derived microfibrillar borate (13-93B3) and silicate (45S5) bioactive glass in a simulated body fluid," *J. Mater. Sci. Mater. Med.*, vol. 24, no. 3, pp. 583–595, 2013.
- [209] U. A. Okonkwo and L. A. DiPietro, "Diabetes and wound angiogenesis," *Int. J. Mol. Sci.*, vol. 18, no. 7, p. 1419, 2017.
- [210] S. Kaya, M. Cresswell, and A. R. Boccaccini, "Mesoporous silica-based bioactive glasses for antibiotic-free antibacterial applications," *Mater. Sci. Eng. C Mater. Biol. Appl.*, vol. 83, pp. 99–107, 2018.
- [211] L. Bi *et al.*, "Effect of bioactive borate glass microstructure on bone regeneration, angiogenesis, and hydroxyapatite conversion in a rat calvarial defect model," *Acta Biomater.*, vol. 9, no. 8, pp. 8015–8026, 2013.
- [212] J. Zhou *et al.*, "In vivo and in vitro studies of borate based glass micro-fibers for dermal repairing," *Mater. Sci. Eng. C Mater. Biol. Appl.*, vol. 60, pp. 437–445, 2016.
- [213] K. Schuhladen, L. Stich, J. Schmidt, A. Steinkasserer, A. R. Boccaccini, and E. Zinser, "Cu, Zn doped borate bioactive glasses: antibacterial efficacy and dose-dependent in vitro modulation of murine dendritic cells," *Biomater. Sci.*, vol. 8, no. 8, pp. 2143–2155, 2020.
- [214] S. Chen *et al.*, "In vitro stimulation of vascular endothelial growth factor by borate-based glass fibers under dynamic flow conditions," *Mater. Sci. Eng. C Mater. Biol. Appl.*, vol. 73, pp. 447–455, 2017.
- [215] A. S. Brydone, D. Meek, and S. Maclaine, "Bone grafting, orthopaedic biomaterials, and the clinical need for bone engineering," *Proc. Inst. Mech. Eng. H*, vol. 224, no. 12, pp. 1329–1343, 2010.
- [216] M. Kellomäki, H. Niiranen, K. Puumanen, N. Ashammakhi, T. Waris, and P. Törmälä, "Bioabsorbable scaffolds for guided bone regeneration and generation," *Biomaterials*, vol. 21, no. 24, pp. 2495–2505, 2000.
- [217] R. J. O'Keefe and J. Mao, "Bone tissue engineering and regeneration: from discovery to the clinic--an overview," *Tissue Eng. Part B Rev.*, vol. 17, no. 6, pp. 389–392, 2011.
- [218] J. S. Cho and Y. C. Kang, "Synthesis of spherical shape borate-based bioactive glass powders prepared by ultrasonic spray pyrolysis," *Ceram. Int.*, vol. 35, no. 6, pp. 2103–2109, 2009.

- [219] A. Yao, D. Wang, W. Huang, Q. Fu, M. N. Rahaman, and D. E. Day, "In vitro bioactive characteristics of borate-based glasses with controllable degradation behavior," *J. Am. Ceram. Soc.*, vol. 90, no. 1, pp. 303–306, 2007.
- [220] W. C. Lepry, S. Naseri, and S. N. Nazhat, "Effect of processing parameters on textural and bioactive properties of sol–gel-derived borate glasses," *J. Mater. Sci.*, vol. 52, no. 15, pp. 8973–8985, 2017.
- [221] M. Turk and A. M. Deliormanlı, "Electrically conductive borate-based bioactive glass scaffolds for bone tissue engineering applications," *J. Biomater. Appl.*, vol. 32, no. 1, pp. 28–39, 2017.
- [222] Y. Gu, W. Huang, M. N. Rahaman, and D. E. Day, "Bone regeneration in rat calvarial defects implanted with fibrous scaffolds composed of a mixture of silicate and borate bioactive glasses," *Acta Biomater.*, vol. 9, no. 11, pp. 9126–9136, 2013.
- [223] W. Jia *et al.*, "Glass-activated regeneration of volumetric muscle loss," *Acta Biomater.*, vol. 103, pp. 306–317, 2020.
- [224] J. K. Leach, D. Kaigler, Z. Wang, P. H. Krebsbach, and D. J. Mooney, "Coating of VEGF-releasing scaffolds with bioactive glass for angiogenesis and bone regeneration," *Biomaterials*, vol. 27, no. 17, pp. 3249–3255, 2006.
- [225] W. C. Lepry and S. N. Nazhat, "Highly bioactive sol-gel-derived borate glasses," *Chem. Mater.*, vol. 27, no. 13, pp. 4821–4831, 2015.
- [226] N. J. Thyparambil, L. C. Gutgesell, C. C. Hurley, L. E. Flowers, D. E. Day, and J. A. Semon, "Adult stem cell response to doped bioactive borate glass," *J. Mater. Sci. Mater. Med.*, vol. 31, no. 2, p. 13, 2020.
- [227] S. Sengupta, M. Michalek, L. Liverani, P. Švančárek, A. R. Boccaccini, and D. Galusek, "Preparation and characterization of sintered bioactive borate glass tape," *Mater. Lett.*, vol. 282, no. 128843, p. 128843, 2021.
- [228] X. Liu *et al.*, "Bioactive borate glass scaffolds: in vitro and in vivo evaluation for use as a drug delivery system in the treatment of bone infection," *J. Mater. Sci. Mater. Med.*, vol. 21, no. 2, pp. 575–582, 2010.
- [229] A. M. Deliormanlı, "Size-dependent degradation and bioactivity of borate bioactive glass," *Ceram. Int.*, vol. 39, no. 7, pp. 8087–8095, 2013.
- [230] K. Zhang, H. Yan, D. C. Bell, A. Stein, and L. F. Francis, "Effects of materials parameters on mineralization and degradation of sol-gel bioactive glasses with 3D-ordered macroporous structures," *J. Biomed. Mater. Res. A*, vol. 66, no. 4, pp. 860–869, 2003.

- [231] W.-T. Jia, Q. Fu, W.-H. Huang, C.-Q. Zhang, and M. N. Rahaman, "Comparison of borate bioactive glass and calcium sulfate as implants for the local delivery of teicoplanin in the treatment of methicillin-resistant *Staphylococcus aureus*-induced osteomyelitis in a rabbit model," *Antimicrob. Agents Chemother.*, vol. 59, no. 12, pp. 7571–7580, 2015.
- [232] N. C. Lindfors *et al.*, "Bioactive glass S53P4 as bone graft substitute in treatment of osteomyelitis," *Bone*, vol. 47, no. 2, pp. 212–218, 2010.
- [233] N. Emanuel, Y. Rosenfeld, O. Cohen, Y. H. Applbaum, D. Segal, and Y. Barenholz, "A lipid-and-polymer-based novel local drug delivery system--BonyPid™: from physicochemical aspects to therapy of bacterially infected bones," *J. Control. Release*, vol. 160, no. 2, pp. 353–361, 2012.
- [234] O. S. Kluin, H. C. van der Mei, H. J. Busscher, and D. Neut, "Biodegradable vs non-biodegradable antibiotic delivery devices in the treatment of osteomyelitis," *Expert Opin. Drug Deliv.*, vol. 10, no. 3, pp. 341–351, 2013.
- [235] T. Hui *et al.*, "Treatment of osteomyelitis by liposomal gentamicin-impregnated calcium sulfate," *Arch. Orthop. Trauma Surg.*, vol. 129, no. 10, pp. 1301–1308, 2009.
- [236] K. Kanellakopoulou *et al.*, "Treatment of experimental osteomyelitis caused by methicillin-resistant *Staphylococcus aureus* with a synthetic carrier of calcium sulphate (Stimulan®) releasing moxifloxacin," *Int. J. Antimicrob. Agents*, vol. 33, no. 4, pp. 354–359, 2009.
- [237] W.-T. Jia, S.-H. Luo, C.-Q. Zhang, and J.-Q. Wang, "In vitro and in vivo efficacies of teicoplanin-loaded calcium sulfate for treatment of chronic methicillin-resistant *Staphylococcus aureus* osteomyelitis," *Antimicrob. Agents Chemother.*, vol. 54, no. 1, pp. 170–176, 2010.
- [238] J. Ning *et al.*, "Synthesis and in vitro bioactivity of a borate-based bioglass," *Mater. Lett.*, vol. 61, no. 30, pp. 5223–5226, 2007.
- [239] X. Zhang *et al.*, "Teicoplanin-loaded borate bioactive glass implants for treating chronic bone infection in a rabbit tibia osteomyelitis model," *Biomaterials*, vol. 31, no. 22, pp. 5865–5874, 2010.
- [240] Z. Xie, X. Cui, C. Zhao, W. Huang, J. Wang, and C. Zhang, "Gentamicin-loaded borate bioactive glass eradicates osteomyelitis due to *Escherichia coli* in a rabbit model," *Antimicrob. Agents Chemother.*, vol. 57, no. 7, pp. 3293–3298, 2013.
- [241] L. L. Hench, "Bioactive materials: the potential for tissue regeneration," *J. Biomed. Mater. Res.*, vol. 41, no. 4, pp. 511–518, 1998.

- [242] S. Das *et al.*, “The induction of angiogenesis by cerium oxide nanoparticles through the modulation of oxygen in intracellular environments,” *Biomaterials*, vol. 33, no. 31, pp. 7746–7755, 2012.
- [243] A. R. Boccaccini, D. S. Brauer, and L. Hupa, *Bioactive glasses: Fundamentals, technology and applications*. Cambridge, England: Royal Society of Chemistry, 2016.
- [244] V. Mouriño, J. P. Cattalini, and A. R. Boccaccini, “Metallic ions as therapeutic agents in tissue engineering scaffolds: an overview of their biological applications and strategies for new developments,” *J. R. Soc. Interface*, vol. 9, no. 68, pp. 401–419, 2012.
- [245] F. Baino, G. Novajra, V. Miguez-Pacheco, A. R. Boccaccini, and C. Vitale-Brovarone, “Bioactive glasses: Special applications outside the skeletal system,” *J. Non Cryst. Solids*, vol. 432, pp. 15–30, 2016.
- [246] B. Gupta, J. B. Papke, A. Mohammadkhah, D. E. Day, and A. B. Harkins, “Effects of chemically doped bioactive borate glass on neuron regrowth and regeneration,” *Ann. Biomed. Eng.*, vol. 44, no. 12, pp. 3468–3477, 2016.
- [247] L. M. Marquardt, D. Day, S. E. Sakiyama-Elbert, and A. B. Harkins, “Effects of borate-based bioactive glass on neuron viability and neurite extension: Borate-based Bioactive Glass,” *J. Biomed. Mater. Res. A*, vol. 102, no. 8, pp. 2767–2775, 2014.
- [248] M. Monsigny, A.-C. Roche, P. Midoux, and R. Mayer, “Glycoconjugates as carriers for specific delivery of therapeutic drugs and genes,” *Adv. Drug Deliv. Rev.*, vol. 14, no. 1, pp. 1–24, 1994.
- [249] T. M. Allen and P. R. Cullis, “Drug delivery systems: entering the mainstream,” *Science*, vol. 303, no. 5665, pp. 1818–1822, 2004.
- [250] H. Tölli, S. Kujala, K. Levonen, T. Jämsä, and P. Jalovaara, “Bioglass as a carrier for reindeer bone protein extract in the healing of rat femur defect,” *J. Mater. Sci. Mater. Med.*, vol. 21, no. 5, pp. 1677–1684, 2010.
- [251] D. W. Hutmacher, “Scaffolds in tissue engineering bone and cartilage,” *Biomaterials*, vol. 21, no. 24, pp. 2529–2543, 2000.
- [252] X. Liu, M. N. Rahaman, and D. E. Day, “In vitro degradation and conversion of melt-derived microfibrinous borate (13-93B3) bioactive glass doped with metal ions,” *J. Am. Ceram. Soc.*, vol. 97, no. 11, pp. 3501–3509, 2014.

- [253] Y. Zhang *et al.*, “Evaluation of injectable strontium-containing borate bioactive glass cement with enhanced osteogenic capacity in a critical-sized rabbit femoral condyle defect model,” *ACS Appl. Mater. Interfaces*, vol. 7, no. 4, pp. 2393–2403, 2015.

## II. THE ANTIBACTERIAL PROPERTIES OF FOUR BIOACTIVE CHRONIC WOUND REPAIR COMPOSITIONS

Sarah Fakher and David Westenberg

### ABSTRACT

Chronic wound infections are not only a prevalent medical issue but also a multifaceted problem that significantly impacts healthcare systems worldwide. Biofilms formed by pathogenic bacteria are fundamental virulence factors implicated in the complexity and persistence of bacterial-associated wound infections, leading to prolonged recovery times and increased risk of infection. This study aims to investigate the antibacterial effectiveness of commonly employed bioactive wound healing compositions with a particular emphasis on their action against common bacterial pathogens implicated in chronic wound infections to identify optimal wound product compositions. The three bacterial species, *Staphylococcus epidermidis*, *Escherichia coli*, and *Pseudomonas aeruginosa*, were examined in this study as they are grounded in their clinical relevance and the different challenges they present in the treatment of wound infections. The antibiofilm effectiveness differed extensively among the biomaterials tested and slightly among the bacterial species. Particularly, copper and zinc doped borate bioactive glass wound products inhibited three clinically relevant bacteria in both planktonic and biofilm forms. Ion release profiles demonstrated a linear correlation between the metal ions and the antibiofilm effectiveness of the materials.



## 1. INTRODUCTION

Wound infections remain a significant concern within clinical practice, affecting a substantial patient population and posing serious health risks. Chronic wounds, such as diabetic ulcers, venous leg ulcers, and pressure ulcers, are particularly susceptible to infection due to the compromised nature of the affected tissue (1). About 2.5% of people in the US and 6.5 million people worldwide are affected by chronic wounds, and a huge amount of money is spent annually on chronic wound treatment-associated medical costs—more than \$25 billion are spent annually in the US, leading to extensive healthcare resource utilization and a considerable economic burden (2, 3). Endogenous and exogenous infections caused by pathogenic bacteria cause wounds to stagnate and become chronic, leading to severe consequences (4). Several clinical treatments such as systematic antibiotics, ointments, and surgical debridement do not effectively alter the microenvironment of chronic wounds (5, 6). To manage chronic wounds, numerous attempts have been made, particularly developing bioactive materials with specialized bio-functional properties such as promoting dermal repair, releasing cytokines and growth factors, and promoting angiogenesis (7, 8). Because bacterial infections contribute to a significant number of chronic wounds, strategic approaches are needed to identify potent versatile antibacterial biomaterials.

The pathophysiology of wound infections is complex, with bacterial biofilms playing a critical role (9). Bacteria within biofilms can be up to 1,000 times more resistant to antibiotics compared to their planktonic forms. Biofilms are structured communities of bacteria that are adherent to a surface and embedded within a self-

produced extracellular polymeric substance (EPS), which protects the bacteria from environmental stressors, including the host's immune response and antibiotic treatments (10). It is estimated that biofilms are responsible for over 60% of microbial infections in the body, with their presence in wounds significantly impairing healing and increasing the risk of chronic infection (11, 12). Conventional wound care practices, including the use of systemic antibiotics, do not address biofilm-associated infections, leading to a cycle of chronic inflammation, tissue destruction, and delayed wound healing (13, 14). Furthermore, the horizontal gene transfer among biofilm communities contributes to the rapid spread of antibiotic resistance, complicating treatment protocols (15).

Strategies for treating chronic wound infections include debridement for removing necrotic tissues and bacteria; however, bacterial regrowth occurs due to insufficient bacterial elimination (16). Other strategies include systemic antibiotics and wound dressings, which yield poor clinical outcomes (17). A variety of wound care products are available commercially, ranging from traditional dressings to advanced bioactive materials. These include alginate dressings, hydrocolloids, foam dressings, antimicrobial dressings containing silver or iodine, and growth factor-based therapies. While these products aim to manage wound exudate, maintain a moist wound environment, and prevent infection, their efficacy varies, and few are effective against biofilms (18, 19). Most wound repair bioactive materials are primarily synthesized to promote the cellular and extracellular wound environment, overlooking microbial inhibition which is essential for proper wound healing. For optimal, accelerated wound healing, a balance between biological enhancement and antibacterial effectiveness is needed.

*S. epidermidis*, *E. coli*, and *P. aeruginosa* were selected for this study due to their distinct physiological characteristics and their notable roles in wound infections (20). *S. epidermidis* is a gram-positive bacterium that is part of the normal skin flora but can become opportunistic in the context of implanted medical devices. It is known for its ability to form robust biofilms on surfaces, which is a major virulence factor contributing to its pathogenicity in wound infections (21). *S. epidermidis* is implicated in over 70% of prosthetic infections due to its biofilm-forming capabilities (22). *E. coli*, a gram-negative bacterium, is commonly found in the intestinal flora but can be pathogenic when introduced to extraintestinal sites such as open wounds. It has been associated with a range of infections and is notorious for its rapid rate of antibiotic resistance acquisition (23). *P. aeruginosa*, another gram-negative bacterium, is inherently resistant to many antibiotics and disinfectants, making it a formidable pathogen in the context of chronic wounds (24). It is capable of surviving in a wide range of environments and is particularly known for its chronic infections in cystic fibrosis patients and its ability to form biofilms, which are highly resistant to phagocytosis and antibiotics. *P. aeruginosa* is found in approximately 20% of chronic wound infections and has been associated with increased morbidity and mortality (25).

Data on the prevalence of these bacteria in wound infections highlight the urgent need for effective treatments. By investigating the efficacy of four different wound-healing bioactive compositions against these diverse bacteria, the study aims to address a broad spectrum of biofilm-related issues in wound care. Most biomaterials are specifically synthesized to display potent biological functionalities and biocompatibility in terms of molecular and biochemical capabilities. Given the increasing number of

wound-healing bioactive materials that primarily focus on promoting skin repair, it is critical to identify optimal biomaterials.

This study tested four bioactive wound repair compositions: (1) a collagen matrix biomaterial sourced from bovine and is primarily used for treating chronic wounds with varying degrees of exudate (2) a multi-layered synthetic polymeric matrix that incorporates minimal quantities of metallic and ionic silver designed for wound care management (3) a borate bioactive glass wound matrix with a porous fiber and microsphere architecture (4) a borate bioactive glass fiber matrix enhanced with copper and zinc.

Collagen-based matrices play a pivotal role in wound healing due to their ability to mimic the body's natural extracellular matrix, thereby promoting tissue regeneration and repair. However, these natural collagen scaffolds can be susceptible to rapid degradation within the wound environment. This is often attributed to elevated levels of proteases, such as matrix metalloproteinases (MMPs), which are frequently overexpressed in chronic, non-healing wounds (26). As these collagen matrices break down, they can hinder cellular infiltration and differentiation, crucial steps in the healing process. Moreover, the incorporation of silver into these synthetic collagen matrices has been shown to enhance their therapeutic potential (27). Silver possesses broad-spectrum antimicrobial properties and can be integrated into the matrix to help prevent bacterial colonization and infection, which are common complications in wound management. However, to mitigate the cytotoxicity of silver, it is critical to control its release from the collagen matrix (28). The inherent properties of collagen to the rapid release of the metal

ions, resulting in a short-term therapeutic ion concentration needed for sustained antibacterial activity.

Natural polymer-based wound dressings, with their inherent biological compatibility and structural resemblance to the ECM, hold significant promise for three-dimensional scaffolding in advanced wound dressing applications. These organic polymers, synthesized by various organisms, include both proteins and carbohydrates, and they are biodegradable and biocompatible due to their hydrophilic nature (29, 30). However, one of the primary challenges with natural polymers is the variability in their properties, which can fluctuate based on the biological source and various environmental factors. Besides, these materials can be prone to microbial contamination (31, 32).

To address several limitations in wound healing, borate bioactive glasses (BBGs), in particular, have gained considerable attention owing to their therapeutic wound-healing potential through maintaining cell activity and angiogenesis. Furthermore, enhanced BBGs release ions that can disrupt bacterial cell membranes, interfere with DNA replication, and promote angiogenesis and fibroblast proliferation, all of which are beneficial for wound healing (33, 34). As BBGs contact an aqueous environment, they undergo a series of chemical transformations to form a hydroxyapatite (HAP) layer within some hours depending on the dissolution medium. HAP formation is the critical mechanism for the development of a chemical bond between the biomaterial and tissue, or bone-tissue bonding. It has been demonstrated that BBG ion disintegration induces gene expression related to cell differentiation and proliferation as well as displays antibacterial properties. Moreover, the higher degradation rate of BBGs enhances their biocompatibility and biomedical applications, and their chemical flexibility renders them

potential for metal doping to further promote their biological performance and antimicrobial properties (33).

## 2. RESULTS

### 2.1. ANTIBACTERIAL EFFECTIVENES

Microlyte yielded a slight 2.5 log reduction in *S. epidermidis*, whereas Puracol Plus and Mirragen demonstrated lower efficacy with 2 and 1 log reductions, respectively, suggesting a lower capacity to disrupt the biofilm integrity or to penetrate the bacterial cell wall of *S. epidermidis*. A bactericidal effect of a 6-log reduction was achieved by the GL1605 (Figure 2A). *E. coli* showed a slightly higher susceptibility to Microlyte and Puracol Plus achieving a 4 and 4.5 log reduction, respectively, while Mirragen displayed a reduced 3 log reduction. *E. coli* was not detected after 9 hours of contact with the GL1605 (Figure 2B). A 3-log reduction was observed with Microlyte, 3.5 log reduction with Puracol Plus, and a 2-log reduction with Mirragen was observed for *P. aeruginosa* (Figure 2C). However, complete inhibition of *P. aeruginosa* was achieved by GL1605 after 24 hours (Figure 2C). The enhanced performance of GL1605 across all tested bacterial species highlights its potential for broad-spectrum antibacterial applications, particularly multi-drug resistant bacteria in wound infections.

### 2.2. TIME-COURSE STUDY

Similar results were observed in *S. epidermidis* and *E. coli*. Microlyte and Mirragen achieved a small reduction in bacterial count after 9 hours (Figure 3A). Puracol Plus was

slightly more effective, reducing the bacterial presence to a greater extent. GL1605 achieved a more potent bactericidal effect within the same timeframe. Both Microlyte and Mirragen showed moderate antibacterial activity against *E. coli*, and Puracol Plus exhibited a slightly higher reduction. However, GL1605 displayed a bactericidal effect after only 6 hours (Figure 3B). Microlyte and Mirragen exhibited a bacteriostatic effect in *P. aeruginosa* during the first 6 hours and increased after 9 hours (Figure 3C). Puracol Plus displayed an enhanced antibacterial effect, with a significant decrease in bacterial counts after 9 hours. Notably, GL1605 demonstrated superior antibacterial properties, with a marked bacterial reduction within 6 hours (Figure 3C). These findings suggest that while all tested materials possess some degree of antibacterial activity, there is a clear gradation in their action. GL1605 exhibited a rapid and pronounced bactericidal effect against all tested bacterial species, suggesting its potential advantage in wound healing.

### **2.3. BIOFILM EFFECTIVENESS**

The efficacy of different wound care materials against bacterial biofilms was evaluated at two time points: 24 and 48 hours of biomaterial contact. *S. epidermidis* biofilms demonstrated a limited reduction of less than a 1-log decrease in contact with Puracol Plus and Mirragen for 24 hours (Figure 4A). Microlyte showed a moderate reduction capability with approximately a 1-log reduction at 24 hours, which increased marginally by an additional 0.5 log by 48 hours. In stark contrast, GL1605 exhibited a substantial biofilm reduction of 4 logs at the 24-hour interval, progressing to complete biofilm eradication at 48 hours (Figure 4A). Both Microlyte and Mirragen initially did

not demonstrate a significant reduction in *E. coli* biofilms. However, a slight increase in biofilm reduction was observed after 48 hours (Figure 4B). Puracol Plus exhibited a more

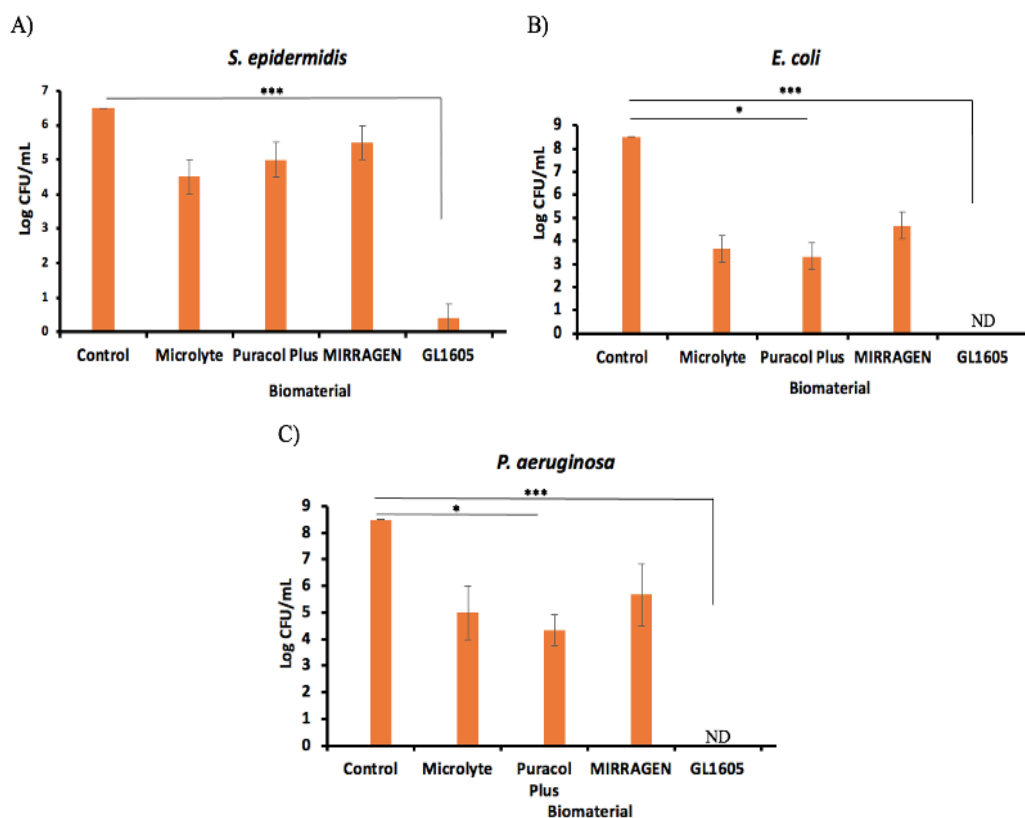


Figure 1. Antibacterial effectiveness of the biomaterials after 24 hours of contact with the bacterial species.

pronounced antibiofilm effect with a 2-log reduction after 48 hours. GL1605 showed a potent antibiofilm effect, achieving a remarkable 5-log reduction within 24 hours and complete biofilm elimination after 48 hours (Figure 4B). In contact with *P. aeruginosa*, Microlyte, Puracol Plus, and Mirragen initially had a negligible impact on biofilm



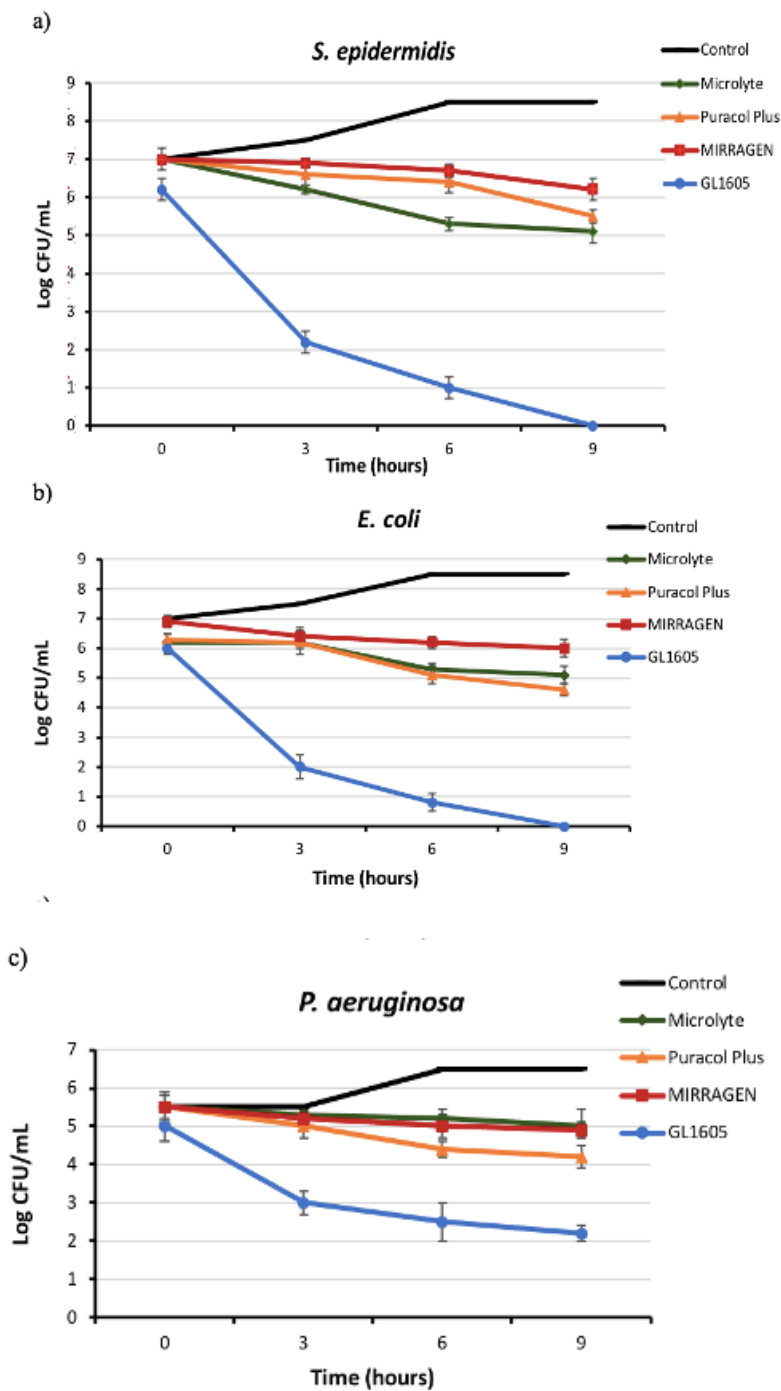


Figure 2. Time course study of the antibacterial effectiveness of the biomaterials.

reduction at 24 hours (Figure 4C). After 48 hours, Puracol Plus demonstrated a slight increase in biofilm reduction efficiency.

Whereas the GL1605 significantly reduced the *P. aeruginosa* biofilms. These results demonstrate the variable efficacy of different wound care compositions in disrupting biofilms. The potent antibiofilm activity of GL1605 among all tested bacterial species is indicative of its advanced therapeutic formulation, which appears to facilitate effective penetration and disruption of the biofilms' ECM.

#### **2.4. ELEMENT RELEASE**

The rate of ion release is a critical factor in determining the antimicrobial activity of the material. In Microlyte and Puracol Plus, the concentration of silver released over the four days was not high. Mirragen exhibited a progressive release of boron over four days. However, the antibiofilm activity observed was minimal, which indicates that boron displays minimal antibacterial properties. In contrast, the GL1605 samples demonstrated a more promising result, with both copper and zinc ions showing a higher release on day 2 which was sustained over the subsequent four days. The GL1605 also inhibited biofilms after 2 days of contact, suggesting a direct relationship between the ion release rates and antibiofilm activity. The correlation between the biofilm reduction and the metal-ion release concentration from the biomaterials is shown in Figure 5. The observed data demonstrates a clear linear correlation between biofilm log reduction and the corresponding release of antimicrobial elements, indicating that the efficacy of biofilm inhibitions is directly proportional to the concentration of active elements present. In the case of boron, the data indicates a subdued response, as only a marginal increase in log reduction was recorded.

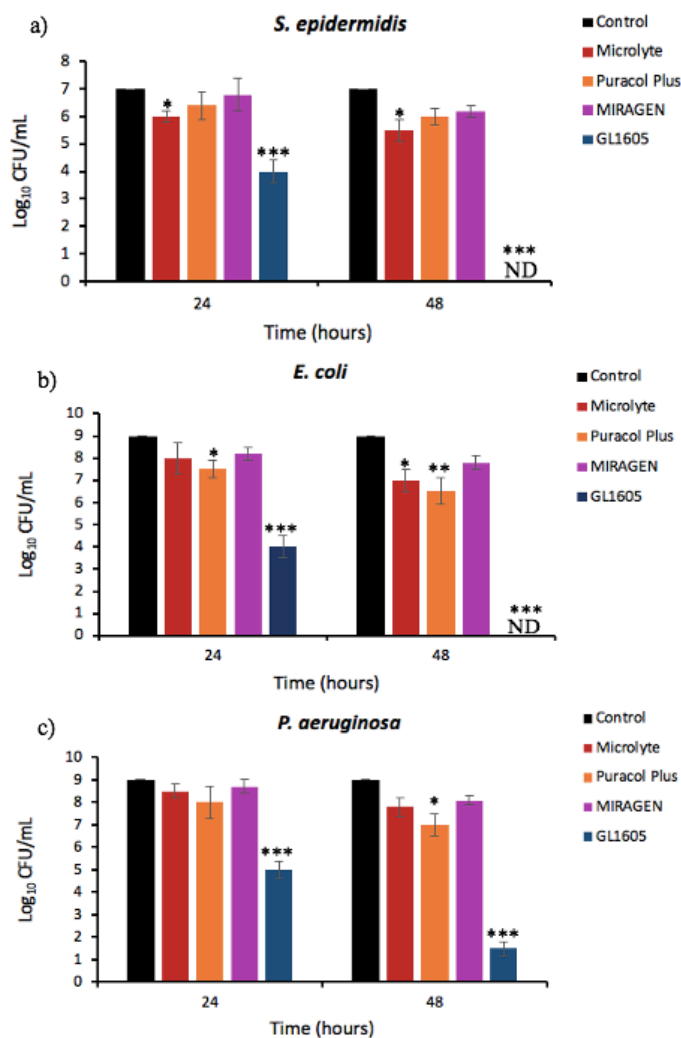


Figure 3. Antibiofilm effectiveness of the biomaterials after 24 and 48 hours of contact.

This suggests that while boron possesses some antibiofilm properties, its efficacy may be limited, requiring higher concentrations or synergistic combinations with other agents to achieve significant biofilm control. Silver resulted in more pronounced antibiofilm activity, achieving up to 2 log reductions. Silver's well-documented antimicrobial properties are reflected in this level of efficacy, which is likely attributed to its ability to disrupt microbial cell walls and potent anti biofilm activities.

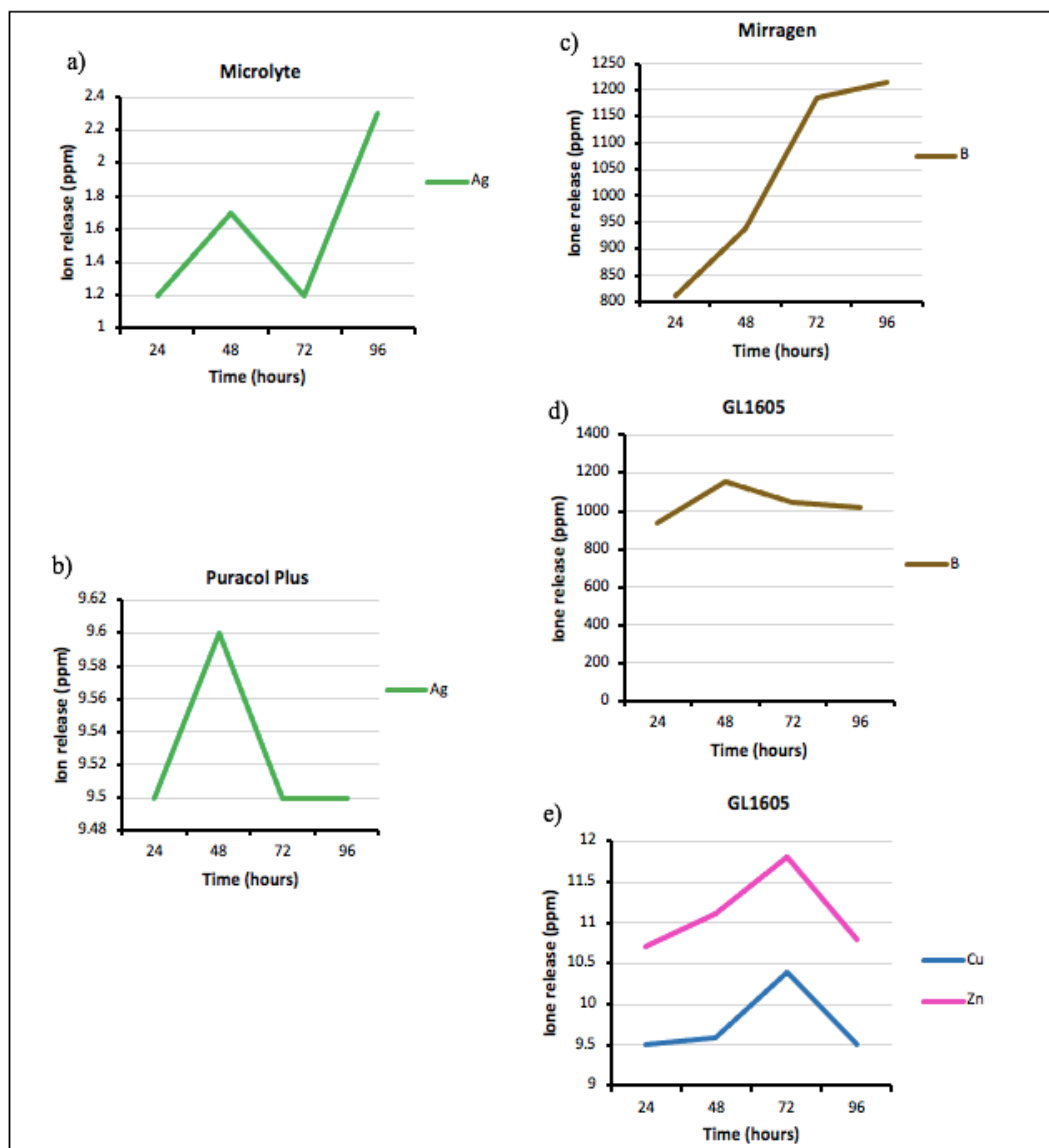


Figure 4. Element release profile from the biomaterials over four days

Copper exhibited slightly superior antibacterial effectiveness compared to zinc. This finding is consistent with the known oligodynamic effect of copper, which has a broad spectrum of antimicrobial action, including the disruption of bacterial cell membranes, denaturation of proteins, and interference with metabolic processes interfere with DNA replication. However, it's important to note that using silver as an antimicrobial is

balanced by concerns over toxicity and the potential for resistance if used indiscriminately.

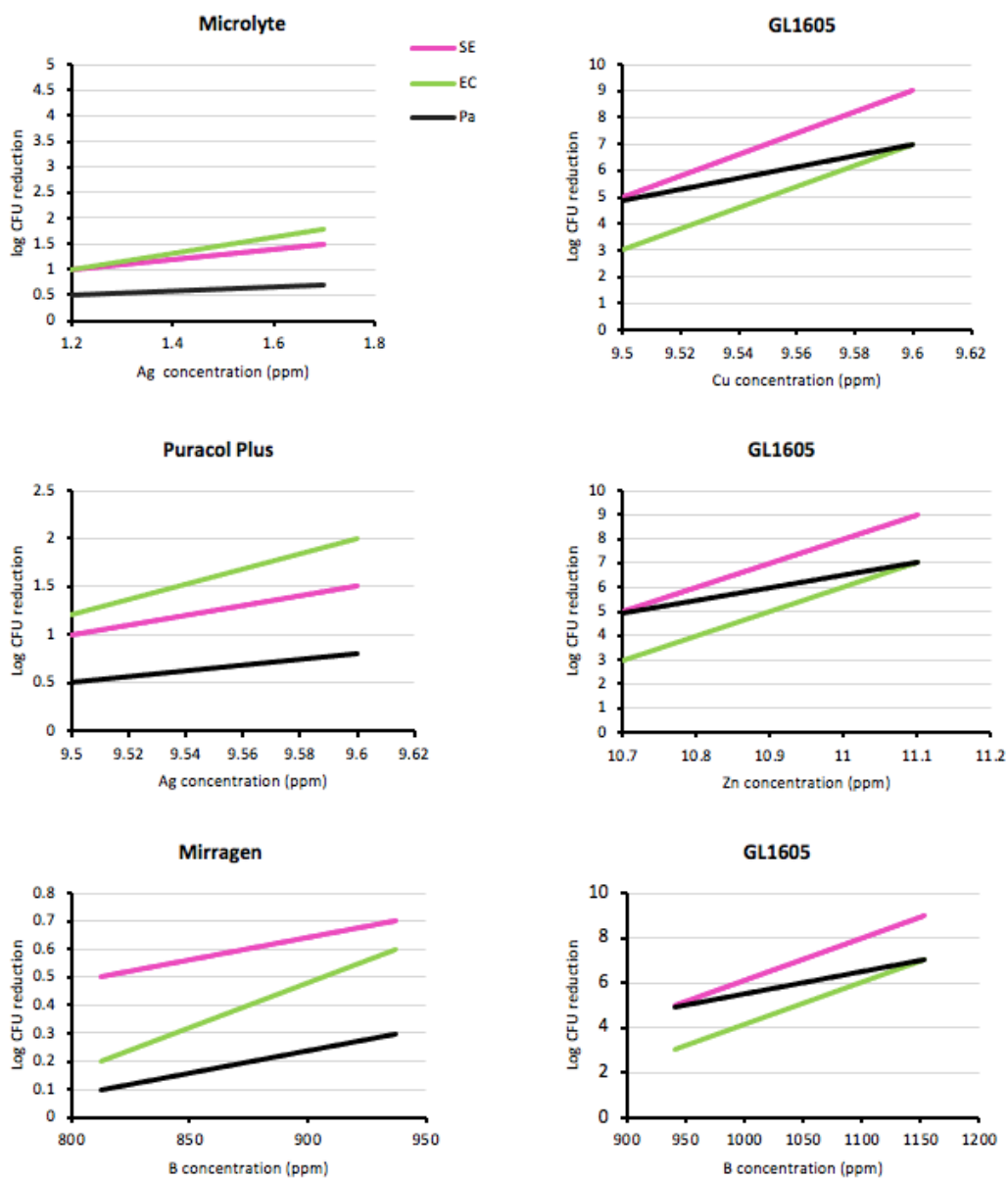


Figure 5. Correlation Between Element-Induced Biofilm Log Reduction and Element Release. This graph displays the varying antibiofilm efficacies of boron, silver, copper, and zinc.

Copper and zinc resulted in higher log reductions, pointing to their strong antibacterial properties.

### 3. DISCUSSION

Wound healing is a dynamic process comprising four interrelated phases. During the initial phase, immediate post-injury, the body's hemostatic response triggers an accumulation of platelets and inflammatory cells that adhere to the ECM collagen. This results in the release of clotting factors, such as fibronectin, which facilitate blood clotting and vasoconstriction to prevent further bleeding. The second phase, the inflammatory stage, follows right after injury, spanning from 24 hours to around 4 to 6 days. It involves the formation of a fibrin clot and the activation of the complement system, leading to the migration of neutrophils due to vasodilation. This phase is crucial for clearing the wound bed of debris and preventing infection (35). However, bacterial infections are common during this stage and can significantly hinder the healing process (Fig.4). These infections can disrupt the normal immune response and delay healing by continuing inflammation, damaging tissues, and impairing the function of fibroblasts and myofibroblasts vital for tissue repair (36, 37).

The proliferation phase, the third stage, begins 2 to 3 days post-injury and lasts until the wound is closed. This stage is characterized by epithelialization, the formation of new granulation tissue, and the development of a new ECM. Fibroblast proliferation and collagen deposition are key activities during this period. Finally, the remodeling stage completes the healing process by regenerating and maturing the wound area. The ECM transforms, with collagen type III being replaced by type I, enhancing the tensile

strength of the newly formed tissue. Infections can severely impair this remodeling process by causing persistent inflammation, leading to scar formation and weakening the structural integrity of the healed skin (35, 38).

The implications of *S. epidermidis*, *E. coli*, and *P. aeruginosa* in wound infections and chronic wounds are significant (39). *S. epidermidis* biofilms are problematic in surgical wounds and can lead to systemic infections if not properly managed. *E. coli*, can cause severe problems when wound contamination occurs, particularly in abdominal surgeries. Its biofilms can exacerbate infections, especially in immunocompromised patients, leading to persistent inflammation and delayed wound healing. *P. aeruginosa* is one of the most common pathogens found in chronic wound infections, particularly in burns and diabetic foot ulcers. Its biofilms protect it from hostile environments and treatments, often leading to chronic infections that are difficult to eradicate and frequently recur, contributing to prolonged hospital stays and increased medical costs.

The comparative analysis of the antibacterial efficacy of wound care products against *S. epidermidis*, *E. coli*, and *P. aeruginosa* provides crucial insights into their clinical relevance. The 24-hour contact study revealed differential effectiveness among the products, with varying degrees of bacterial reduction. Notably, the antibacterial potency varied not only among the different products but also with the bacterial species, reflecting the complex interplay between the antimicrobial agents in the wound care products and the diverse defense mechanisms employed by each type of bacteria.

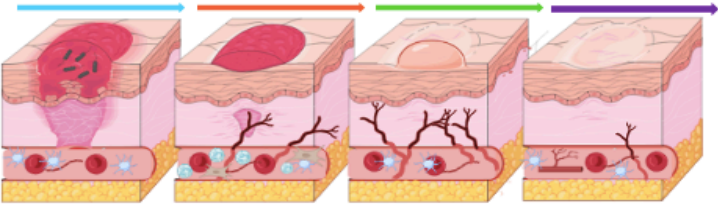
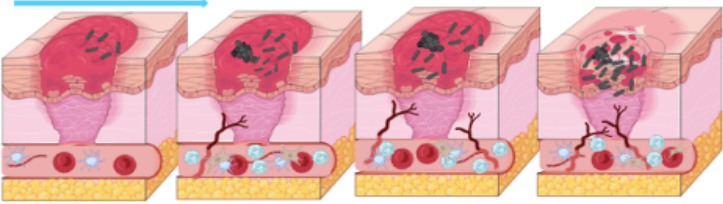
Normal wound healing				
Wound healing stages	<p><b>Homeostasis</b></p> <p>The healing process is immediately initiated with vasoconstriction, platelet aggregation, and clot formation, with platelets releasing growth factors.</p>	<p><b>Inflammation</b></p> <p>The inflammatory phase peaks within 24-48 hours, and usually subsides by 3-4 days. White blood cells clear contaminants, setting the stage for new tissue development.</p>	<p><b>Proliferation</b></p> <p>The proliferation phase typically starts around day 3 or 4 and can continue for 2-3 weeks. This phase is characterized by re-epithelialization, angiogenesis, granulation tissue formation, and collagen deposition. Vascular supply is restored and new tissue forms.</p>	<p><b>Remodeling</b></p> <p>Remodeling can begin around week 3. The wound matures as collagen is remodeled, increasing the wound's tensile strength. Cellular activity decreases, and the extracellular matrix is refined and organized. The repaired tissue eventually reaches approximately 80% of its original tensile strength, with the formation of a scar being the final outcome.</p>
Chronic (Infected) wound healing				
Wound healing stages	<p><b>Homeostasis</b></p> <p>Homeostasis is delayed due to ongoing inflammation and infection. As a result, clot formation is unstable, causing continuous exudation and impaired provisional matrix.</p>	<p><b>Inflammation</b></p> <p>The inflammatory phase can last from weeks to months. Elevated levels of white blood cells and ROS contribute to ongoing tissue destruction, inhibiting the proliferation phase, and the healing process.</p>	<p><b>Proliferation</b></p> <p>The proliferation phase is significantly delayed in chronic wounds. The ongoing inflammation and infection prevent the progression to or completion of the proliferation phase. Cells involved in this phase are often dysfunctional, leading to insufficient granulation tissue and angiogenesis, which results in poor wound fill and lack of structural integrity of the new tissue.</p>	<p><b>Remodeling</b></p> <p>Chronic wounds rarely achieve effective remodeling, structural and functional integrity of the skin is compromised, resulting in a high risk of wound recurrence and often leading to a non-healing state.</p>

Figure 6. Schematic of the four stages of normal and chronically infected wound healing process. Wound healing is a complex process that consists of four distinct overlapping stages: homeostasis, inflammation, proliferation, and remodeling. Chronic infected wounds do not go through the wound-healing stages to heal completely.

The differential effectiveness observed can be attributed to several factors, including the unique biofilm-forming capabilities inherent to each bacterial species, which can impede the penetration and activity of antimicrobial agents. For instance, *S. epidermidis* is known for its robust biofilm production, while gram-negative *E. coli* and *P. aeruginosa* have



different cell wall structures and metabolic pathways that may influence their susceptibility to certain antibacterial agents.

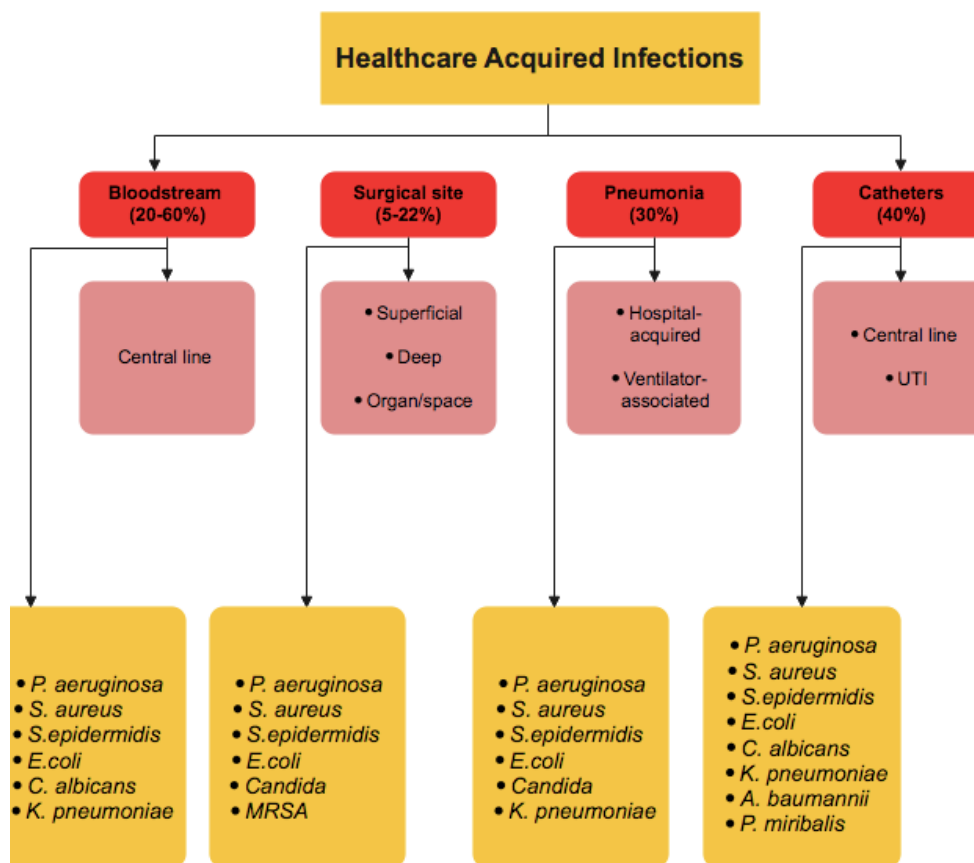


Figure 7. Prevalence of Common Healthcare-Acquired Infections. This chart illustrates the percentage distribution of the most frequently encountered infections in healthcare settings, highlighting the proportional impact of each infection type on patient health.

The GL1605 demonstrated a potent inhibitory effect across all bacterial strains, suggesting its broad-spectrum antibacterial capability. The bactericidal activity of this product, as opposed to the bacteriostatic effect displayed by the other biomaterials, may

have significant clinical implications, especially in the treatment of severe or recalcitrant infections where complete eradication of bacteria is critical.

To discern the kinetics of these antibacterial effects, a time-course study was performed, measuring the antibacterial activity at 3-hour intervals up to 9 hours. This dynamic assessment aimed to identify which materials exerted the most rapid antibacterial action. The observed trends suggest that the Microlyte, Puracol Plus, and Mirragen exhibited a gradual onset of antibacterial activity, which could align with the slower bacterial disruption integrity or delayed interaction with bacterial cell walls. The GL1605, however, displayed more rapid and pronounced antibacterial properties, achieving a substantial effect within the initial hours of contact, which is particularly relevant in a clinical context where the early suppression of bacterial growth can be critical in preventing the establishment of infection and promoting a favorable healing environment. Such efficacy might be attributed to the copper and zinc dopants in the glass which can disrupt bacterial homeostasis more efficiently.

In the context of the study, the findings elucidate distinct antibacterial profiles for each of the wound care compositions tested. Microlyte began to exhibit antibacterial properties incrementally over the observation period. This could suggest its utility in clinical scenarios where a gradual release of antimicrobial agents is preferable, perhaps in the management of chronic wounds where prolonged exposure to antimicrobials is necessary to maintain a clean wound bed and prevent colonization. Some clinical trials indicated that Microlyte showed effective antibacterial properties after 3 days, indicating its potential for preventing infections from occurring (40). Mirragen, on the other hand, also showed a progressive antibacterial action, albeit to a different extent. The

characteristics of Mirragen could make it suitable for applications where wound care requires a delicate balance between managing bacterial load and promoting tissue regeneration. This is particularly pertinent in wounds where tissue growth is the priority.

Puracol Plus demonstrated a somewhat more pronounced antibacterial effect within the same timeframe. Its efficacy profile indicates a potential for use in a broader range of wound care scenarios, including those where more immediate microbial control is needed to prevent infection or in the early stages of wound healing when the risk of infection is highest. On the other hand, GL1605's performance was noted for its rapid onset of antibacterial activity. This suggests that GL1605 could be instrumental in acute care settings or the initial treatment of highly contaminated wounds. Its rapid action could help to quickly reduce bacterial colonization, preventing the establishment of biofilms. The porosity of Puracol Plus was assessed by a previous study, and SEM images revealed that it has very high porosity, which is essential for cell adhesion and wound healing, however, the study indicated that the antibacterial effectiveness of this biomaterial could be promoted by enhancing it with antimicrobial peptides (41). Another study noted that the slow antibacterial effectiveness of the Puracol can be ascribed to its dense structure which has a low bacterial penetration capacity (42).

Each material's temporal pattern of antibacterial activity emphasizes the importance of tailored wound care strategies. The choice of a wound care product may thus be heavily influenced by the specific needs of the wound environment, the stage of wound healing, and the nature of the bacteria present. This study's insights into the varied antibacterial kinetics of these materials underscore the need for personalized wound care regimens and may inform future product development and clinical practice. Further

investigation into the specific mechanisms by which these materials exert their antibacterial effects would likely yield valuable information for optimizing wound care management.

The study's findings on the antibiofilm effectiveness of the wound care materials provide important insights for the discussion of chronic wound management. The ability of these materials to disrupt and reduce biofilms of *S. epidermidis*, *E. coli*, and *P. aeruginosa* was assessed at 24 and 48 hours of contact to reflect their potential use in clinical settings. Microlyte, Puracol Plus, and Mirragen compositions showed a limited capacity to reduce the biofilm densities, particularly against *S. epidermidis* and *E. coli*. This could suggest that while they may possess antimicrobial properties, their formulation may not be optimized for penetrating the extracellular matrix of biofilms. This is a critical consideration, as biofilms present a substantial barrier to wound healing due to their complex structure and resistance to penetration by antimicrobial agents. *P. aeruginosa*, known for its robust biofilm-forming ability and intrinsic resistance, these materials exhibited a low antibiofilm effectiveness. The initial ineffectiveness of Microlyte, Puracol Plus, and Mirragen to significantly disrupt biofilms of *P. aeruginosa* suggests that their mode of action may not be adequately equipped to tackle this resilient pathogen. However, an increase in antibiofilm activity over time with Puracol Plus indicates some potential for managing biofilms in extended-care settings. GL1605, in contrast, exhibited a notable ability to reduce all biofilms. The material's performance against biofilms suggests a formulation that is potentially more potent in its action, which can be particularly beneficial in acute or severe infections where rapid biofilm disruption is essential.

The superior performance of GL1605 can be attributed to the presence of copper and zinc dopants, which are well-documented for their antimicrobial properties. Copper ions are known to disrupt bacterial cell walls and interfere with intracellular enzymes, leading to increased oxidative stress within bacterial cells. Zinc also plays a multifaceted role in antimicrobial activity, including the disruption of membrane integrity and the inhibition of bacterial growth and metabolism. A study performed by Jung et al. observed the bactericidal effects of the GL1605 in inhibiting biofilms after 48 hours compared to Mirragen which was mostly effective in reducing only the planktonic bacteria (43).

The efficacy of Puracol Plus, which also showed commendable antibacterial activity, can be associated with its silver content. Silver ions have a broad-spectrum antimicrobial effect that is well-established in the literature, functioning through multiple pathways such as binding to bacterial DNA, RNA, and proteins, thereby inhibiting bacterial replication and function. The presence of silver in Puracol Plus likely contributes to its ability to reduce both planktonic bacterial populations and biofilm structures.

In contrast, Mirragen and Microlyte displayed limited degrees of antibacterial effectiveness. Microlyte contains silver; however, the exact concentration and the bioavailability of the silver ions within the product are unknown. The silver concentration in Microlyte might be below the threshold required to exert a significant antimicrobial effect, or the release kinetics of the ions are not optimized for immediate antimicrobial action. Mirragen, which does not contain any known metal ion dopants with antimicrobial properties, showed the least antibacterial activity.

The correlation between the antibiofilm efficacy of bioactive materials and their constituent metal dopants was further examined. Boron, silver, copper, and zinc display antibacterial properties, with silver, copper, and zinc being extensively documented for their capacity to inhibit and disrupt bacterial growth and biofilm formation (43). Silver ions have been shown to possess potent antibacterial activity by disrupting bacterial cell walls and interacting with thiol groups in proteins, leading to cell death. Similarly, copper ions can penetrate bacterial cells and generate reactive oxygen species (ROS), which can damage DNA, proteins, and lipids, leading to cell death. Zinc is known to interfere with membrane function and protein synthesis, and it can also disrupt biofilm structure by destabilizing the matrix (43). In contrast, boron's antibacterial properties are considerably less pronounced. The antimicrobial mechanism of boron is less clearly defined but is hypothesized to involve the disruption of enzymatic activity and membrane function. The comparison of these materials highlights the importance of the matrix composition in the release kinetics of metal ions. The bioactive glass composition of GL1605, characterized by its high biodegradability, facilitated a fast and controlled release of copper and zinc ions in contrast to the compositions of Microlyte and Puracol Plus, which did not support a similarly rapid silver release.

Overall, the discussion reflects the complexity of biofilm management in wound care and highlights the differential effects of wound care materials over time. The findings reiterate the necessity for effective wound treatment compositions that address the recalcitrance of bacterial biofilms. This study highlighted the potential of enhanced BBGs in rapidly inhibiting biofilms and underscored the contribution of such dopants to the antimicrobial efficacy of wound care materials. The optimal antibiofilm activity is not

solely dependent on the presence of antibacterial metals but is also critically influenced by the rate at which these ions are made available in the wound environment. Future research should focus on optimizing material compositions to enhance ion release rates, exploring synergistic combinations of metals, and developing targeted delivery mechanisms to exploit the full potential of these bioactive materials in the prevention and treatment of biofilm-related infections.

#### 4. MATERIALS AND METHODS

**Biomaterials and sample preparation:** Four biomaterials were used in this study; their compositions, main characteristics, and respective names are presented in Table 1.

Grooves were formed on the biomaterials' surface to enhance their absorption surface area and ensure their absolute contact with the solution. **In vitro antibacterial assay:**

Three bacterial species were selected for the present study as they are commonly implicated in chronic wound infections. All isolates were purchased from the American Type Culture Collection (ATCC): *S. epidermidis* (ATCC 6538), *E. coli* (ATCC 27853), and *P. aeruginosa* (ATCC 9637). Antibacterial tests were carried out in three triplicates.

The bacteria were plated on TSA Petri dishes (60 x 15 mm) and incubated overnight at 37 °C under aerobic conditions. TSB was used as the culture medium for the bacterial growth- one colony was transferred to the medium and incubated overnight at 37 °C under aerobic conditions in a shaker incubator until an exponential growth phase was achieved. Bacterial cultures were diluted into the media containing the sample. Before

plating, all tubes were vortexed until the sample was precipitated. Bacterial samples were inoculated with a concentration of  $10^8$  CFU/mL.

Table 1. Commercially available wound healing biomaterials assessed in this study

<b>Biomaterial</b>	<b>Composition</b>	<b>Dopants</b>	<b>Bioactive properties</b>
Microlyte® (Imbed BIOSCIENCES)	Bioresorbable matrix for partial and full thickness wounds	Ag (<25 ug/cm <sup>2</sup> )	<ul style="list-style-type: none"> <li>▪ Facilitates wound granulation</li> <li>▪ Maintains a physiologically moist environment</li> <li>▪ Promotes vascularization, cell migration, and tissue formation</li> </ul>
PURACOL PLUS® (Medline Industries, Inc)	Collagen matrix for partial thickness wounds	Ag (1%)	<ul style="list-style-type: none"> <li>▪ Stimulates fibroblastic activity</li> <li>▪ Promotes ECM formation</li> </ul>
Mirragen® Bioactive Glass (ETS Wound Care)	Borate-based glass fiber matrix (51.6B <sub>2</sub> O <sub>3</sub> –20CaO–12K <sub>2</sub> O–5MgO–6Na <sub>2</sub> O–4% P <sub>2</sub> O <sub>5</sub> , in mol %) for acute and chronic wounds	—	<ul style="list-style-type: none"> <li>▪ Promotes cell growth, tissue regeneration, and wound closure</li> <li>▪ Accelerates wound healing</li> <li>▪ Reduces inflammation</li> </ul>
GL1605 Bioactive Glass (MO Sci)	Enhanced borate glass fiber matrix (51.6B <sub>2</sub> O <sub>3</sub> –20CaO–12K <sub>2</sub> O–5MgO–6Na <sub>2</sub> O–4% P <sub>2</sub> O <sub>5</sub> –1%ZnO–0.4%CuO, in mol %). for acute and chronic wounds	Zn (1%) Cu (0.4%)	<ul style="list-style-type: none"> <li>▪ Promotes angiogenesis, cell differentiation, and tissue formation</li> <li>▪ Accelerates wound healing</li> </ul>

In vitro antibiofilm assay: The standard optical density measurement assay was used to evaluate the bacterial biofilm formation. Bacterial biofilms were assessed using the crystal violet staining assay, and the optical density was read at a wavelength of 600 nm.



Fixed biofilms were stained with 1% crystal violet, and the excess stain was thoroughly rinsed off with dH<sub>2</sub>O. Then, 30% acetic acid solution was added to the wells to distain the bound biofilms. A spectrophotometry was used to assess biofilm formation. The bacterial suspensions were added to a 24-well culture plate, and the plate was incubated at 37°C for 24 h under static conditions to allow for biofilm adhesion and formation. Following 24 h the plate was rinsed with PBS to remove planktonic bacteria. Wells containing only dH<sub>2</sub>O were used as controls. Adhered biofilms were treated with the materials, and stimulated body fluid was used as the media. The plates were incubated for 48 h at 37°C, followed by quantification of the biofilms every 24 h.

Element release profile: The element release amount was measured by inductively coupled plasma mass spectroscopy (ICP-MS). Aliquots were diluted 1:1000 in aqueous 1% HNO<sub>3</sub>. The quantification of elements was based on standard element calibration of Ag, B, Cu, and Zn. Ion release was read by an acquisition system. Before ICP-MS was performed, samples were purified by a 0.45 µm syringe filter.

Statistical analysis: All experiments were performed in three replicates, and data are presented as the mean ± standard deviation. The antibacterial effective values exhibited/did not exhibit normal distribution as inferred by the Shapiro-Wilk test. For the data that exhibited a normal distribution, a parametric hypothesis was used for data comparison and vice versa. A one-way ANOVA with a Tukey post hoc test was performed, and a statistical significance was set at 0.05. (\*  $p \leq 0.05$ , \*\*  $p \leq 0.01$ , \*\*\*  $p \leq 0.001$ ).

## REFERENCES

1. Rahim K, Saleha S, Zhu X, Liang H, Basit A, Franco OL. 2016. Bacterial contribution in chronicity of wounds. *Microbial Ecology* 73:710–721.
2. Sen CK, Gordillo GM, Roy S, Kirsner RS, Lambert L, Hunt TK, Gottrup F, Gurtner GC, Longaker MT. 2009. Human skin wounds: A major and snowballing threat to public health and the economy. *Wound Repair and Regeneration* 17:763–771.
3. Queen D, Harding K. 2023. What's the true costs of wounds faced by different healthcare systems around the world? *International Wound Journal* 20:3935–3938.
4. Pfalzgraff A, Brandenburg K, Weindl G. 2018. Antimicrobial peptides and their therapeutic potential for bacterial skin infections and wounds. *Frontiers in Pharmacology* 9.
5. Pereira SG, Moura J, Carvalho E, Empadinhas N. 2017. Microbiota of Chronic Diabetic Wounds: Ecology, impact, and potential for Innovative Treatment Strategies. *Frontiers in Microbiology* 8.
6. Burgess JL, Wyant WA, Abujamra BA, Kirsner RS, Jozic I. 2021. Diabetic Wound-Healing Science. *Medicina-lithuania* 57:1072.
7. Przekora A. 2020. A concise review on tissue engineered artificial skin grafts for chronic wound treatment: Can we reconstruct functional skin tissue in vitro? *Cells* 9:1622.
8. Solanki D, Vinchhi P, Patel MM. 2023. Design considerations, formulation approaches, and strategic advances of hydrogel dressings for chronic wound Omega 8:8172–8189.
9. Bjarnsholt T. 2013. The role of bacterial biofilms in chronic infections. *APMIS* 121:1–58.
10. Sharma D, Misba L, Khan AU. 2019. Antibiotics versus biofilm: an emerging battleground in microbial communities. *Antimicrobial Resistance and Infection Control* 8.
11. Høiby N, Ciofu O, Johansen HK, Song Z, Moser C, Jensen PØ, Molin S, Givskov M, Tolker-Nielsen T, Bjarnsholt T. 2011. The clinical impact of bacterial biofilms. *International Journal of Oral Science* 3:55–65.
12. Percival SL, Emanuel C, Cutting K, Williams DW. 2011. Microbiology of the skin and the role of biofilms in infection. *International Wound Journal* 9:14–32.

13. Kadam S, Shai S, Shahane A, Kaushik KS. 2019. Recent advances in Non-Conventional Antimicrobial Approaches for chronic wound biofilms: Have we found the 'Chink in the armor'? *Biomedicines* 7:35.
14. Mihai MM, Preda M, Lungu II, Gestal MC, Popa MI, Holban AM. 2018. Nanocoatings for Chronic Wound Repair—Modulation of microbial colonization and biofilm formation. *International Journal of Molecular Sciences* 19:1179.
15. Lerminiaux NA, Cameron ADS. 2019. Horizontal transfer of antibiotic resistance genes in clinical environments. *Canadian Journal of Microbiology* 65:34–44.
16. Bowler PG. 2002. Wound pathophysiology, infection and therapeutic options. *Annals of Medicine* 34:419–427.
17. Neğuț I, Grumezescu V, Grumezescu AM. 2018. Treatment strategies for infected wounds. *Molecules* 23:2392.
18. Kolimi P, Narala S, Nyavanandi D, Youssef AAA, Dudhipala N. 2022. Innovative treatment strategies to Accelerate wound healing: Trajectory and recent advancements. *Cells* 11:2439.
19. Kim HS, Sun X, Lee JH, Kim H, Fu X, Leong KW. 2019. Advanced drug delivery systems and artificial skin grafts for skin wound healing. *Advanced Drug Delivery Reviews* 146:209–239.
20. Hassan MA, El-Aziz SA, Elbadry HM, El-Aassar SA, Tamer TM. 2022. Prevalence, antimicrobial resistance profile, and characterization of multi-drug resistant bacteria from various infected wounds in North Egypt. *Saudi Journal of Biological Sciences* 29:2978–2988.
21. Montanaro L, Arciola CR. 2013. A review of the clinical implications of anti-infective biomaterials and infection-resistant surfaces. *Biomaterials* 34:8018–8029.
22. Brown MM, Horswill AR. 2022. *Staphylococcus epidermidis* and its dual lifestyle in skin health and infection. *Nature Reviews Microbiology* 21:97–111.
23. Braz VS, Melchior K, Moreira CG. 2020. *Escherichia coli* as a Multifaceted Pathogenic and Versatile Bacterium. *Frontiers in Cellular and Infection Microbiology* 10.
24. Vetrivel A, Ramasamy M, Vetrivel P, Natchimuthu S, Arunachalam S, Kim GS, Murugesan R. 2021. *Pseudomonas aeruginosa* Biofilm Formation and Its Control. *Biologics* 1:312–336.
25. Reynolds D, Kollef MH. 2021. The Epidemiology and Pathogenesis and Treatment of *Pseudomonas aeruginosa* Infections: An Update. *Drugs* 81:2117–2131.

26. Mathew-Steiner SS, Roy S, Sen CK. 2021. Collagen in wound healing. *Bioengineering* 8:63.
27. Qian Y, Zhou X, Zhang F, Diekwisch TGH, Luan X, Yang J. 2019. Triple PLGA/PCL scaffold modification including silver impregnation, collagen coating, and electrospinning significantly improve biocompatibility, antimicrobial, and osteogenic properties for orofacial tissue regeneration. *ACS Applied Materials & Interfaces* 11:37381–37396.
28. Paladini F. 2019. Antimicrobial silver nanoparticles for wound healing Application: progress and future trends. *Materials* 12:2540.
29. Kalva SN, Augustine R, Mamun AA, Dalvi YB, Vijay N, Hasan A. 2021. Active agents loaded extracellular matrix mimetic electrospun membranes for wound healing applications. *Journal of Drug Delivery Science and Technology* 63:102500.
30. Gobi R, Ravichandiran P, Babu RS, Yoo DJ. 2021. Biopolymer and Synthetic Polymer-Based Nanocomposites in wound dressing Applications: a review. *Polymers* 13:1962.
31. Karoyo AH, Wilson LD. 2021. A review on the design and hydration properties of natural Polymer-Based hydrogels. *Materials* 14:1095.
32. Sheokand B, Vats M, Kumar A, Srivastava CM, Bahadur I, Pathak SR. 2023. Natural polymers used in the dressing materials for wound healing: Past, present and future. *Journal of Polymer Science* 61:1389–1414.
33. Ege D, Zheng K, Boccaccini AR. 2022. Borate Bioactive Glasses (BBG): bone regeneration, wound healing applications, and future directions. *ACS Applied Bio Materials* 5:3608–3622.
34. Westenberg DJ, Viswanathan R, Kadyk DL, Hibbs S, Kopel J, Day DE. 2021. Evaluation of three Borate-Bioactive Glass compositions for antibacterial applications. *Advances in Microbiology* 11:646–656.
35. Karoyo AH, Wilson LD. 2021. A review on the design and hydration properties of natural Polymer-Based hydrogels. *Materials* 14:1095.
36. Sheokand B, Vats M, Kumar A, Srivastava CM, Bahadur I, Pathak SR. 2023. Natural polymers used in the dressing materials for wound healing: Past, present and future. *Journal of Polymer Science* 61:1389–1414.
37. Ege D, Zheng K, Boccaccini AR. 2022. Borate Bioactive Glasses (BBG): bone regeneration, wound healing applications, and future directions. *ACS Applied Bio Materials* 5:3608–3622.

38. Westenberg DJ, Viswanathan R, Kadyk DL, Hibbs S, Kopel J, Day DE. 2021. Evaluation of three Borate-Bioactive Glass compositions for antibacterial applications. *Advances in Microbiology* 11:646–656.
39. Mayet N, Choonara YE, Kumar P, Tomar LK, Tyagi C, Du Toit LC, Pillay V. 2014. A comprehensive review of advanced biopolymeric wound healing systems. *Journal of Pharmaceutical Sciences* 103:2211–2230.
40. Sorg H, Tilkorn DJ, Hager S, Hauser J, Mirastschijski U. 2016. Skin Wound Healing: An update on the current knowledge and concepts. *European Surgical Research* 58:81–94.
41. Han G, Ceilley RI. 2017. Chronic Wound Healing: A review of current management and Treatments. *Advances in Therapy* 34:599–610.
42. Landén NX, Li D, Ståhle M. 2016. Transition from inflammation to proliferation: a critical step during wound healing. *Cellular and Molecular Life Sciences* 73:3861–3885.
43. Bessa LJ, Fazii P, Di Giulio M, Cellini L. 2013. Bacterial isolates from infected wounds and their antibiotic susceptibility pattern: some remarks about wound infection. *International Wound Journal* 12:47–52.
44. BioSpace. 2023. Spartan Medical launches concentric attack on surgical site infections. BioSpace. <https://www.biospace.com/article/releases/spartan-medical-launches-concentric-attack-on-surgical-site-infections/>.
45. Lozeau LD, Grosha J, Kole D, Prifti F, Dominko T, Camesano TA, Rolle MW. 2017. Collagen tethering of synthetic human antimicrobial peptides cathelicidin LL37 and its effects on antimicrobial activity and cytotoxicity. *Acta Biomaterialia* 52:9–20.
46. Capella-Monsonís H, Tilbury MA, Wall JG, Zeugolis DI. 2020. Porcine mesothelium matrix as a biomaterial for wound healing applications. *Materials Today Bio* 7:100057.
47. Jung SB, Day T, Boone T, Buziak B, Omar A. 2019. Anti-biofilm activity of two novel, borate based, bioactive glass wound dressings. *Biomedical Glasses* 5:67–75.

### III. THE ANTIBIOFILM EFFICACY OF METAL-ION DOPED BORATE BIOACTIVE GLASS: A COMPREHENSIVE PREDICTIVE MODELING APPROACH FOR INFECTION CONTROL IN HEALTHCARE SETTINGS

Sarah Fakher and David Westenberg

#### ABSTRACT

Health Care Acquired Infections (HAIs) pose significant challenges in medical settings, primarily due to their resistance to conventional treatment methods. The role of bacterial biofilms in exacerbating these infections is well-documented, making them particularly difficult to eradicate. Despite numerous research efforts, an effective solution to combat these infections remains elusive. This study aims to explore the potential of undoped and metal-ion (copper and zinc) doped borate bioactive glasses as a novel approach to inhibit bacterial species commonly implicated in HAIs: *Staphylococcus epidermidis*, *Escherichia coli*, and *Pseudomonas aeruginosa*. The study analyzed the efficacy of both direct and indirect applications of the borate bioactive glass (BBGs) on severe biofilms pre-formed under static and dynamic growth conditions, acknowledging the critical role of bacterial biofilms in the complexity and persistence of these infections. A comprehensive predictive modeling was developed, simulating diverse clinically relevant conditions. Results demonstrate a significant reduction in bacterial growth within 2 days under direct application and within 3 days for indirect application of copper and zinc-doped borate bioactive glasses. These findings were consistent across the three bacterial species, in both static and dynamic conditions, underscoring the potential of metal-ion

doped borate bioactive glasses as an effective approach in combating HAIs complicated by biofilms.

## 1. INTRODUCTION

Health Care Acquired Infections (HAIs), characterized by their persistent nature and resistance to conventional treatment methods, represent a significant global health challenge. Acquired by patients during their stay in healthcare facilities, these infections contribute to increased morbidity and mortality rates and have a profound impact on healthcare systems worldwide (1). HAIs encompass a wide range of infections, from surgical site infections to pneumonia and urinary tract infections, often complicated by the presence of resilient bacterial biofilms (2). HAIs are a significant global health burden, affecting millions of patients annually. In the US alone, HAIs account for an estimated 1.7 million infections and 99,000 associated deaths each year (3). Globally, HAIs have a prevalence of about 10% in developed countries and up to 25% in developing countries (1, 4). These infections lead to prolonged hospital stays, long-term disability, increased resistance of microorganisms to antimicrobials, massive additional financial burden, and longer hospitalization (5, 6).

Central to the challenge of HAIs is the role of bacterial biofilms, which are communities of microorganisms that adhere to surfaces and are embedded in a self-produced extracellular matrix (ECM). This matrix shields the bacteria from antimicrobial agents and the host immune system, contributing to the chronic and recurrent nature of these infections (7). Biofilms are particularly challenging in the context of indwelling

medical devices, where they can establish persistent infections that are resistant to conventional antibiotics. Over 60% of HAIs, particularly those related to implanted medical devices, are ascribed to bacterial biofilms. The presence of biofilms on medical devices and hospital surfaces significantly complicates treatment, as bacteria in biofilms can be up to 1,000 times more resistant to antibiotics compared to their planktonic form (8). These biofilms are also a known cause of persistent infections like osteomyelitis (9). Overall, biofilms contribute to over 80% of microbial infections in the human body (10). The study of biofilms is therefore crucial for understanding the pathogenesis of HAIs and developing effective treatment strategies.

Among the bacterial species implicated in HAIs, *S. epidermidis*, *E. coli*, and *P. aeruginosa* are notable for their prevalence and impact (11-13). *S. epidermidis* is frequently associated with catheter-related bloodstream infections and prosthetic device infections, owing to its ability to form robust biofilms (14). *E. coli*, a common cause of urinary tract and surgical site infections, presents challenges due to its increasing resistance to antibiotics (15). *P. aeruginosa*, known for its intrinsic resistance mechanisms, is a common pathogen in ventilator-associated pneumonia and burn wound infections (16). These pathogens are notorious for their biofilm-forming capabilities and are responsible for a range of infections; for instance, *P. aeruginosa* alone accounts to more than 10% of all HAIs (17). Moreover, the ability of these bacteria to form biofilms and evade standard treatments makes them formidable pathogens in healthcare settings.

In the context of HAIs, antibiotic resistance presents a formidable challenge to conventional medicine (18). Even though the evolution of antibiotic resistance is a natural phenomenon, it has been significantly accelerated by the overuse and misuse of



antibiotics. In healthcare environments and clinical settings, the frequent and sometimes inappropriate use of antibiotics has led to the emergence of multidrug-resistant organisms, transforming once easily treatable infections into serious health threats (19). According to the CDC, about 2.8 million antibiotic-resistant infections occur in the US each year, causing more than 35,000 deaths (20). Globally, the WHO has identified antibiotic resistance as one of the top ten global public health threats, with predictions of up to 10 million deaths per year by 2050 if no action is taken (21, 22). The impact of antibiotic resistance is particularly acute in the case of HAIs, where patients are often exposed to a high load of antibiotics that not only select for resistant strains but also allow for the horizontal transfer of resistance genes among different bacterial species (23). These resistant strains are often involved in biofilm formation, which further complicates treatment as biofilms provide a protective environment that enhances bacterial survival against antibiotics. This synergy between antibiotic resistance and biofilm formation necessitates the development of innovative approaches, beyond traditional antibiotics, to effectively manage HAIs and curb the rise of antibiotic resistance.

In the quest to address the challenges posed by HAIs and bacterial biofilms, BBGs have emerged as a promising biomaterial (24-26). BBGs are recognized for their biodegradability, biological activity, and ability to support bone growth (26). Their properties outperform other types of BGs, making them suitable for diverse medical applications, including bone repair and wound healing. These properties include enhanced bioactivity, the ability to support tissue regeneration, and the controlled release of therapeutic ions (27, 28).

BBGs can be enhanced by integrating metals like silver, zinc, and notably copper (24). Copper, recognized for its role in promoting angiogenesis, does so through the stimulation of key growth factors such as fibroblast growth factor-2 (FGF-2) and vascular endothelial growth factor (VEGF) (29). It's also instrumental in driving mesenchymal cells toward osteogenic differentiation and curtailing the activity of osteoclasts. Furthermore, copper's involvement in collagen fiber crosslinking is vital for bone ossification (30). Its antibacterial efficacy against various pathogens like is well-established (31, 32). The proposed mechanism suggests that copper ions, through electrostatic attraction, bind to the negatively charged peptidoglycan of the bacterial cell wall, especially affecting gram-negative bacteria by irreparably damaging their structural proteins. This process is potentially driven by the generation of reactive hydroxyl radicals, which can impede cellular development by oxidizing proteins and lipids (33,34). Besides, zinc ions stand out as particularly effective against bacterial biofilms, offering several therapeutic benefits. Known for its enzymatic role and its importance in DNA replication, zinc is essential for bone formation and, when released from BGs, zinc can induce oxidative stress within bacterial cells or cause harm to the bacterial membrane, contributing to its antimicrobial action (35, 36).

The integration of metallic ions into the chemical structure of BBGs represents a cutting-edge approach to creating materials with enhanced antibacterial properties. The inclusion of copper and zinc is particularly strategic as they are well-recognized for their broad-spectrum antimicrobial activity and potential to disrupt biofilm formation (33, 36). Moreover, copper and zinc ions are increasingly being utilized due to their established antimicrobial efficacy and relatively low cytotoxicity at minimal concentrations. The

antibacterial mechanisms of copper and zinc ions combined are multifaceted: they can interfere with bacterial cell membrane integrity, promote the generation of reactive oxygen species that damage cellular components, and bind to proteins, impeding bacterial metabolic processes (37). Moreover, the incorporation of these ions into BBGs also contributes to the materials' bio-functionality, promoting healing processes in biological tissues(38). The controlled release of these ions can also provide sustained antibacterial activity, which is crucial in medical applications such as wound healing and bone regeneration (39,40). This ensures that the antibacterial effect persists for the duration required to prevent infection.

Despite the promising attributes of BBGs and the recognized antimicrobial roles of copper and zinc, there is a notable gap in the comprehensive evaluation of metal-ion doped biomaterials under clinically relevant conditions. Most studies to date have focused on isolated aspects of BBG functionality or employed *in vitro* and *in vivo* models that do not fully replicate the complex and dynamic environment of HAIs in patients. There is a pressing need for an integrated approach that encompasses both direct and indirect applications of BBGs in various growth conditions, including static and dynamic biofilm cultures. Such an approach is essential for developing a deeper understanding of the potential of BBGs in combating HAIs, particularly those complicated by biofilms, and for advancing the field of infection control and bioactive material application in clinical settings. This research aims to fill this gap by providing a comprehensive and scientifically rigorous examination of the efficacy of copper and zinc-doped BBGs against HAIs. By focusing on the interaction of these glasses with bacterial biofilms of key species implicated in HAIs and considering the complex interplay of factors that

influence infection dynamics, the study seeks to offer new insights and potential solutions to a problem that continues to challenge healthcare systems worldwide.

## 2. RESULTS

### 2.1. STATIC BIOFILM GROWTH

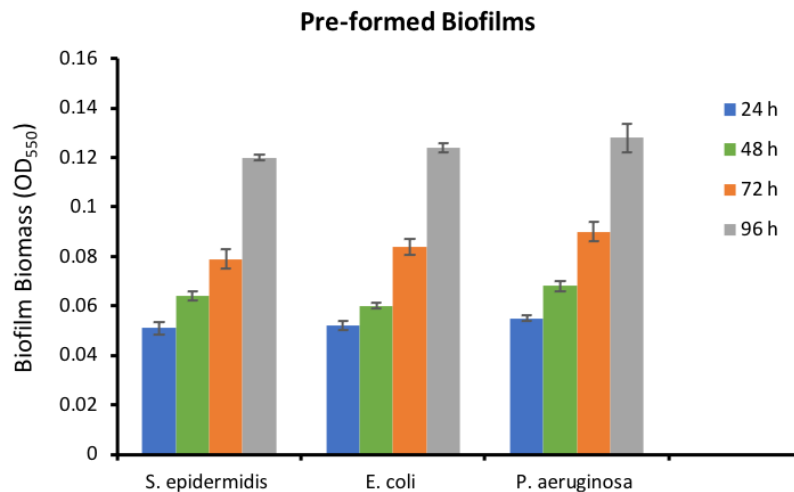
In the study of biofilm formation dynamics, bacterial cultures were incubated under static conditions at a controlled temperature of 37°C. The extent of biofilm biomass was quantitatively analyzed utilizing the crystal violet staining method. This assay relies on absorbance measurement through spectrophotometry and facilitates the evaluation of biofilm mass by quantifying the optical density (OD) of stained biofilms. Daily measurements were recorded over four days, and the results were compared to the optical density cut-off value (OD<sub>c</sub>), which was determined to be 0.02. This enabled the classification of biofilms into categories based on their adherence levels and biomass: non-adherent, weak, moderate, or severe. Data indicated that all tested bacterial strains achieved an adherent biofilm mode within 24 hours (Fig.1). Notably, *S. epidermidis* demonstrated the formation of severe biofilms by the third day. In contrast, *E. coli* and *P. aeruginosa* reached a similar level of severe biofilm formation by the fourth day (Fig.1). Severe biofilms were selected as the test subjects to assess the efficacy of the BGs in inhibiting or disrupting biofilm formation. This approach aims to rigorously evaluate of the BGs' antimicrobial properties, particularly their ability to counteract robust biofilm structures, which are often resistant to conventional antimicrobial treatments.

## 2.2. BBG DIRECT/INDIRECT APPLICATION ON STATIC BIOFILMS

Upon direct application of GL1605 to *S. epidermidis* biofilms, there was an observed 4-log decrease in bacterial count within the initial 24-hour period, progressing to a 5-log reduction at the 48-hour mark. No biofilms were detected (Figure 2A) after that. In contrast, MIRRAGEN's direct application resulted in a 2-log reduction, with an incremental 1-log reduction over the succeeding 72-hour period, stabilizing after that until the 96-hour (Figure 2A). Indirect application of GL1605 on *S. epidermidis* achieved a 4.5-log reduction after 72 hours, with no biofilm detectable at 96 hours (Figure 2B). This indirect modality rendered MIRRAGEN considerably less potent against *S. epidermidis*, achieving a three-log reduction.

The antibiofilm effects against *E. coli* were also notable; direct application of GL1605 led to a three-log reduction at 24 hours, with a pronounced decline and a bactericidal effect observed by 48 hours (Figure 2C), and complete biofilm eradication by 96 hours.

MIRRAGEN demonstrated a peak efficacy of four-log reduction at 96 hours, indicating its relatively inefficient antibiofilm effectiveness (Figure 2C). When applied indirectly, GL1605 effected a 5.5-log reduction at 72 hours against *E. coli*, with no detectable bacteria at 96 hours (Figure 2D), while MIRRAGEN's indirect application achieved only a three-log reduction after 96 hours. For *P. aeruginosa*, direct application of GL1605 achieved a bacteriostatic effect at 24 hours and a bactericidal effect with a 4.5-log reduction by 48 hours, beyond which no bacteria were detectable (Figure 2E). Indirect application of the GL1605 achieved bactericidal effectiveness after 72 hours (Figure 2F). MIRRAGEN's efficacy against *P. aeruginosa* was minimal in both direct and indirect applications when compared to the other bacterial strains (Figure 2F).



Biofilm	Time (hours)	Average OD ± SD	Adherence	Biofilm formation
<i>S. epidermidis</i>	24 h	0.051 ± 0.003	(+/-)	Weak
	48 h	0.064 ± 0.002	(+)	Moderate
	72 h	0.079 ± 0.004	(+)	Moderate
	96 h	0.120 ± 0.001	(++)	Severe
<i>E. coli</i>	24 h	0.052 ± 0.002	(+/-)	Weak
	48 h	0.060 ± 0.001	(+)	Moderate
	72 h	0.084 ± 0.003	(++)	Severe
	96 h	0.124 ± 0.002	(++)	Severe
<i>P. aeruginosa</i>	24 h	0.055 ± 0.001	(+/-)	Weak
	48 h	0.068 ± 0.002	(+)	Moderate
	72 h	0.090 ± 0.004	(++)	Severe
	96 h	0.128 ± 0.005	(++)	Severe

Figure 1. Static biofilm development of *S. epidermidis*, *E. coli*, and *P. aeruginosa*.

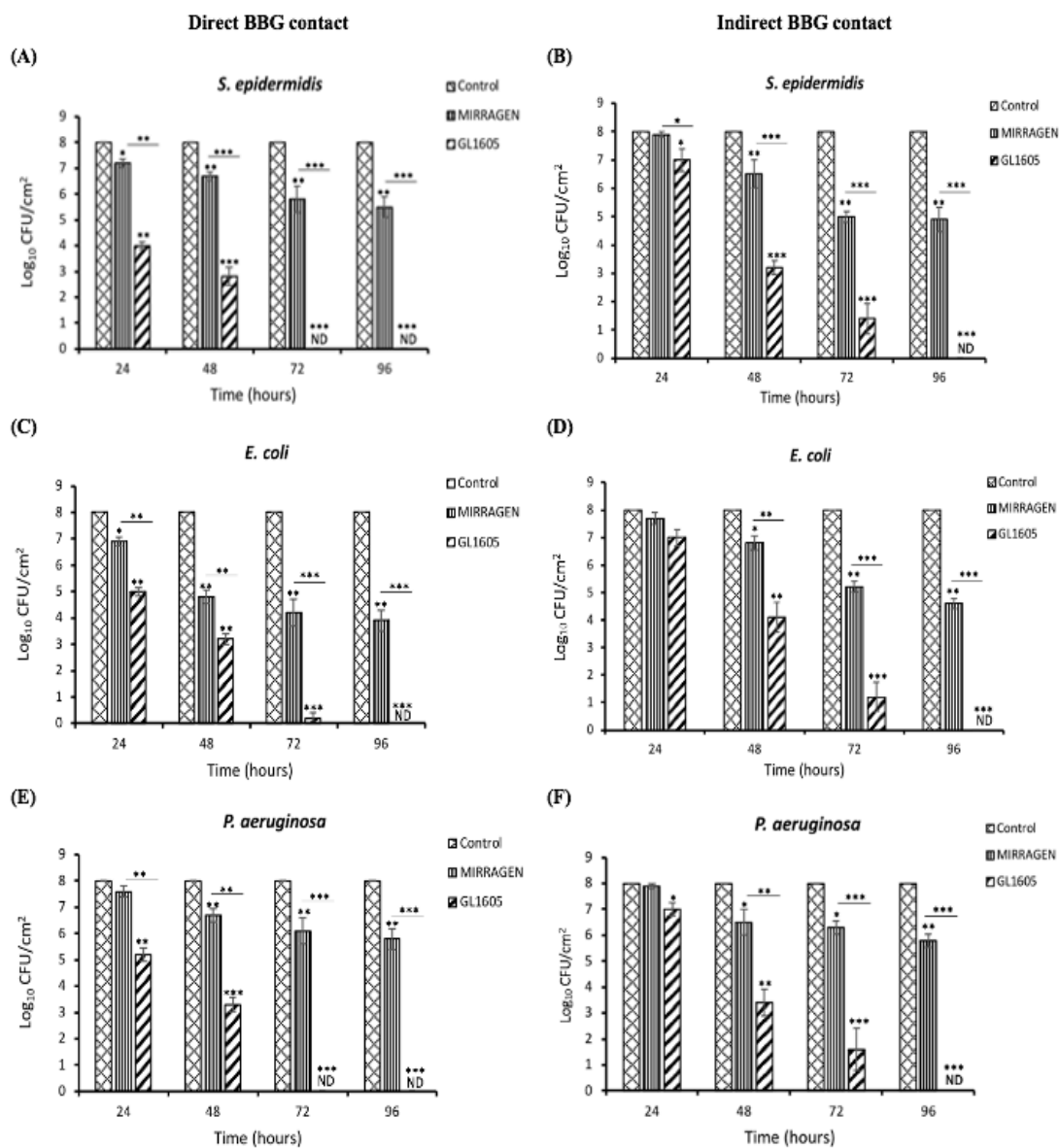


Figure 2. Borate bioactive glass direct and indirect application on severely pre-formed static biofilms. The BBG was applied to the biofilms directly (A, C, D) and indirectly (B, D, F). Treated biofilms were incubated 4 days and cell viability was measured every 24 hours. Results are expressed as the mean  $\pm$  standard deviation from three replicates. \* $P < 0.05$ ; \*\* $P < 0.01$ ; \*\*\* $P < 0.001$

Direct application of BBGs substantively accelerated anti-biofilm activity among all tested bacterial species relative to the indirect application.

The GL1605 demonstrated a pronounced and rapid antibiofilm efficacy against both gram-positive and gram-negative bacteria within a 48-hour contact period. Conversely, MIRRAGEN only achieved bacteriostatic effects following four days of exposure.

The differential responses to direct versus indirect BBG application can be attributed to the immediate bioavailability of ionic species at the biofilm interface in direct application, which may exert a more pronounced osmotic or ionic stress on the biofilm. In contrast, the indirect approach relies on the diffusion of ions through the biofilm structure, which may be impeded by the biofilm's extracellular polymeric substance, especially in gram-negative bacteria with their characteristic outer membrane barriers.

### 2.3. SCANNING ELECTRON MICROSCOPY (SEM)

SEM of the untreated control showed the undisturbed state of the bacterial biofilms (Figure 3A, B, C). *S. epidermidis* appears as dense, circular clusters, characteristic of staphylococcal biofilms (Figure 3A), with a homogeneous extracellular matrix indicative of a mature biofilm. *E. coli* (Figure 3B), presents a tightly organized rod-shaped cell structure within a smooth matrix, while *P. aeruginosa* (Figure 3C) also exhibits its typical rod shape, embedded within a thick, structured matrix. Following MIRRAGEN treatment, changes are subtle. *S. epidermidis* (Figure 3D) shows initial signs of biofilm disaggregation, with circular cells beginning to separate. *E. coli* cells (Figure 3E) display a slight separation, indicating early biofilm destabilization. *P. aeruginosa* shows a less dense arrangement with a somewhat disrupted matrix (Figure 3F). In contrast, after GL1605 treatment, *S. epidermidis* reveals distorted, disorganized circular cells, with a disrupted matrix suggesting significant biofilm degradation (Figure 3G). The rod-shaped



cells of *E. coli* (Figure 3H) exhibit pronounced damage and disrupted integrity, while *P. aeruginosa* (Figure 3I) shows severe cell and matrix damage, with cells appearing lysed. The pronounced morphological changes from their typical shapes and the compromised matrix integrity across all specimens underscore GL1605's potent antibiofilm efficacy.

For *S. epidermidis* biofilms, the SEM analysis indicated that indirect MIRRAGEN application did not result in a significant reduction in biofilm formation. The presence of ECM structures connecting biofilm clusters is observed, as indicated by the yellow arrows (Figure 3J). These ECM structures appeared to facilitate the persistence of viable cells within the biofilm, potentially contributing to the limited disruption seen. Similarly, *E. coli* biofilms subjected to indirect MIRRAGEN application did not yield biofilm disruption (Figure 3K). Although there were some dead cells within the biofilm matrix, most cells remained viable. Notably, the viable cells were observed to aggregate, likely due to the presence of ECM, which appeared to play a role in maintaining the structural integrity of the biofilm. In contrast to the observations with *S. epidermidis* and *E. coli*, the indirect application of MIRRAGEN to *P. aeruginosa* biofilms did not lead to any significant reduction (Figure 3L). SEM analysis revealed an absence of dead cells within the biofilm matrix, indicating that the biofilm structure remained largely intact.

For GL1605 on *S. epidermidis*, SEM images indicated the presence of very few intact cells, and no aggregated biofilm structures were noted (Figure 3M). Conversely, GL1605 application on *E. coli* biofilms yielded no detected viable cells, with the presence of cell debris suggesting significant cell morphological damage (Figure 3N). A similar pattern was observed in the case of *P. aeruginosa* subjected to GL1605

application, where damaged dead cells were visible, and no intact cells were detected within the biofilm (Figure 3O).

These SEM findings collectively suggest that the effects of BBG application on biofilm disruption vary depending on the bacterial species. While some instances showed limited disruption with a predominance of viable cells, others exhibited pronounced damage and reduced viability, indicating the need for further investigation into the mechanisms underlying these variations. Additional complementary assays and analyses are needed to gain a comprehensive understanding of the interplay between the BBGs and biofilm formation in diverse bacterial strains. The impact of GL1605 on cell viability is markedly evident. The integrity of the cells' structure, particularly the cell membrane, is crucial for viability, and the images after GL1605 treatment show significant disruption. In contrast to the control groups where the biofilms appear intact and cellular shapes are well-defined, the GL1605-treated biofilms display a loss of structural definition, with cells exhibiting signs of lysis or severe damage. This disruption of cell integrity is indicative of compromised cell viability, affirming the efficacy of GL1605 in not only disrupting biofilm architecture but also in effectively reducing the population of viable bacteria within these structures.

#### **2.4. BIOFILM DYNAMIC GROWTH**

To investigate the dynamics of bacterial growth in a dynamic environment, biofilms were pre-formed using a CDC biofilm reactor. In this reactor, bacterial cultures are subjected to continuous nutrient flow and shear forces, simulating conditions closer to those found in natural and clinical settings. A constant infusion of TSB and consistent

shear stress provided by the reactor's design support more rapid biofilm development compared to static conditions. The monitoring of biofilm formation was conducted through frequent OD measurements every four hours over a 24-hour period, rather than the 24-hour intervals used in static studies, due to the accelerated biofilm growth dynamics under continuous flow conditions. The ODC for the dynamic study was determined to be 0.07 (Fig.4). Results revealed that *E. coli* and *P. aeruginosa* developed severe biofilms within just 16 hours of incubation in the reactor. *S. epidermidis*, although slower, followed suit by forming severe biofilms by 20 hours (Figure 4). The faster biofilm formation by *E. coli* and *P. aeruginosa* can be attributed to their inherent rapid growth rates, efficient adherence mechanisms, and possibly their ability to better utilize the continuous nutrient supply in the dynamic system.

The severe biofilms formed under these dynamic conditions were then selected for the BBGs treatment, aimed to assess the effectiveness of BBGs in inhibiting or disrupting pre-formed biofilms. The effectiveness of BBGs against such robust biofilm structures is particularly significant as these are known to exhibit considerable resistance to conventional antimicrobial treatments.

## **2.5. BBG DIRECT/INDIRECT APPLICATION ON DYNAMIC BIOFILMS**

Direct application of MIRRAGEN to *S. epidermidis* dynamically growing cultures yielded a moderate reduction of approximately 2 log units within the initial 4 days of contact (Figure 5A) Conversely, the direct application of GL1605 exhibited 4-log reduction within 48 hours, indicative of a bactericidal effect (Figure 5A).

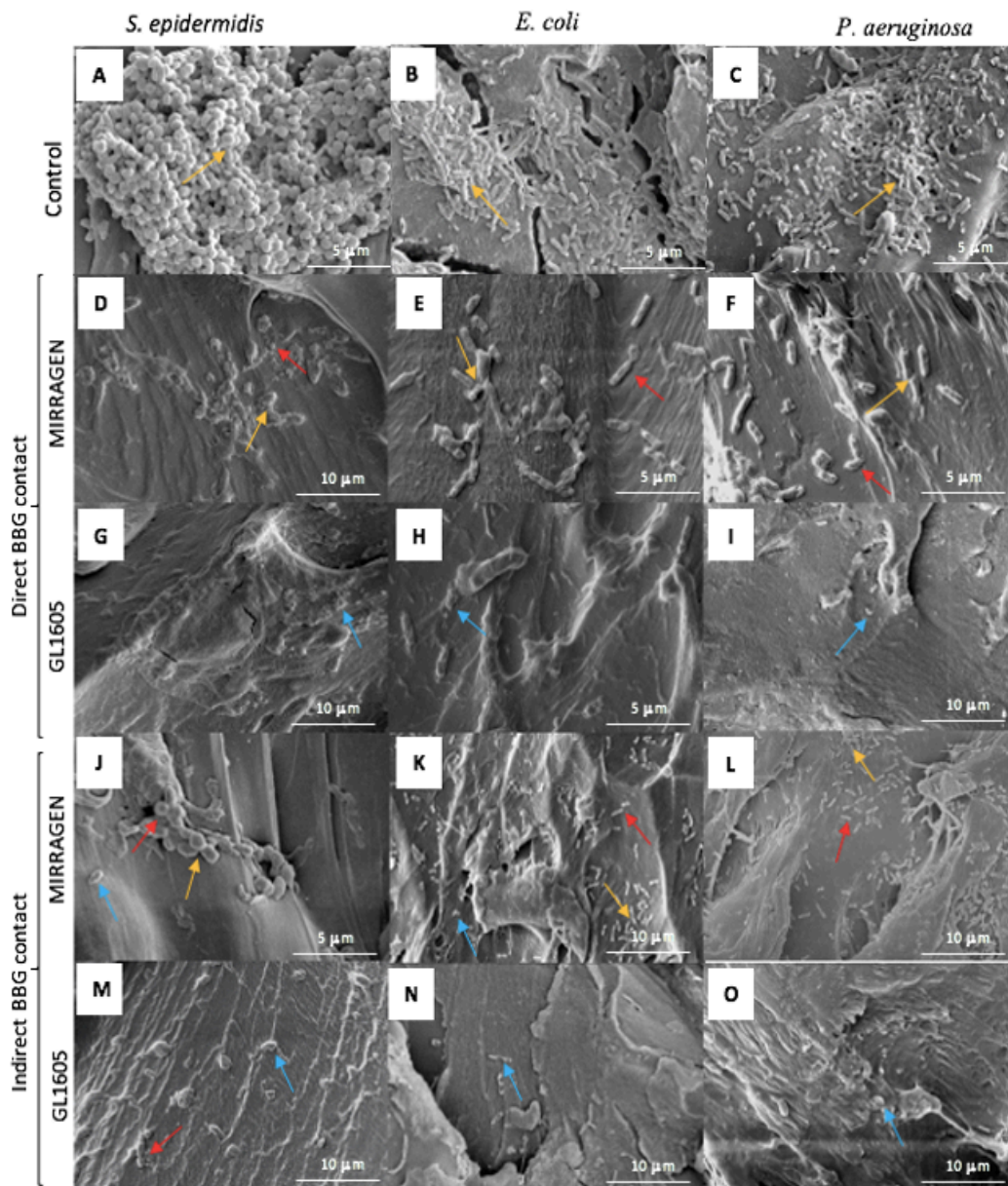
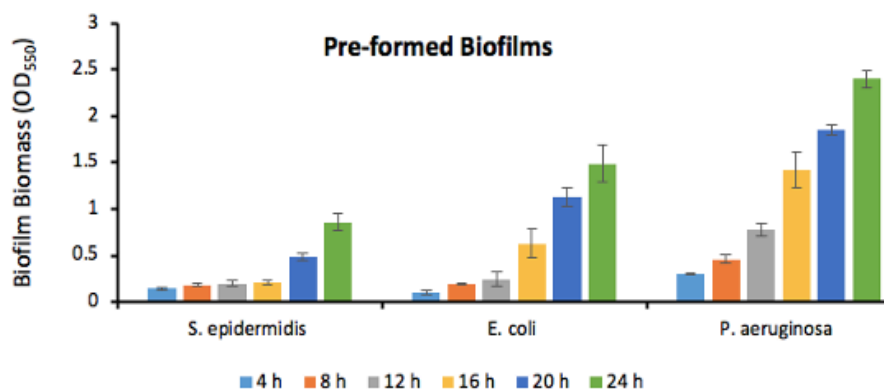


Figure 3. SEM. (A, B, C) biofilms before BBG treatment after 48 hours. (D, E, F) direct MIRRAGEN application. (G, H, I) Direct GL1605 application. (J, K, L) indirect MIRRAGEN application. (M, N, O) indirect GL1605 application. Yellow arrows indicate the presence of ECM, red arrows indicate viable cells, and blue arrows indicate dead cells

Although a slightly diminished effect was observed between 48 and 96 hours, the antibacterial efficacy remained substantial. Indirect MIRRAGEN contact with *S.*

*epidermidis* displayed a similar trend to direct application, with no marked reduction in bacteria (Figure 5B).



Biofilm	Time (hours)	Average OD ± SD	Adherence	Biofilm formation
<i>S. epidermidis</i>	4 h	0.14 ± 0.02	(+/-)	Weak
	8 h	0.17 ± 0.002	(+)	Moderate
	12 h	0.19 ± 0.002	(+)	Moderate
	16 h	0.22 ± 0.03	(+)	Moderate
	20 h	0.44 ± 0.04	(++)	Severe
	24 h	0.78 ± 0.09	(++)	Severe
<i>E. coli</i>	4 h	0.10 ± 0.01	(+/-)	Weak
	8 h	0.19 ± 0.01	(+)	Moderate
	12 h	0.25 ± 0.08	(+)	Moderate
	16 h	0.63 ± 0.15	(++)	Severe
	20 h	1.12 ± 0.11	(++)	Severe
	24 h	1.50 ± 0.09	(++)	Severe
<i>P. aeruginosa</i>	4 h	0.32 ± 0.03	(++)	Severe
	8 h	0.46 ± 0.5	(++)	Severe
	12 h	0.78 ± 0.08	(++)	Severe
	16 h	1.42 ± 0.19	(++)	Severe
	20 h	1.85 ± 0.05	(++)	Severe
	24 h	2.40 ± 0.4	(++)	Severe

Optical density cut-off value (OD<sub>c</sub>) = 0.07

Legend: (-) non-adherent; (+/-) weakly adherent; (+) moderately adherent; (++) strongly adherent.

Determination of biofilm production: non-adherent (OD ≤ OD<sub>c</sub>), weak (OD<sub>c</sub> < OD ≤ 2 OD<sub>c</sub>), moderate (2 OD<sub>c</sub> < OD ≤ 4 OD<sub>c</sub>), and severe (4 OD<sub>c</sub> < OD)

Figure 4. Dynamic biofilm development of *S. epidermidis*, *E. coli*, and *P. aeruginosa*. Biofilms were formed in a CDC biofilm reactor for 24 hours. The OD was measured every 4 hours. All results are expressed as the mean ± standard deviation from three replicates.

indirect application of GL1605, however, exhibited a substantial 3.8-log reduction after 72 hours, indicating that it required an additional day to achieve the same bactericidal effect as direct application (Figure 5B).

Direct application of MIRRAGEN to dynamically growing *E. coli* cultures resulted in a bacteriostatic effect, with a 2-log unit reduction observed after 96 hours (Figure 5C). In contrast, direct application of GL1605 produced a rapid and potent 5.6-log reduction within 48 hours, eradicating the bacteria after 96 hours. (Figure 5C) Similarly, indirect MIRRAGEN application on *E. coli* cultures demonstrated a 2-log reduction after 96 hours, indicating its limited impact. The indirect application of GL1605, though less effective than direct application, still achieved a notable 4.5 log unit reduction within 72 hours (Figure 5D).

Dynamic growth of *P. aeruginosa* displayed more resilience to MIRRAGEN's direct application, resulting in only 1-log reduction after 96 hours. In contrast, direct application of GL1605 exhibited a more substantial 4-log reduction within 48 hours, with a gradual increase in efficacy over the subsequent 48 hours (Figure 5D). Similarly, indirect MIRRAGEN application on *P. aeruginosa* cultures did not induce significant bacterial reduction. However, the indirect application of GL1605 displayed a significant 4.5-log reduction after 72 hours, highlighting its potency in achieving bactericidal effects (Figure 5E).

A detailed investigation revealed the variable efficacy of MIRRAGEN and the GL1605 when applied directly and indirectly to dynamically pre-formed bacteria. These results underscore the importance of considering the specific bacterial strain and variant

when assessing the antibacterial and antibiofilm properties of MIRRAGEN, highlighting the potential use of GL1605 in achieving potent bactericidal effects.

## 2.6. SCANNING ELECTRON MICROSCOPY (SEM)

SEM images of untreated *S. epidermidis*, *E. coli*, and *P. aeruginosa* biofilms reveal dense, compact structures (Figure 6A, B, C). These biofilms, marked by a robust extracellular matrix ECM, exhibit characteristics crucial for resilience, such as three-dimensional architecture and cellular cohesion. Following MIRRAGEN treatment, SEM analysis shows early signs of biofilm disassembly in *S. epidermidis* (Figure 6D), *E. coli* (Figure 6E), and *P. aeruginosa* (Figure 6F), with a slight reduction in cell numbers, although significant viable populations persist, as indicated by the presence of ECM. GL1605 treatment, however, resulted in pronounced disorganization of biofilm architecture across all species. *S. epidermidis* biofilms display extensive morphological changes (Figure 6G), *E. coli* exhibited significant cellular damage (Figure 6H), and *P. aeruginosa* also presented extensive cell disruption (Figure I). The presence of dead cells suggests a potent bactericidal effect of GL1605, likely due to its destabilizing action on the ECM and direct disruption of cell membranes.

SEM imaging was performed 72 hours after indirect application of MIRRAGEN and the GL1605 on the dynamically pre-formed biofilms. The SEM analysis of *S. epidermidis* biofilms subjected to indirect MIRRAGEN application revealed that the biofilm integrity remained largely unaffected when compared to the control group. Intact biofilms were prominently observed, with the presence of ECM (Figure 3J), which is responsible for maintaining the structural integrity of the biofilm, emphasizing their role

in biofilm resilience. Similarly, the indirect application of MIRRAGEN on *E. coli* biofilms did not disrupt the biofilm matrix significantly; SEM analysis indicated no damaged cells within the biofilm matrix. Instead, a limited number of cells appeared to be disassociated from the biofilm structure, suggesting that MIRRAGEN treatment had minimal effect on *E. coli* biofilm stability (Figure 3K). Following indirect MIRRAGEN application on *P. aeruginosa* biofilms, MIRRAGEN did not induce significant biofilm disruption. Intriguingly, the biofilm structure remained robust, displaying strong aggregates similar to those observed in the untreated control group (Figure 3L).

For the GL1605 application on *S. epidermidis*, SEM images showed signs of cellular damage, as indicated by the blue arrows (Figure 6M). *E. coli* treated with the GL1605 biofilms resulted in damaged, disintegrated cells, along with the presence of cell debris and morphologically altered cells (Figure 6N). Similar observations were noted for *P. aeruginosa* subjected to GL1605 application, wherein damaged dead cells were prominent, accompanied by the presence of substantial cell debris (Figure 6O). Few viable cells were discernible, further substantiating pronounced effects on biofilm integrity.

### 3. DISCUSSION

Despite the potential of BBGs, a comprehensive understanding of their application in clinical settings is lacking. Current literature often presents fragmented insights, with a notable gap in studies that simulate different clinical conditions.



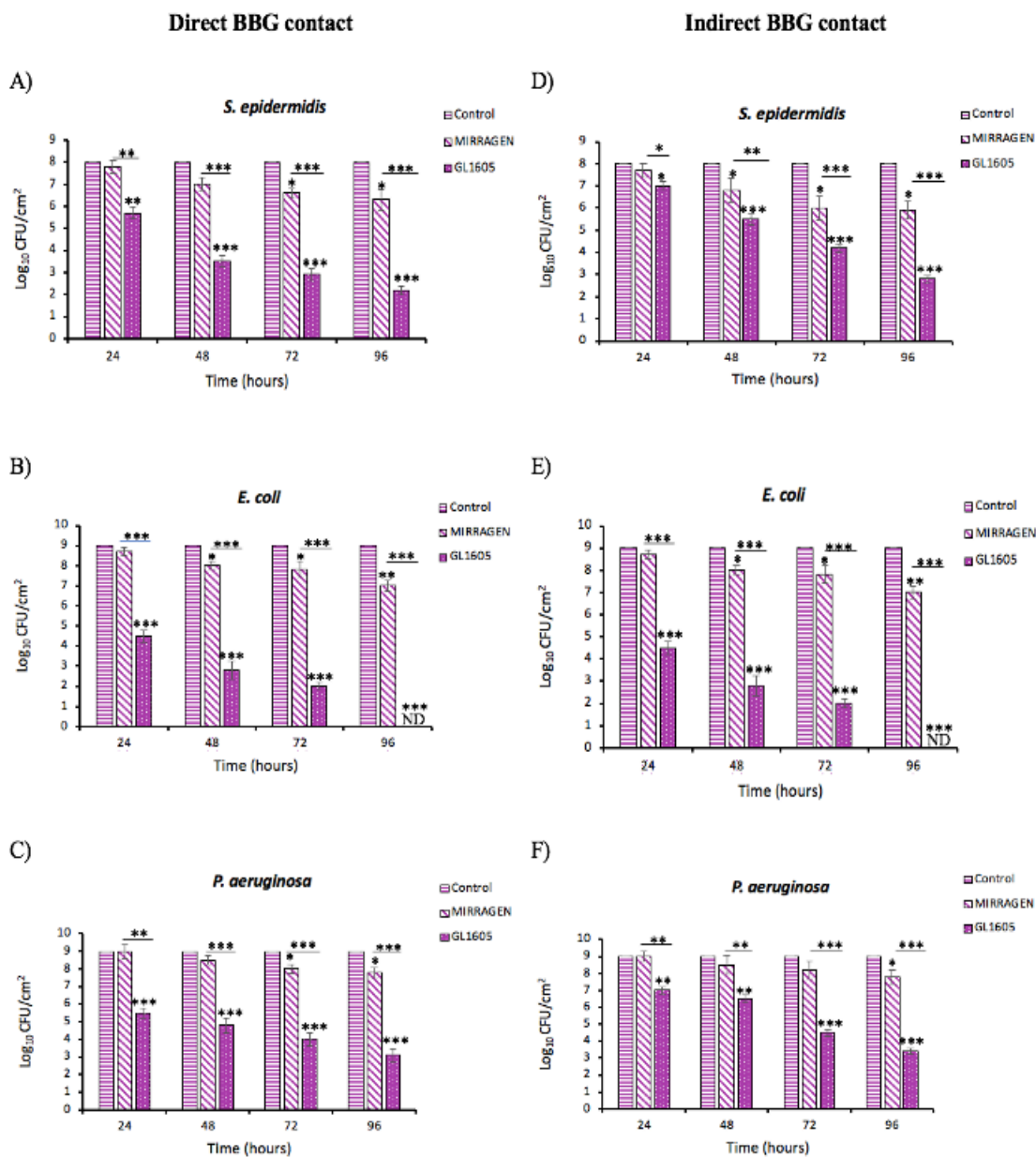


Figure 5. Borate bioactive glass direct and indirect application on severely pre-formed static biofilms. The BBG was applied to the biofilms directly (A, C, D) and indirectly (B, D, F). Treated biofilms were incubated 4 days and cell viability was measured every 24 hours. Results are expressed as the mean  $\pm$  standard deviation from three replicates. \*P < 0.05; \*\*P < 0.01; \*\*\*P < 0.001

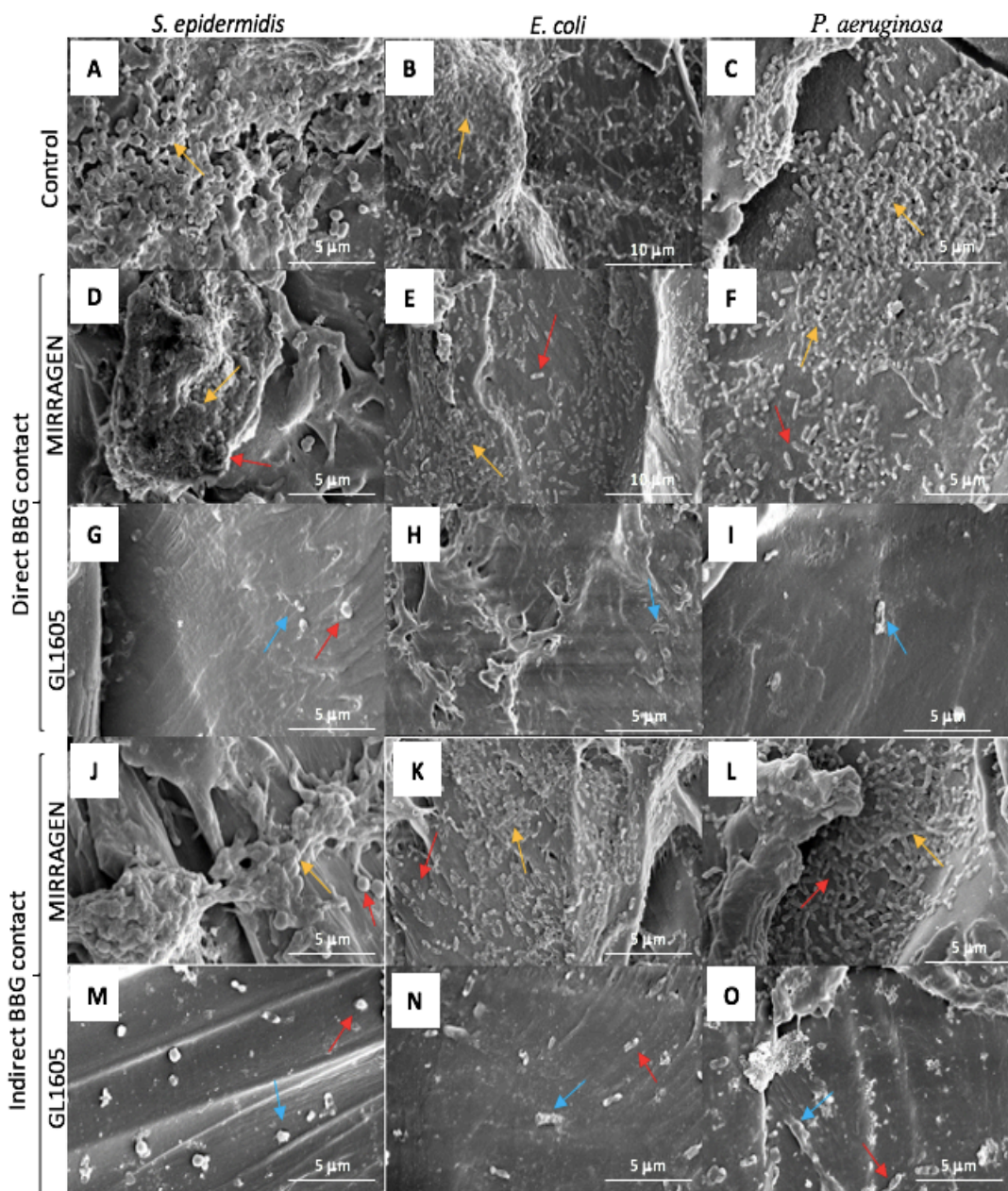


Figure 6. SEM. (A, B, C) biofilms before BBG treatment after 48 hours. (D, E, F) direct MIRRAGEN application. (G, H, I) Direct GL1605 application. (J, K, L) indirect MIRRAGEN application. (M, N, O) indirect GL1605 application. Yellow arrows indicate the presence of ECM, red arrows indicate viable cells, and blue arrows indicate dead cells

This gap is critical as HAIs continue to evolve in complexity, with antibiotic resistance posing an ever-increasing challenge. This research aims to bridge this gap by providing a

comprehensive analysis of the efficacy of BBGs, particularly focusing on their interaction with the biofilms of key bacterial species. By incorporating a multi-faceted approach that includes both direct and indirect applications of BBGs in static and dynamic growth conditions, this study seeks to offer a nuanced understanding of how these innovative materials can be effectively utilized to minimize HAIs.

Exploring the biofilm formation dynamics, the research employed a methodical approach to incubate bacterial cultures under static conditions to replicate the stable environment often found in clinical settings, where biofilms pose significant treatment challenges. Biofilm biomass was determined using the crystal violet assay; this assay exploits the principle of differential staining, wherein the crystal violet dye preferentially binds to the biofilm matrix and bacterial cells. The spectrophotometric analysis then allows for the quantification of this binding by measuring the OD of the stained biofilms, thereby providing an indirect but reliable estimate of biofilm mass.

The use of a predetermined OD<sub>c</sub> of 0.02 served as a threshold to distinguish between biofilm categories. Biofilm classification into non-adherent, weak, moderate, or severe biofilms enabled a nuanced interpretation of biofilm formation levels, which is essential for assessing the potential risk associated with biofilm-related infections and the efficacy of antimicrobial agents. The study's findings that all tested bacterial strains were capable of adherent biofilm formation within the initial 24-hour period highlight their capacity to establish surfaces. Notably, the progression to severe biofilm formation differed among the species, with *S. epidermidis* reaching a severe mode by the third day, while *E. coli* and *P. aeruginosa* required an additional day. This temporal difference may

reflect the inherent biological and physiological differences among the species, such as cell surface structures, biofilm matrix components, and growth rates.

Selecting severe biofilms for BBG efficacy assessment is a deliberate strategy to challenge the BGs with the most resilient biofilm structures. These severe biofilms are characterized by a dense ECM and a high cell density, which confer a heightened resistance to antimicrobial agents, making them a formidable model for testing. The ECM not only serves as a physical barrier but also plays a role in gene regulation, signaling, and community behavior within the biofilm, further complicating eradication efforts.

The dynamics of biofilm formation in a CDC biofilm reactor can be significantly different from static cultures due to the flow conditions that more closely mimic the natural environment of bacteria in host tissues or industrial settings. The physical characteristics of biofilm growth environments play a crucial role in shaping biofilm morphology and influencing the effectiveness of antimicrobial treatments. Moreover, dynamic conditions can lead to more heterogeneous and irregular biofilm structures that may show a different response to treatments compared to biofilms grown under static conditions.

The accelerated biofilm formation by *E. coli* and *P. aeruginosa* in a CDC biofilm reactor, as compared to *S. epidermidis*, can be attributed to their faster growth rates, efficient adhesion mechanisms, rapid EPS production, shear resistance, responsive genetic regulation, and effective quorum sensing. These factors are supported by evidence from microbial physiology and genomic studies, and they underscore the challenges posed by these organisms in biofilm-associated infections. These differences are well-documented in scientific literature, which shows that *P. aeruginosa*, for instance,

has biofilm phenotypes that are less susceptible to treatments when formed under certain conditions, highlighting their resilience and adaptability in forming biofilms. The intricate biofilm formation mechanisms and control pathways of these bacteria have been extensively studied, providing insights into their abilities to establish biofilms rapidly in dynamic environments. Studies have shown that *E. coli* can double in 20 minutes under optimal conditions, while *P. aeruginosa* and *S. epidermidis* typically have longer doubling times. Research comparing the biofilm formation capabilities of these bacteria under flow conditions has consistently reported faster biofilm formation by *E. coli* and *P. aeruginosa*. Additionally, genomic analyses reveal a higher number of genes related to adhesion and stress response in these bacteria, which may provide a genetic basis for their rapid biofilm formation abilities (14-16).

Previous studies have highlighted that the intricate regulatory systems of *P. aeruginosa* and *E. coli* contribute to their rapid biofilm development. These bacteria utilize advanced communication and control processes that facilitate quicker biofilm formation (41). In a study examining biofilm formation by various clinical isolates (42), it was observed that certain strains of *E. coli* and *P. aeruginosa* had a significantly greater ability to form biofilms compared to other strains. This ability was determined through both a microtiter plate method and SEM. The study found a strong association between specific pulsed-field type (PFT) groups and biofilm formation capabilities in these bacteria. Additionally, a correlation between the biofilm formation and the site of isolate collection was observed, indicating that clinical strains isolated from non-fluid sites such as tissues and respiratory tracts had a higher proportion of biofilm strains. This suggests

that the biofilm-forming capacity of these bacteria can vary significantly depending on their genetic makeup and the environment from which they are isolated.

This research not only provides insight into the biofilm formation capabilities of different bacterial species but also sets a foundational understanding for the evaluation of BBGs in a clinically relevant scenario. The BBGs' performance against severe biofilms could provide valuable data regarding their potential as alternative or adjunctive therapies in managing of biofilm-associated infections. The ability of metal-ion doped BBGs to disrupt or inhibit these complex structures could lead to novel anti-biofilm strategies, especially important in the context of increasing antibiotic resistance and the need for new antimicrobial strategies. In evaluating the anti-biofilm efficacy of the two BBG compositions, this study implemented both direct and indirect treatment methods. Direct application represents the physical incorporation of the BBGs into the biofilm matrix, whereas indirect application represents BBG dissolution products, encompassing a spectrum of released ions, into the biofilm environment.

Results demonstrate a significant reduction in biofilms within 2 days under direct application and within 3 days for indirect application of the GL1605. These findings were consistent across the three bacterial species, in both static and dynamic conditions, underscoring the potential of metal-ion doped BBGs as an effective approach to minimize HAIs complicated by biofilms. These four conditions were chosen to mimic the diverse environments encountered in clinical settings. Our findings indicate that the GL1605 demonstrates enhanced ant-biofilm properties. Specifically, bacterial growth was inhibited within 2 days under direct GL1605 application and within 3 days for indirect application. These results were consistent across all three bacterial species tested, under

both static and dynamic conditions. The study highlights the significance of metal-ion doping (particularly copper and zinc) in improving the biological functionalities of BBGs.

The application of Mirragen and GL1605 to the *S. epidermidis*, *E. coli*, and *P. aeruginosa* biofilms in a dynamic growth environment has yielded varying results. Directly applied Mirragen showed limited biofilm reduction capabilities, likely due to its inability to effectively disrupt the biofilm's ECM barrier, with *P. aeruginosa* biofilms exhibiting resilience, possibly due to their dense matrix and efficient resistance mechanisms. In contrast, GL1605 demonstrated significant bactericidal effects directly, suggesting an enhanced ability to penetrate or disassemble the biofilm structure. When applied indirectly, Mirragen's effects remained minimal, indicating that the mode of delivery is crucial for its efficacy. However, GL1605 retained a strong bactericidal impact even with indirect application, highlighting its potential for sustained action and deeper penetration into the biofilms of each bacterial species. This suggests that the metal dopants and delivery method of BBGs are critical determinants of their antimicrobial effectiveness, particularly under the challenging conditions of dynamic biofilm growth. In a comparative analysis, Jung et al. (43) observed that GL1605 demonstrated a rapid inhibitory effect on *P. aeruginosa* biofilms, achieving significant inhibition within four hours.

The indirect application of GL1605 also resulted in significant reductions in biofilm density. This suggests that the soluble ionic forms are sufficient to penetrate the biofilm matrix, disrupting its integrity over time. In contrast, MIRRAGEN's dissolution products demonstrated a markedly less effective anti-biofilm action, particularly against

*P. aeruginosa*. In contrast, MIRRAGEN exhibited a bacteriostatic effect, which was only observed after an extended period of 48 hours.

In assessing the effectiveness of GL1605 against bacterial biofilms grown under static and dynamic conditions, it has been observed that the bactericidal effect is similar in both environments, albeit with a slightly more pronounced effect under dynamic conditions. This can be attributed to the enhanced penetration and distribution of bioactive agents in a fluid dynamic environment, which increases the exposure of the bacterial biofilm to the antimicrobial agent, potentially leading to a higher log reduction in bacterial counts. The observed bactericidal effect of GL1605 after 48 hours in direct contact under both growth conditions may be attributed to the direct interaction and immediate bioavailability of the BBGs to the biofilm matrix and bacterial cells. However, when applied indirectly, the effectiveness of GL1605 requires a longer period (72 hours) to achieve a similar level of biofilm reduction, which can be due to the time needed for the bioactive components to diffuse through the biofilm matrix to reach the bacterial cells.

The scientific discussion around the effectiveness of GL1605 against bacterial biofilms is consistent with the understanding that the mode of growth and the method of application of the antimicrobial agent are critical factors in determining treatment outcomes. The detailed mechanisms of action, however, would require further investigation and could be substantiated by microbiological studies focusing on biofilm permeability, agent diffusion rates, and the impact of fluid dynamics on bacterial biofilm structures. BBGs' direct and indirect application on static and dynamic biofilms is summarized in Figure 7 (44-51).



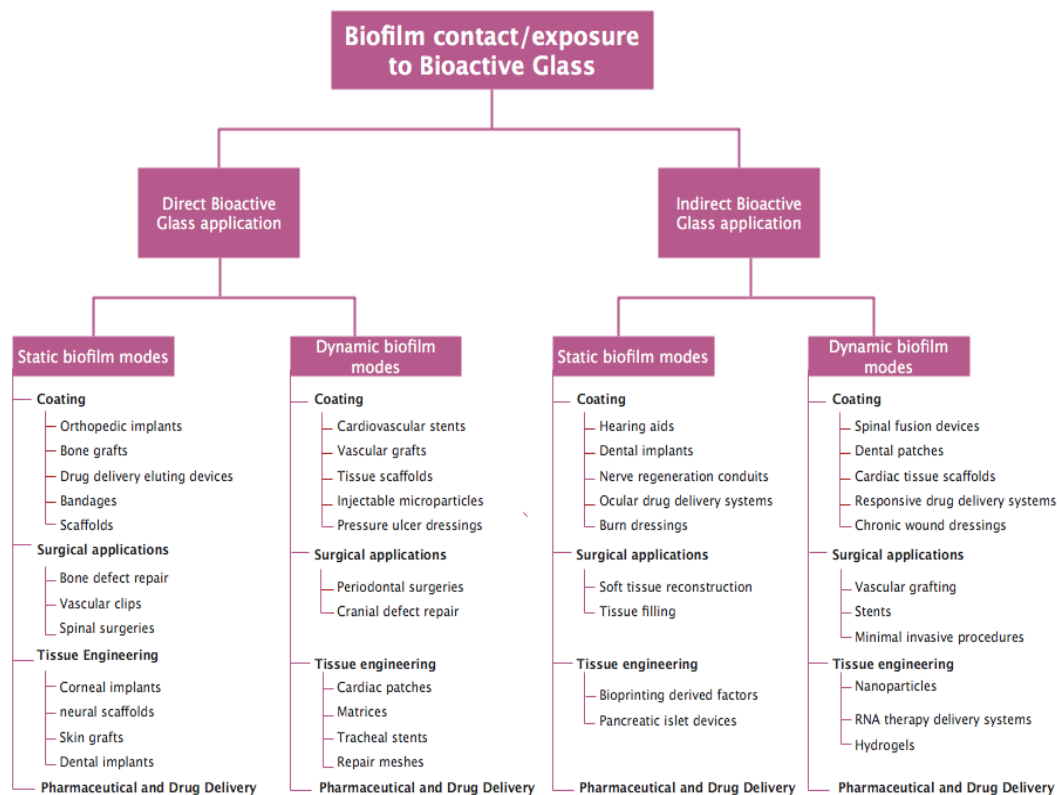


Figure 7. Summary of the clinical scenarios represented by the direct/indirect BBG application of static/dynamic biofilm modes.

In SEM analyses of bacterial biofilms, similar morphological characteristics and viable cell reductions were noted for both statically and dynamically grown biofilms. However, dynamically grown control biofilms exhibited a more disordered and aggregated appearance, particularly in *S. epidermidis*. This could be due to the enhanced nutrient flow and shear forces in dynamic environments, affecting biofilm integrity and promoting a more heterogeneous structure.

The dynamic growth conditions in a bioreactor can significantly influence biofilm morphology. The constant flow of nutrients enhances bacterial metabolism, leading to more rapid growth and biofilm maturation. Shear forces, meanwhile, can selectively

remove weaker parts of the biofilm, promoting a more irregular and “wobbly” appearance as only the most adherent cells and matrix components persist. This can lead to a more heterogeneous biofilm structure, with varying degrees of density and thickness, potentially affecting the biofilm's overall resilience and its response to antimicrobial agents. Furthermore, the shear stresses can induce a variable shear that may influence the biofilm's coverage and structure, leading to areas with increased density and thickness in regions experiencing the greatest variance in shear.

In the untreated controls, SEM images depict *S. epidermidis*, *E. coli*, and *P. aeruginosa* with intact, densely compacted biofilms, characterized by a robust ECM that supports the biofilm's three-dimensional architecture and cellular cohesion, crucial for the biofilm's resilience. Upon treatment with MIRRAGEN, *S. epidermidis* displayed a slightly disaggregated matrix, indicative of the beginning of biofilm breakdown, which is mirrored in the treatments of *E. coli* and *P. aeruginosa*. Although the biofilms remained largely intact, these subtle morphological changes suggest a compromise in the structural integrity of the biofilm matrix and potential alterations in cell surface interactions. The treatment with GL1605 yielded a stark contrast; the biofilms of *S. epidermidis* exhibit significant morphological alterations, characterized by a disrupted and disorganized extracellular matrix. *E. coli* showed considerable cellular damage, pointing to a profound impact on cell viability. *P. aeruginosa* similarly displayed extensive damage, with disrupted cells and a compromised matrix.

These observations underscore the critical influence of the GL1605 composition on anti-biofilm activity. The presence of ZnO and CuO in GL1605 enhanced its anti-biofilm efficacy against both gram-positive and gram-negative bacteria. The direct application

ensures immediate interaction of these ions with the biofilm, intensifying their impact. Indirect application, while effective, showed a delayed response due to the time required for the dissolution products to infiltrate and act upon the biofilm structure. Zinc is recognized for its role in impairing bacterial cell membrane integrity and inhibiting biofilm formation. Copper, while being toxic to bacterial cells at higher concentrations, can at trace levels disrupt bacterial metabolic processes and induce oxidative stress, leading to cell death. This synergistic effect of zinc and copper, along with the foundational ionic matrix of GL1605, is likely instrumental in its rapid bactericidal action observed in the direct application. Within 24 hours, a considerable log reduction in bacterial count was documented for *S. epidermidis*, escalating to complete biofilm eradication by 48 hours. Conversely, the absence of these trace elements in MIRRAGEN may account for its comparatively subdued anti-biofilm efficacy. While still capable of inducing log reductions in the bacterial count, MIRRAGEN required a longer exposure duration to exhibit bacteriostatic effects, demonstrating the pivotal role of trace elements in the GL1605's anti-microbial profile. The trace elements ZnO and CuO in GL1605 markedly potentiate its anti-biofilm effects, suggesting that their inclusion could be pivotal for the development of BBGs tailored for enhanced bactericidal applications. A study conducted by Schuhladen et al. (52) demonstrated the antibacterial effectiveness of copper and zinc doped BBGs against *E. coli* and *S. aureus* within 24 hours; however, the study found that the antibacterial effects of the BBGs varied depending on their composition. Other studies have observed that BBGs doped with minor concentrations of copper and zinc displayed a broad-spectrum antibacterial activity (53, 54).

#### 4. MATERIALS AND METHODS

**Bacteria Strain and Growth Conditions:** Bacterial isolates were chosen because of their use in various applications including standard assays and models, their known pathogenicity as well as their ability to form well-established biofilms.

All isolates were purchased from the American Type Culture Collection (ATCC) and included *Staphylococcus epidermidis* ATCC 6538, *Pseudomonas aeruginosa* ATCC 27853, *Escherichia coli* ATCC 9637. The strains were subcultured on tryptic soy agar (TSA) and incubated overnight at 37°C. A single bacterial colony from an overnight culture was resuspended in 5 mL of Tryptic Soy Broth (TSB) and incubated at 37 °C on a rotary shaker at 220 rpm.

**Biofilm growth:** Bacterial inoculum was diluted to obtain a bacterial count of about  $10^8$  CFU/mL, corresponding to an optical density (OD) of 0.05-0.09 at 600nm. The inoculum was added to a 96-microtiter well plate and supplemented with 2% glucose. The plate was incubated at 37 °C for 24 h, 48 h, 72, and 96 h, and the biofilm-forming ability was assessed at each time point using the crystal violet assay. For SEM analysis, polycarbonate coupons were placed in the well plate with the added bacterial inoculum. After severe biofilm development- determined by a crystal violet assay-, the coupons were rinsed three times in PBS. Dynamic cultivation of biofilms was carried out in a CDC biofilm reactor (BioSurfaces Technologies Corporation, Bozeman, MN, USA). Polycarbonate coupons were secured using the rods designed for a standard CDC biofilm reactor. Bacterial colonies were introduced into 500 mL of TSB for an overnight incubation at 37 °C. Subsequently, 1 mL of this bacterial culture was transferred into the

biofilm reactor. The reactor was then positioned on a heating plate, which was set to 34°C and the baffle was set to rotate at 130 rpm, this was done for a period of 24 hours to facilitate batch growth. In the next stage, a 10% TSB solution (300 mg/L) was employed in the Continuous Flow, Stirred Tank Reactor (CFSTR) configuration, ensuring a flow of approximately 6.9 mL/min for an extra 24 hours. Post this phase, rods were sterilely detached from the reactor and subjected to three PBS rinses. To ascertain the count of colony-forming units, a dilution method by 10-fold increments was performed. Prior to the biofilm harvest, the coupons underwent three PBS washes to eliminate any non-adherent cells. Finally, the biofilms were removed from the coupons using 1 mL of PBS.

**Biofilm biomass assessment:** Static biofilms: The microtitre well plates were aerobically incubated statically at 37°C. The biofilms were then washed with PBS three times to remove planktonic cells. The adhered biofilms in each well were then stained with crystal violet solution for 30 minutes, and the excess stain was rinsed. The well plate was rinsed with dH<sub>2</sub>O 3 times and allowed to air dry. 33% acetic acid was added to each well. The crystal violet dye was allowed to solubilize for 30 minutes, and the OD was at 595 nm using a 50 UV-Vis Spectrometer microplate reader.

**Reagents and materials:** A Simulated Body Fluid (SBF) medium with a similar ionic composition to human plasma was prepared to mimic the physiological conditions upon the BG interaction with the biofilms. A BBG, trade-named MIIRAGEN (51.6B<sub>2</sub>O<sub>3</sub>–20CaO–12K<sub>2</sub>O–5MgO–6Na<sub>2</sub>O–4% P<sub>2</sub>O<sub>5</sub>, in mol %) was used as the undoped BBG. Copper and zinc-doped BBG, trade-named GL1605 (51.6B<sub>2</sub>O<sub>3</sub>–20CaO–12K<sub>2</sub>O–5MgO–6Na<sub>2</sub>O–4% P<sub>2</sub>O<sub>5</sub>–1%ZnO–0.4%CuO, in mol %). The GL1605 was approved by the USFDA in 2018 and is currently used only for treating wounded animals and as a bone

grafting implant component. Both BBGs were provided by the Mo-Sci Corporation, Rolla, MO, USA.

**Anti-biofilm testing:** The coupons containing the pre-formed biofilms were added to a 24-well plate. For the direct BBG contact, 3 biopsy punches (6 mm in diameter) of the BBG were added to the plate along with SBF. Untreated glass wool was used as the negative control. The plate was for 24 h, 48 h, 72 h, and 96h. At each time point, the sample was plated on TSA plates at 37 °C for 24 hours and CFUs were observed. Experiments were performed in three replicates. For the indirect BBG contact, BBGs were added to SBF with a concentration of 170 mg/L and 140 mg/L for MIRGGAEN and the GL1605 respectively. The solution was incubated for 24 h, 48 h, 72 h, and 96 h and filtered at each time point using a 0.45-micron syringe filter. The filtrates were added to the coupons, and samples were plated on TSA plates at 37 °C for 24 hours followed by CFUs count.

**Scanning electron microscopy imaging:** SEM was employed to directly visualize the morphology of the biofilms and verify their development on the coupons. The growth of biofilms was achieved using the previously mentioned method. Individual coupons were immersed in a modified Karnovsky's fixative (2.5% glutaraldehyde and 4% formaldehyde) in 0.2 M phosphate-buffered saline (PBS) at pH 7.4, where they remained for a full day at ambient temperature. Following fixation, a graded series of ethanol was used to dehydrate the samples, involving three cycles of 20 minutes each, incrementally up to 100% ethanol, after which they were left to air-dry for no less than 48 hours. For SEM analysis, the coupons were then affixed to specimen stubs using double-sided

carbon tape and gold-palladium sputter coated. All coupons were imaged with a Helios 5 Hydra CX DualBeam SEM.

**Dynamic biofilms:** Scraped-off biofilms were fixed with 95% ethanol and left to incubate for 20 minutes. Following this, the mixture was transferred into microcentrifuge tubes and spun down to settle the fixed biofilms, which were then relocated to a microtiter plate and permitted to air dry. The process for the crystal violet assay was the same as previously mentioned. This procedure was performed in triplicate. The threshold for the OD 595nm for the negative control was established by taking the average OD 595nm from all the negative control wells and adding three times the standard deviation to this mean. Based on this threshold, the strains were classified into three categories of biofilm formation: weak ( $OD_c < OD \leq 2 OD_c$ ), moderate ( $2 OD_c < OD \leq 4 OD_c$ ), and strong ( $4 OD_c < OD$ ).

**Statistical Analysis:** Experiments were performed in three replicates. The data was analyzed by constructing a Time-Kill Curve for bacteria, plotting the logarithm of colony-forming units (CFU) against time. The viability of bacteria before and after treatment across different groups was assessed using a one-way analysis of variance (ANOVA). In cases where the data did not follow a normal distribution, the Kruskal-Wallis one-way analysis of variance on ranks was utilized, followed by the Tukey post hoc test to carry out pairwise multiple comparisons when the results were statistically significant. The findings are presented as the mean  $\pm$  the standard error of the mean. The threshold for significance was a P-value of less than 0.05. Differences were considered significant when the P-value was below this threshold.

## REFERENCES

1. Haque M, Sartelli M, McKimm J, Bakar MA. 2018. Health care-associated infections-An overview. *Infection and Drug Resistance* Volume 11:2321–2333.
2. Pinto H, Simões M, Borges A. 2021. Prevalence and Impact of Biofilms on Bloodstream and Urinary tract Infections: A Systematic Review and Meta-Analysis. *Antibiotics* 10:825.
3. Haque M, McKimm J, Sartelli M, Dhingra S, Labricciosa FM, Islam S, Jahan D, Nusrat T, Chowdhury TS, Catena F, Iskandar K, Catena F, Charan J. 2020. Strategies to Prevent Healthcare-Associated Infections: A Narrative Overview-Risk Management and Healthcare Policy Volume 13:1765–1780.
4. Founou RC, Founou LL. 2017. Clinical and economic impact of antibiotic resistance in developing countries: A systematic review and meta-analysis. *PLOS ONE* 12:e0189621.
5. Marchetti A, Rossiter R. 2013. Economic burden of healthcare-associated infection in US acute care hospitals: societal perspective. *Journal of Medical Economics* 16:1399–1404.
6. Calfee DP. 2012. Crisis in Hospital-Acquired, Healthcare-Associated infections. *Annual Review of Medicine* 63:359–371.
7. Assefa M, Amare A. 2022. Biofilm-Associated Multi-Drug Resistance in Hospital-Acquired Infections: A review. *Infection and Drug Resistance* Volume 15:5061–5068.
8. Caldara M, Belgiovine C, Secchi E, Rusconi R. 2022. Environmental, Microbiological, and Immunological Features of Bacterial Biofilms Associated with Implanted Medical Devices. *Clinical Microbiology Reviews* 35.
9. Khatoon Z, McTiernan CD, Suuronen EJ, Mah T-F, Alarcon EI. 2018. Bacterial biofilm formation on implantable devices and approaches to its treatment and prevention. *Heliyon* 4:e01067.
10. Vestby LK, Grønseth T, Simm R, Nesse LL. 2020. Bacterial Biofilm and its Role in the Pathogenesis of Disease. *Antibiotics* 9:59.
11. Morris SJ, Cerceo E. 2020. Trends, epidemiology, and management of Multi-Drug Resistant Gram-Negative bacterial infections in the hospitalized setting. *Antibiotics* 9:196.



12. Tajeddin E, Rashidan M, Razaghi M, Javadi SSS, Sherafat SJ, Alebouyeh M, Sarbazi MR, Mansouri N, Zali MR. 2016. The role of the intensive care unit environment and health-care workers in the transmission of bacteria associated with hospital acquired infections. *Journal of Infection and Public Health* 9:13–23.
13. Genovese C, La Fauci V, D’Amato S, Squeri A, Anzalone C, Costa GB, Fedele F, Squeri R. 2020. Molecular epidemiology of antimicrobial resistant microorganisms in the 21th century: a review of the literature. *Acta Bio-medica: Atenei Parmensis* 91:256–273.
14. Mack D, Davies A, Harris LG, Jeeves RE, Pascoe B, Knobloch J, Rohde H, Wilkinson TS. 2012. *Staphylococcus epidermidis* in Biomaterial-Associated Infections, p. 25–56. *In Springer eBooks*.
15. Li X, Fan H, Zi H, Hu H-X, Li B, Huang J, Luo P, Zeng X. 2022. Global and regional burden of bacterial antimicrobial resistance in urinary tract infections in 2019. *Journal of Clinical Medicine* 11:2817.
16. Pachori P, Gothalwal R, Gandhi P. 2019. Emergence of antibiotic resistance *Pseudomonas aeruginosa* in intensive care unit; a critical review. *Genes and Diseases* 6:109–119.
17. Raman G, Avendano EE, Chan J, Merchant S, Puzniak L. 2018. Risk factors for hospitalized patients with resistant or multidrug-resistant *Pseudomonas aeruginosa* infections: a systematic review and meta-analysis. *SPRINGER* 7.
18. Mancuso G, Midiri A, Gerace E, Biondo C. 2021. Bacterial antibiotic resistance: the most critical pathogens. *Pathogens* 10:1310.
19. Muteeb G, Rehman T, Shahwan M, Aatif M. 2023. Origin of Antibiotics and antibiotic resistance, and their Impacts on Drug Development: A Narrative review. *Pharmaceuticals* 16:1615.
20. 2022. The biggest antibiotic-resistant threats in the U.S. Centers for Disease Control and Prevention. <https://www.cdc.gov/drugresistance/biggest-threats.html>.
21. Sahli C, Moya S, Lomas JS, Gravier-Pelletier C, Briandet R, Hémadi M. 2022. Recent advances in nanotechnology for eradicating bacterial biofilm. *Theranostics* 12:2383–2405.
22. Atkinson I. 2022. Antibiofilm Activity of biocide metal ions containing bioactive glasses (BGs): a mini review. *Bioengineering* 9:489.
23. Lerminiaux NA, Cameron ADS. 2019. Horizontal transfer of antibiotic resistance genes in clinical environments. *Canadian Journal of Microbiology* 65:34–44.

24. Ege D, Zheng K, Boccaccini AR. 2022. Borate Bioactive Glasses (BBG): bone regeneration, wound healing applications, and future directions. *ACS Applied Bio Materials* 5:3608–3622.
25. Neğu I, Ristoscu C. 2023. Bioactive Glasses for Soft and Hard Tissue Healing Applications—A Short Review. *Applied Sciences* 13:6151.
26. Westenberg DJ, Viswanathan R, Kadyk DL, Hibbs S, Kopel J, Day DE. 2021. Evaluation of three Borate-Bioactive Glass compositions for antibacterial applications. *Advances in Microbiology* 11:646–656.
27. Baino F, Novajra G, Miguez-Pacheco V, Boccaccini AR, Brovarone CV. 2016. Bioactive glasses: Special applications outside the skeletal system. *Journal of Non-Crystalline Solids* 432:15–30.
28. Gupta B, Papke JB, Mohammad-Khāh A, Day DE, Harkins AB. 2016. Effects of chemically doped bioactive borate glass on neuron regrowth and regeneration. *Annals of Biomedical Engineering* 44:3468–3477.
29. Urso E, Maffia M. 2015. Behind the Link between Copper and Angiogenesis: Established Mechanisms and an Overview on the Role of Vascular Copper Transport Systems. *Journal of Vascular Research* 52:172–196.
30. Tang D, Tare RS, Yang L, Williams D, Ou KL. 2016. Biofabrication of bone tissue: approaches, challenges and translation for bone regeneration. *Biomaterials* 83:363–382.
31. Dalecki AG, Crawford CL, Wolschendorf F. 2017. Copper and antibiotics, p. 193–260. *In* *Advances in Microbial Physiology*.
32. Argueta-Figueroa L, Morales-Luckie RA, Vilchis RJS, Olea-Mejía O. 2014. Synthesis, characterization and antibacterial activity of copper, nickel and bimetallic Cu–Ni nanoparticles for potential use in dental materials. *Progress in Natural Science: Materials International* 24:321–328.
33. Zhang H, Yang F, Zhang Q, Hui A, Wang A. 2022. Structural evolution of palygorskite as the nanocarrier of silver nanoparticles for improving antibacterial activity. *ACS Applied Bio Materials* 5:3960–3971.
34. Sousa BC, Massar C, Gleason MA, Cote DL. 2021. On the emergence of antibacterial and antiviral copper cold spray coatings. *Journal of Biological Engineering* 15.
35. Ghosh R, Das S, Mallick SP, Beyene Z. 2022. A review on the antimicrobial and antibiofilm activity of doped hydroxyapatite and its composites for biomedical applications. *Materials Today Communications* 31:103311.

36. Sirelkhatim A, Mahmud S, Seeni A, Kaus NHM, Ann LC, Bakhori SKM, Hasan H, Mohamad D. 2015. Review on Zinc oxide nanoparticles: antibacterial activity and toxicity Mechanism. *Nano-Micro Letters* 7:219–242.
37. Mitra D, Kang E, Neoh KG. 2019. Antimicrobial Copper-Based Materials and Coatings: Potential Multifaceted Biomedical Applications. *ACS Applied Materials & Interfaces* 12:21159–21182.
38. Saidin S, Jumat MA, Amin NAAM, Al-Hammadi ASS. 2021. Organic and inorganic antibacterial approaches in combating bacterial infection for biomedical application. *Materials Science and Engineering: C* 118:111382.
39. Ottomeyer M, Mohammadkah A, Day DE, Westenberg DJ. 2016. Broad-Spectrum antibacterial characteristics of four novel Borate-Based bioactive glasses. *Advances in Microbiology* 06:776–787.
40. Wang H, Zhao S, Zhou J, Yan S, Huang W, Zhang C, Rahaman MN, Wang D. 2014. Evaluation of borate bioactive glass scaffolds as a controlled delivery system for copper ions in stimulating osteogenesis and angiogenesis in bone healing. *Journal of Materials Chemistry B* 2:8547–8557.
41. Cerqueira L, Oliveira JA, Nicolau A, Azevedo NF, Vieira MJ. 2013. Biofilm formation with mixed cultures of *Pseudomonas aeruginosa*/*Escherichia coli* on silicone using artificial urine to mimic urinary catheters. *Biofouling* 29:829–840.
42. Sánchez CJ, Mende K, Beckius ML, Akers KS, Romano DR, Wenke JC, Murray CK. 2013. Biofilm formation by clinical isolates and the implications in chronic infections. *BMC Infectious Diseases* 13.
43. Jung SB, Day T, Boone T, Buziak B, Omar A. 2019. Anti-biofilm activity of two novel, borate based, bioactive glass wound dressings. *Biomedical Glasses* 5:67–75.
44. Zhou P, Garcia BL, Kotsakis GA. 2022. Comparison of antibacterial and antibiofilm activity of bioactive glass compounds S53P4 and 45S5. *BMC Microbiology* 22.
45. Awaid M, Cacciotti I. 2022. Bioactive Glasses with Antibacterial Properties: Mechanisms, Compositions, and Applications. In Book: *Bioactive Glasses and Glass-Ceramics* (pp581-614) 581–614.
46. Cannio M, Bellucci D, Roether JA, Boccaccini DN, Cannillo V. 2021. Bioactive Glass Applications: A Literature Review of human clinical trials. *Materials* 14:5440
47. Dash PA, Mohanty S, Nayak SK. 2023. A review on bioactive glass, its modifications and applications in healthcare sectors. *Journal of Non-Crystalline Solids* 614:122404.

48. Fernandes JS, Gentile P, Pires RA, Reis RL, Hatton PV. 2017. Multifunctional bioactive glass and glass-ceramic biomaterials with antibacterial properties for repair and regeneration of bone tissue. *Acta Biomaterialia* 59:2–11.
49. Baino F, Fiorilli SL, Vitale-Brovarone C. 2016. Bioactive glass-based materials with hierarchical porosity for medical applications: Review of recent advances. *Acta Biomaterialia* 42:18–32.
50. Jones JR, Brauer DS, Hupa L, Greenspan DC. 2016. Bioglass and bioactive glasses and their impact on healthcare. *International Journal of Applied Glass Science* 7:423–434.
51. Baino F. 2019. Biomedical, therapeutic and clinical applications of bioactive glasses. Elsevier eBooks.
52. Schuhladen K, Stich L, Schmidt J, Steinkasserer A, Boccaccini AR, Zinser E. 2020. Cu, Zn doped borate bioactive glasses: antibacterial efficacy and dose-dependent in vitro modulation of murine dendritic cells. *Biomaterials Science* 8:2143–2155.
53. Elmowafy B, Abdelghany AM, Ramadan R, Ghazy R, Meaz TM. 2022. Synthesis, structural characterization, and antibacterial studies of new borate 13-93B3 bioglasses with low copper dopant. *Egyptian Journal of Chemistry* 0:0.
54. Mehrabi T, Mesgar AS. 2022. In vitro biomineralization potential in simulated wound fluid and antibacterial efficacy of biologically-active glass nanoparticles containing B2O3/ZnO. *Colloids and Surfaces B: Biointerfaces* 212:112338.

#### IV. IN VITRO ASSESMENT OF THE ANTI-BIOFILM EFFECTIVENESS OF COPPER AND ZINC ENHANCED BORATE BIOACTIVE GLASS USING PROCESSED MICROSCOPIC IMAGES

##### ABSTRACT

The escalating burden of nosocomial infections presents a formidable challenge to healthcare systems worldwide, leading to increased morbidity, prolonged hospital stays, and elevated healthcare costs. These infections are often resistant to conventional antibiotic therapies due to their association with biofilms which contribute to the persistence and resistance of pathogens. In addressing the challenge of biofilm-associated nosocomial infections, borate bioactive glasses (BBGs) have emerged as promising materials. Doping these glasses with antimicrobial metals could potentially enhance their antibacterial properties to prevent biofilm formation. This study undertakes a rigorous evaluation of the antibiofilm efficacy of copper and zinc-doped BBGs employing processed imaging techniques and machine learning algorithms that allow for the in-depth analysis of biofilms. The study focused on three bacterial species known for their propensity to form biofilms and cause nosocomial infections: *Staphylococcus epidermidis*, *Escherichia coli*, and *Pseudomonas aeruginosa*. Results indicated a marked reduction in biofilm viability morphological disruptions upon treatment with copper and zinc-doped BBGs, highlighting their potential as a novel approach to minimize the persistent challenge of nosocomial infections.

## 1. INTRODUCTION

Nosocomial infections constitute a major health concern globally, significantly impacting patient outcomes and healthcare economics. These infections include a wide range of infections, such as surgical site infections, ventilator-associated pneumonia, and catheter-associated urinary tract infections, among others (1, 2). The Centers for Disease Control and Prevention (CDC) estimates that on any given day, about 1 in 31 hospital patients acquire at least one type of nosocomial infection (3). Moreover, The World Health Organization (WHO) has identified these infections as a critical area of concern, with estimates indicating that millions of patients worldwide are affected annually (4). The persistence and spread of these infections are facilitated by the increasing prevalence of antibiotic-resistant bacteria, making nosocomial infections a critical challenge to manage and control.

A key contributing factor in the challenge of treating nosocomial infections is the ability of many pathogens to form biofilms on both biotic and abiotic surfaces, including medical devices (5). Biofilms are complex, structured communities of bacteria encased in an extracellular polymeric substance (EPS) matrix that they produce. This matrix protects the bacteria from antibiotics and the host immune system, contributing to the chronic nature of biofilm-associated infections (5, 6). Biofilms are known to be up to 1,000 times more resistant to antibiotics than planktonic bacteria, highlighting the need for novel approaches to disrupt biofilm formation and eradicate biofilm-associated pathogens (7).

BBGs represent an innovative class of biomaterials with promising applications in bone regeneration and wound healing. Unlike other bioactive glasses, BBGs exhibit faster degradation rates and higher bioactivity, which can be advantageous in biomedical and clinical applications (8, 9). The incorporation of therapeutic ions into the BBG matrix can further enhance their functionality, providing targeted antimicrobial effects in addition to their regenerative properties (10, 11).

Doping the BBGs with antimicrobial metal ions, particularly, copper and zinc, offers a strategic approach to combating biofilm formation (12, 13). Copper is well-known for its broad-spectrum antimicrobial effects, attributed to its ability to disrupt bacterial cell membranes and interfere with vital cellular processes (14). Zinc, on the other hand, has been shown to inhibit biofilm formation and reduce the virulence of pathogens without significant toxicity to human cells (15). The synergistic inclusion of Cu and Zn into BBGs aims to exploit these antimicrobial properties, targeting biofilm-forming bacteria and preventing nosocomial infections.

*S. epidermidis*, *E. coli*, and *P. aeruginosa* were selected for this study based on their clinical relevance and known ability to cause device-related nosocomial infections. *S. epidermidis* is a commensal bacterium of human skin that has emerged as a leading cause of device-related infections, exploiting compromised host barriers to establish biofilms on indwelling medical devices. Its capacity for biofilm formation is closely linked to the production of polysaccharide intercellular adhesin (PIA), facilitating adherence and accumulation on surfaces (16, 17). *E. coli*, predominantly known as a gut commensal, can act as an opportunistic pathogen when externalized from its native environment. It is responsible for a significant proportion of urinary tract infections (UTIs), many of which

are associated with biofilm formation on urinary catheters (18). *P. aeruginosa* is recognized for its role in chronic infections and its remarkable ability to resist antibiotics, partly due to its biofilm-forming capabilities. This pathogen is a common cause of ventilator-associated pneumonia and infections in burn units, with biofilms contributing to its persistence and resistance (19, 20).

In the context of evaluating the antibiofilm efficacy of Cu/Zn-BBGs, microscopic imaging plays a crucial role. Scanning Electron Microscopy (SEM) is a powerful direct imaging technique that evaluates the biofilms' morphological characteristics with high accuracy (21). SEM helps discern the alterations in the biofilm's architecture with high-resolution imagery, providing insight into the extent of biofilm degradation or inhibition. Furthermore, a comparison of cell morphology between treated and untreated biofilms can yield information on the mechanisms by which these BBGs exert their antibiofilm effects—whether through disruption of the biofilm's protective matrix, direct damage to the bacterial cell walls, or a combination of both (22).

Moreover, automatic segmentation is a potent tool for calculating areas covered by biofilms by partitioning the biofilms into sections. This method overcomes the limitations achieved by common manual thresholding that can yield inaccurate results such as insufficient image resolution for individual cells. Given that the intensity values of the SEM contrast and the biofilms are very similar, manual thresholding makes it difficult to analyze the images. Therefore, this study provides an automatic quantitative SEM analysis to assess the effectiveness of biofilm disruption achieved and to calculate the biofilm area after treatment. Ultimately, the application of machine learning



algorithms in image segmentation provides critical quantitative data that complements the qualitative visual evidence obtained through SEM.

CLSM stands at the forefront of imaging technologies for the study of biofilms, offering deeper insights into their complex structures and behaviors (23, 24, 25). The technique's capacity for high-resolution imaging facilitates the detailed analysis of biofilm disruption and cell death induced by these novel antimicrobial agents. By employing fluorescent stains that differentiate between live and dead cells, CLSM allows for the quantification of treatment-induced cytotoxicity within biofilms, providing a clear picture of the antimicrobial activity of Cu/Zn-BBGs. Furthermore, CLSM allows for the non-invasive, in situ visualization of biofilms in three dimensions by penetrating the depth of biofilms, layer by layer, to generate comprehensive three-dimensional reconstructions (26). This capability is pivotal for understanding the spatial organization and heterogeneity within biofilms, which are critical factors in their resilience and pathogenicity. The three-dimensional insights obtained through CLSM are critical for observing the intricate architecture of biofilms, including the distribution of microbial cells as well as the biofilm's volume, thickness, and confluency (26, 27).

## **2. RESULTS**

### **2.1. ANTIBIOFILM EFFECTIVENESS**

The anti-biofilm effect of the BBGs was assessed quantitatively by examining the CFU (Table 1). The GL1605 was found to markedly reduce the bacterial biofilms compared to the negative control, and results were consistent among the bacterial species.

In contrast, no significant changes were observed with the biofilms treated with Mirragen. GL1605 achieved a statistically significant 4-log reduction in biofilms after 48 h compared to the control, signifying a 10,000-fold decrease in viable bacteria.

Table 1. Log reduction of biofilms after 24 hours and 48 hours of exposure to the bioactive glasses

CFU log reduction after 24 hours			
	Control	Mirragen	GL1605
<i>S. epidermidis</i>	0	1	4 (p<0.01)
<i>E. coli</i>	0	1.5	4.5 (p<0.01)
<i>P. aeruginosa</i>	0	0.5	3.5 (p<0.05)
CFU log reduction after 48 hours			
<i>S. epidermidis</i>	0	2	7 (p<0.001)
<i>E. coli</i>	0	3.5 (p<0.05)	8 (p<0.001)
<i>P. aeruginosa</i>	0	2.5	6.5 (p<0.001)

## 2.2. SEM

SEM images in Figure 1, provide a vivid depiction of the biofilm structures formed by *S. epidermidis*, *E. coli*, and *P. aeruginosa*. These images are provided both before and after the segmentation process. The control images show extensive and resilient biofilm formation. After Mirragen treatment, the SEM images revealed only minor damages to the biofilm structures, suggesting partial disintegration of the biofilms that largely maintained their viability and structural integrity. In contrast, GL1605 treatment exhibited a homogenous disruption of the biofilm architecture, including dead cells and debris.

A critical evaluation of the segmentation accuracy in the SEM images was performed to compare automatic machine learning algorithms with traditional manual thresholding techniques (Fig 1S). The machine learning approach utilized for segmentation is described as employing a diverse array of feature detection methods, including texture filters and edge detection algorithms, which are paramount in training the models to differentiate between the biofilm and the surface in the SEM images. ROIs were randomly positioned on both the biofilm and the surface to provide the algorithm with a variety of training data, which enhances its ability to recognize different features within the images. This automated approach shows several advantages over the manual method. Primarily, it does not depend on the variations in intensity that manual thresholding does, which is particularly beneficial in situations where the SEM images have non-uniform backgrounds. Such non-uniformity can often pose a challenge for manual segmentation, leading to inaccuracies and inconsistencies in the results. Moreover, the automatic method's independence from intensity differences can allow for greater precision in

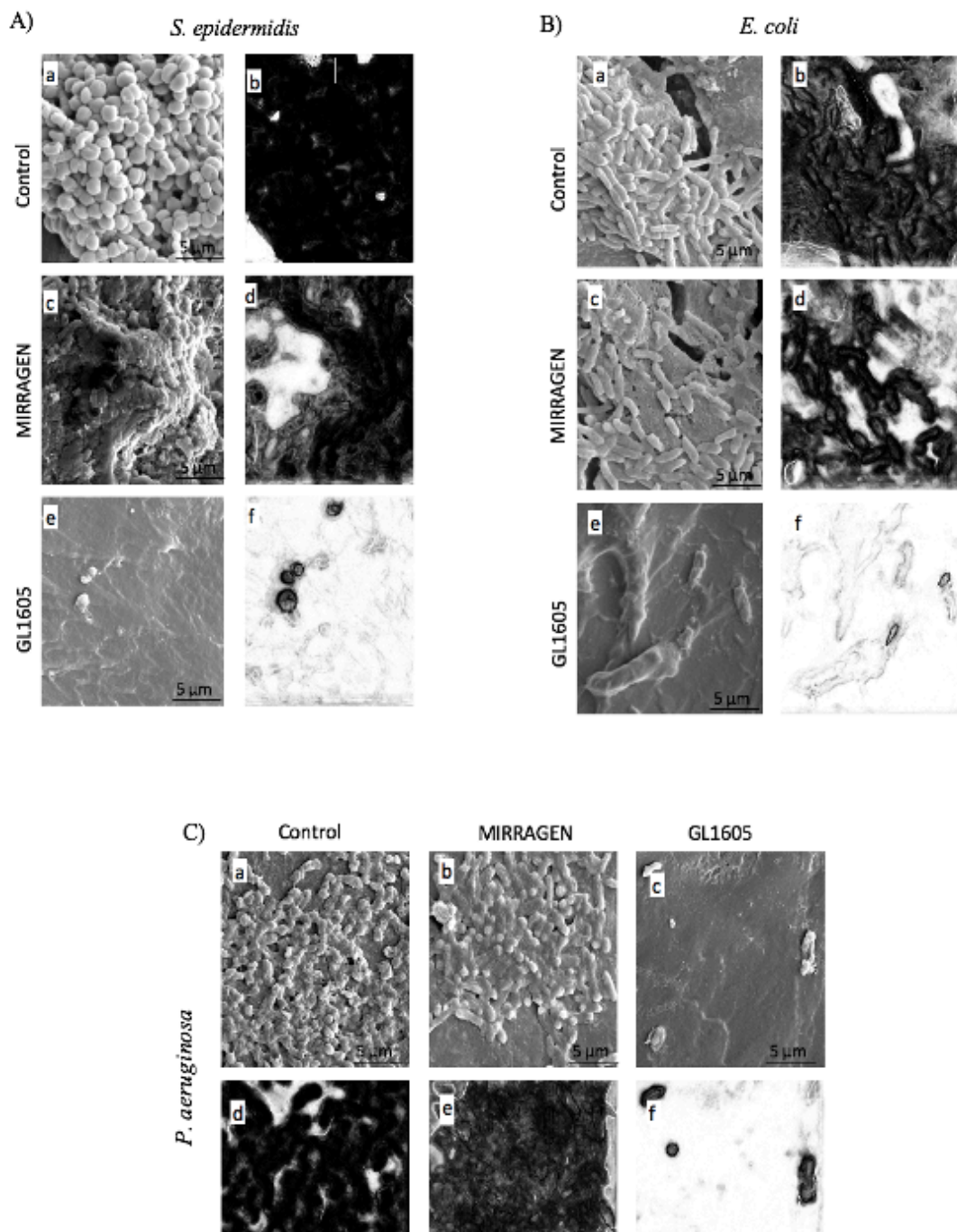


Figure 1. SEM. SEM images of (A) *S. epidermidis*, (B) *E. coli*, and (C) *P. aeruginosa* biofilms (x2500 magnification) (a) control (b) MIRRAGEN treatment (c) GL1605 treatment. (d-f) Whole SEM images segmented automatically, where biofilms and surface are labelled black and white respectively.

identifying the biofilm boundaries, especially when the biofilm and the surface have similar grayscale values. The efficacy of biofilm removal treatments is quantitatively evaluated in Figure 2. Mirragen removed only a few amounts of biofilm. This suggests that while Mirragen possesses some activity against biofilms, it is relatively limited and may not be sufficient for applications requiring substantial biofilm reduction. On the other hand, GL1605 has demonstrated remarkable efficacy, removing upwards of 90% of the biofilms, indicating its potent disruptive effect on the biofilm matrix and capability of penetrating and eliminating the biofilm's structural components.

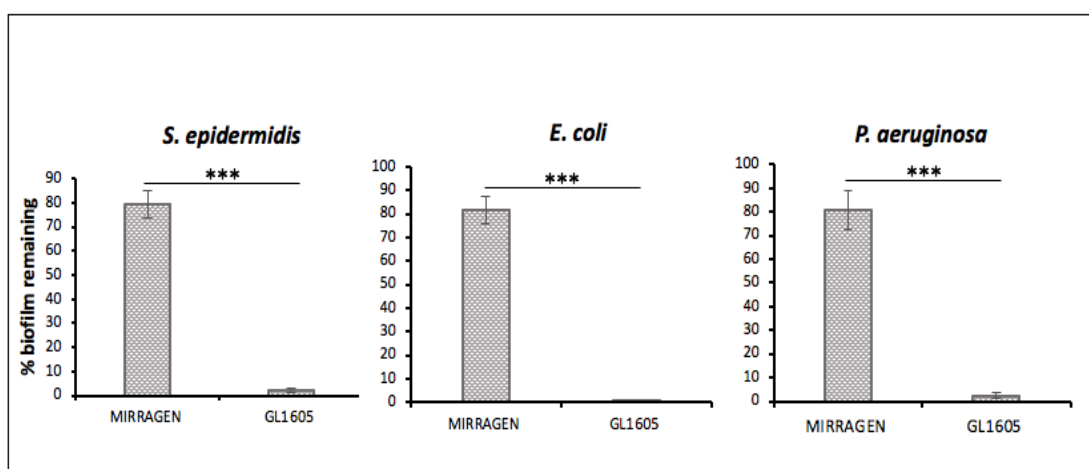


Figure 2. Mean % of remaining biofilms from segmented images after 48 hours of bioactive glass treatment. \*\*\* $p < 0.001$

### 2.3. CLSM

In the *S. epidermidis* control group, a predominant population of viable cells was observed, with minimal presence of dead cells. After Mirragen contact with the biofilms for 48 hours, the viability of the cells did not exhibit significant reduction, and only a

slight increase in the number of nonviable cells was observed. In contrast, GL1605 treatment for the same duration markedly decreased the number of viable cells, with a concurrent increase in the dead cell count (Fig 3A).

Quantitative analysis of fluorescence intensity across the respective channels provided insight into the differential staining between viable and nonviable cells. Treatment with Mirragen yielded fluorescence intensities similar to the control, indicating little to no effect on cell viability. In stark contrast, the GL1605 treatment resulted in a substantial deviation in fluorescence intensities, suggesting a pronounced increase in cell mortality (Fig 3B).

The proportion of live to dead cells was subsequently calculated, revealing that after a 48-hour exposure to Mirragen, less than 10% of the cells were nonviable. On the other hand, GL1605 treatment resulted in a greater than 90% reduction in viable cell count (Fig 3C). Furthermore, the ratio of SYTO to PI fluorescence is depicted in Fig 3D. This ratio was found to be negligible in the GL1605-treated biofilms as opposed to the Mirragen, which retained a ratio similar to that of the untreated control. This indicates that fluorescence emanating from viable cells was significantly higher compared to that of dead cells, underscoring the effectiveness of GL1605 in compromising cell viability.

Similarly, the antibiofilm efficacy of Mirragen and GL1605 against *E. coli* and *P. aeruginosa* demonstrated consistent patterns. Within 48 hours of exposure to Mirragen, a slight decrease in viable cell was observed for both bacterial species. In contrast, GL1605 treatment exhibited a significant reduction in viable cells and a concomitant increase in dead cells. This effect was substantiated by the fluorescence intensity measurements, which indicated a similarity of SYTO dye intensity over PI in biofilms treated with

Mirrugen and the untreated controls. In contrast, for GL1605-treated biofilms, PI intensity was markedly high compared to SYTO.

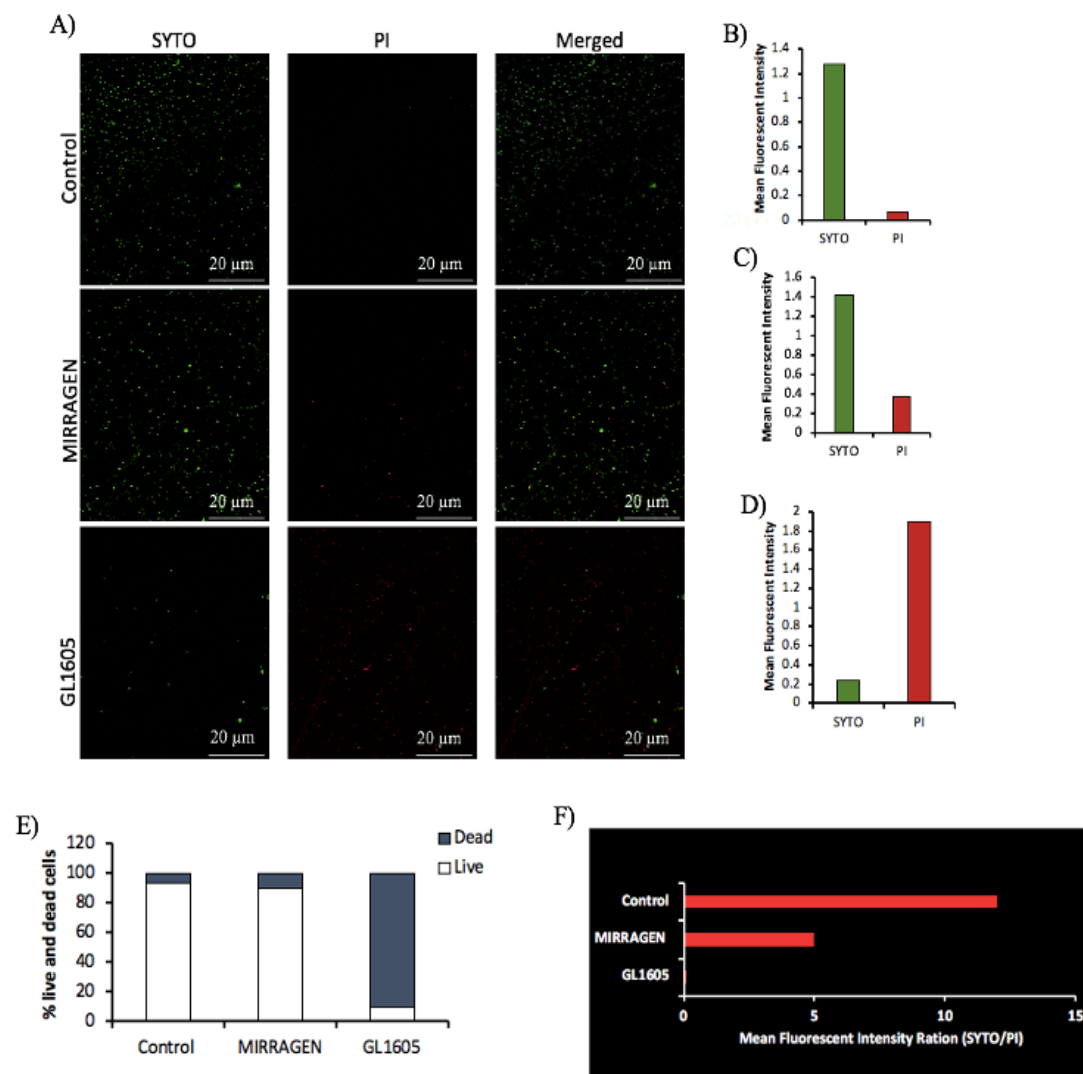


Figure 3. CLSM. (a) Confocal images of *S. epidermidis* before and after bioactive glass treatment for 48 h (b-d) mean fluorescent intensity (e) percentage of live and dead cells remaining (f) ratios of the SYTO and PI fluorescent intensities

Mirrugen exhibited a minimal inhibition effect on the viability of *E. coli* biofilms (Figs 4A, 5A), with only a 5% reduction. In *P. aeruginosa*, approximately a 6% decrease in

viable cell count was achieved. Whereas, GL1605 treatment resulted in a significant reduction of viable cells, exceeding 90% for both *E. coli* and *P. aeruginosa* (Figs 4C, 5C).

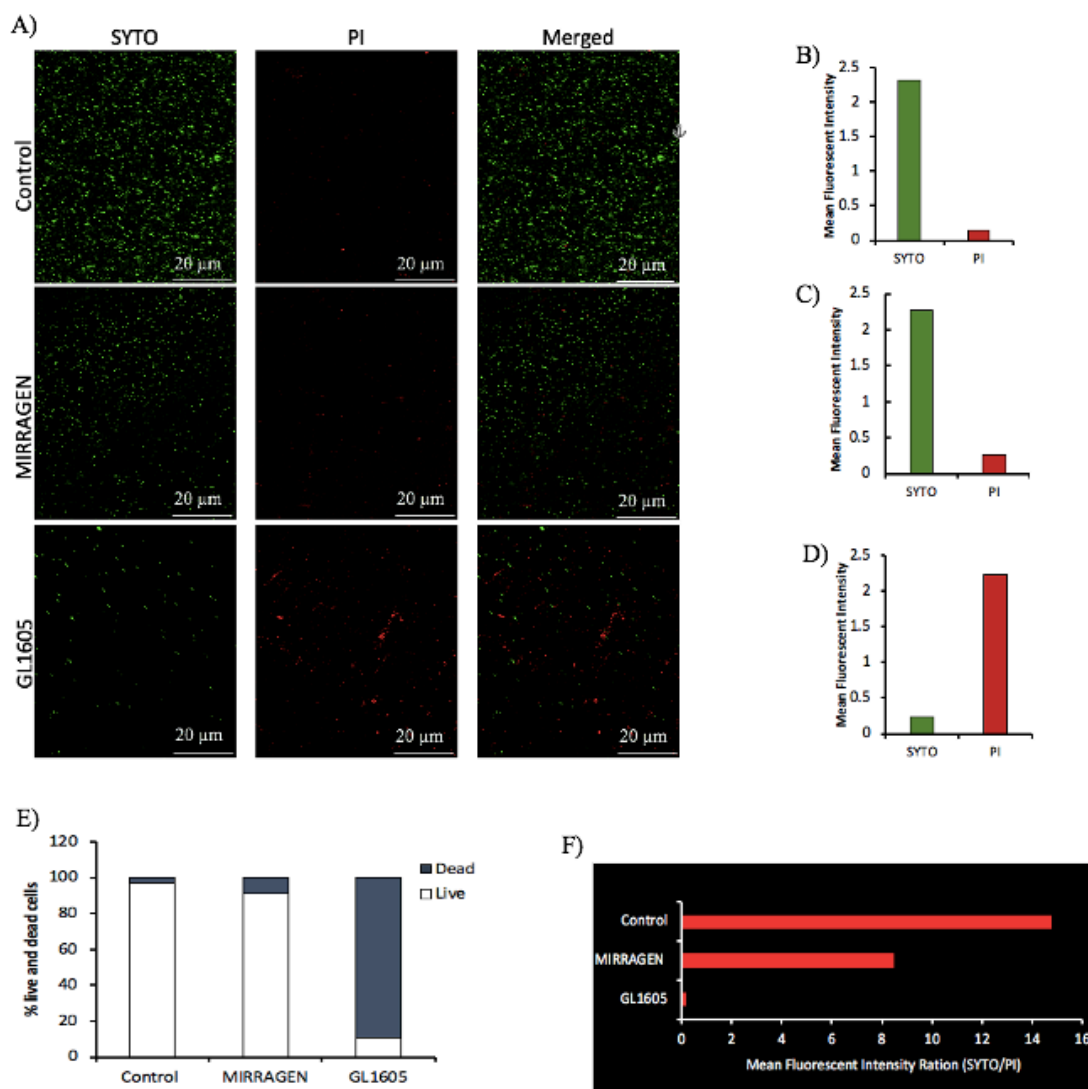


Figure 4. CLSM. (a) Confocal images of *E. coli* before and after bioactive glass treatment for 48 h (b-d) mean fluorescent intensity (e) percentage of live and dead cells remaining (f) ratios of the SYTO and PI fluorescent intensities



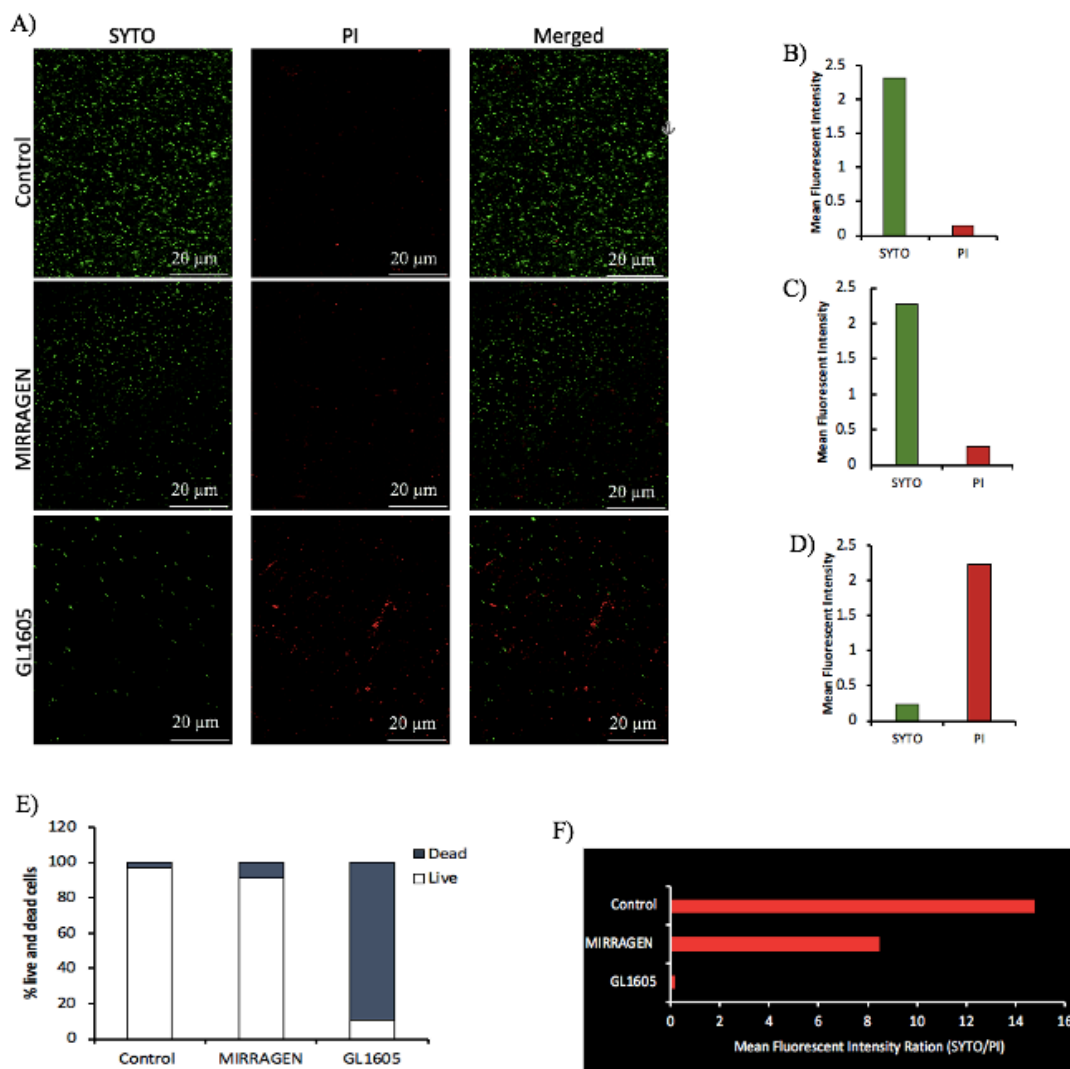


Figure 5. CLSM. (a) Confocal images of *P. aeruginosa* before and after bioactive glass treatment for 48 h (b-d) mean fluorescent intensity (e) percentage of live and dead cells remaining (f) ratios of the SYTO and PI fluorescent intensities.

Moreover, the fluorescence intensity from Mirragen was significantly higher in biofilms treated with Mirragen compared to GL1605 treated biofilm (Figs 4B, 5B). The fluorescent ratios of Mirragen-treated biofilms closely resembled those of the controls (Figs 4D, 5D).

However, the ratios for GL1605-treated biofilms were significantly diminished, reflecting the extensive cellular mortality induced by the treatment.

In *P. aeruginosa*, approximately a 6% decrease in viable cell count was achieved. In stark contrast, GL1605 treatment resulted in a significant reduction of viable cells, exceeding 90% for both *E. coli* and *P. aeruginosa* (Figs 4C, 5C). Moreover, the fluorescence intensity from Mirragen was significantly higher in biofilms treated with Mirragen compared to GL1605 treated biofilm (Figs 4B, 5B). The fluorescent ratios of Mirragen-treated biofilms closely resembled those of the controls (Figs 4D, 5D). However, the ratios for GL1605-treated biofilms were significantly diminished, reflecting the extensive cellular mortality induced by the treatment.

#### **2.4. BIOFILM STRUCTURAL PARAMETERETERS**

The 3D reconstruction images derived from CLSM demonstrated the effectiveness of the GL1605 in disrupting the biofilms' spatial structures and eliminating some dead cells, indicating its potential to kill and eliminate bacterial biofilms (Figs 6A, 7A, 8A). The GL1605 resulted in a high reduction in the biofilm volume (Figs 6B, 7B, 8B) and the overall biofilm thickness compared to the Mirragen (Figs 6C, 7C, 8C). Results were similar in the three bacterial species. *P. aeruginosa* biofilms exhibited a notable increased biovolume and overall thickness, which can be attributed to their prolific EPS production that leads to the formation of complex, multi-layered structures. However, upon treatment with compound GL1605 for 48 hours, a reduction in both biofilm thickness and biovolume was observed. This indicates that GL1605 possesses biofilm-disruptive

properties, potentially targeting and degrading the EPS matrix or impeding its production, thus compromising the structural integrity of the biofilm.

Three-dimensional reconstructions generated from the CLSM provided a visual and quantitative assessment of the impact of GL1605 on bacterial biofilms. The GL1605 effectively compromised the spatial organization of the biofilms and facilitated the removal of dead cells. Furthermore, a significant reduction in both the volume and the overall thickness of the biofilms was exhibited when treated with GL1605, as compared to those treated with Mirragen; effects were consistent across the biofilms of all three bacterial species studied.

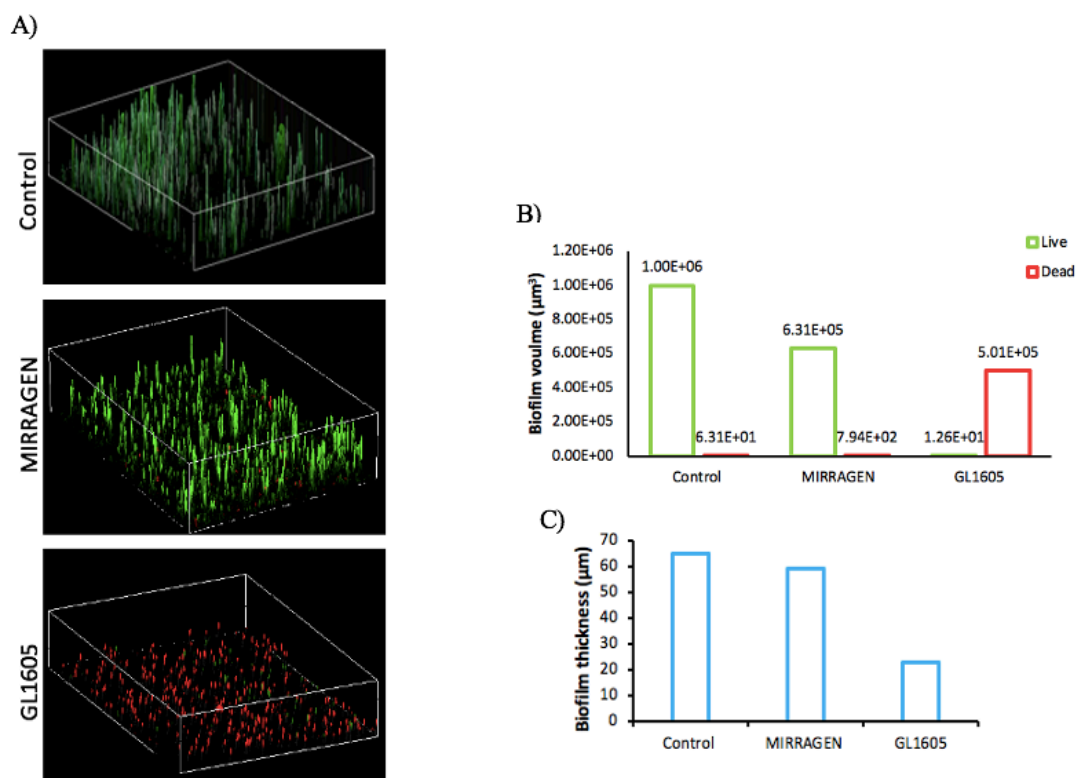


Figure 6. Biofilm structural parameters. (a) 3D biofilm architecture of *S. epidermidis* from CLSM images (b) biofilm's biovolume (c) Impact of bioactive glass treatment on the overall biofilm mean thickness.

For *E. coli*, Mirragen was more effective, with a 54% eradication rate, suggesting a slightly better but still incomplete ability to disrupt the biofilm structure. However, its efficacy against *P. aeruginosa* was markedly low, with only 11%. In contrast, GL1605 displayed a remarkably potent biofilm eradication capability, with a consistent 100% success rate across all tested biofilm species. This indicates that GL1605 is not only effective but also consistently so across a range of biofilm types, which is particularly significant given the varied physiologies and biofilm-forming mechanisms.

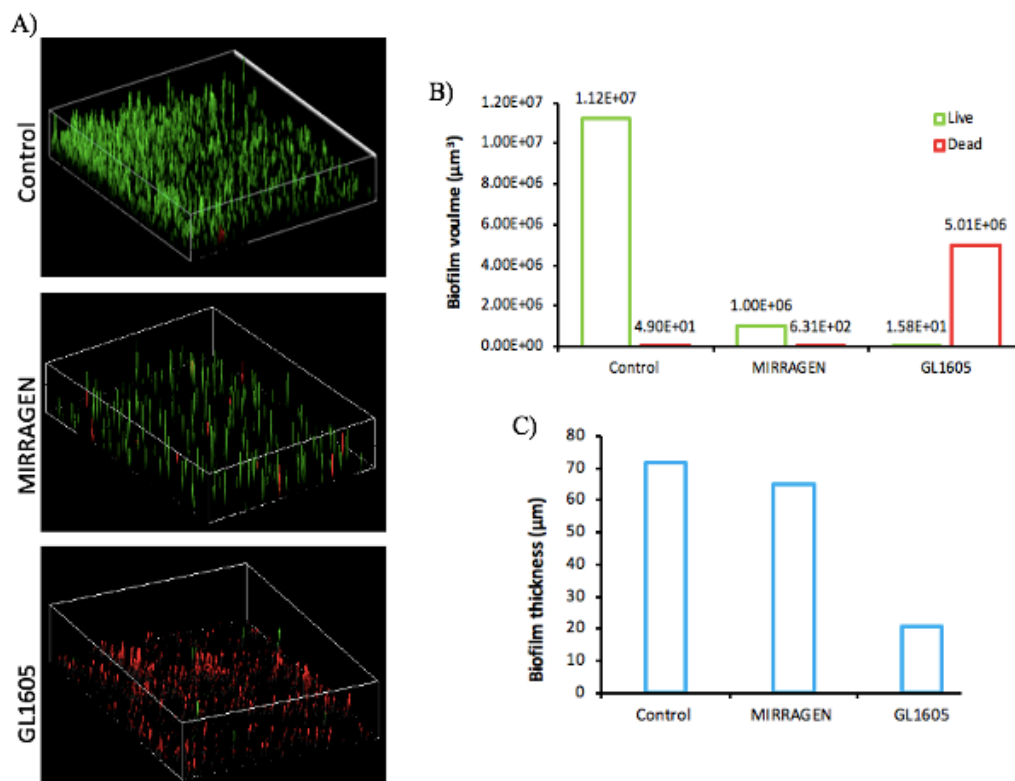


Figure 7. Biofilm structural parameters. (a) 3D biofilm architecture of *E. coli* from CLSM images (b) biofilm's biovolume (c) Impact of bioactive glass treatment on the overall biofilm mean thickness

The structural parameters of biofilm volume and thickness are critical indicators of biofilm robustness and resilience. Biofilm volume corresponds to the total biomass and is a measure of the three-dimensional space occupied by the bacterial community within the biofilm. Thickness, on the other hand, reflects the depth of the biofilm and is related to the diffusion gradients for nutrients and waste products, as well as the penetration of antimicrobial agents. A reduction in these parameters implies that GL1605 disrupts biofilm integrity, likely impairing the biofilm's defensive capabilities and reducing its potential to withstand antimicrobial penetration and immune clearance.

A mathematical formula was used to calculate the Antiseptic Biofilm Eradication (ABE%) to assess the impact level of Mirragen and GL1605 on the biofilms.

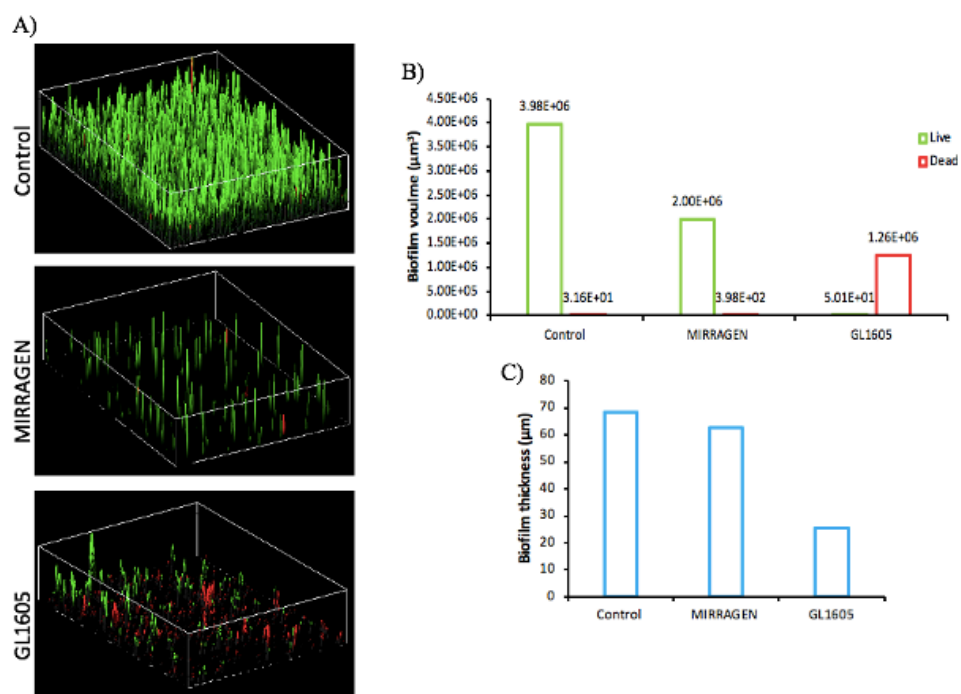


Figure 8. Biofilm structural parameters. (a) 3D biofilm architecture of *P. aeruginosa* from CLSM images (b) biofilm's biovolume (c) Impact of bioactive glass treatment on the overall biofilm mean thickness.

This formula consists of two components: the biofilm fluorescent intensity and the biofilm-covered area (calculated by Image j). Figure 9 shows a comparable biofilm eradication capacity for Mirragen and GL1605. Mirragen achieved a 41% reduction in biofilm mass for *S. epidermidis*, which, while notable, indicates a less than half reduction and suggests that a significant portion of the biofilm remains intact post-treatment.

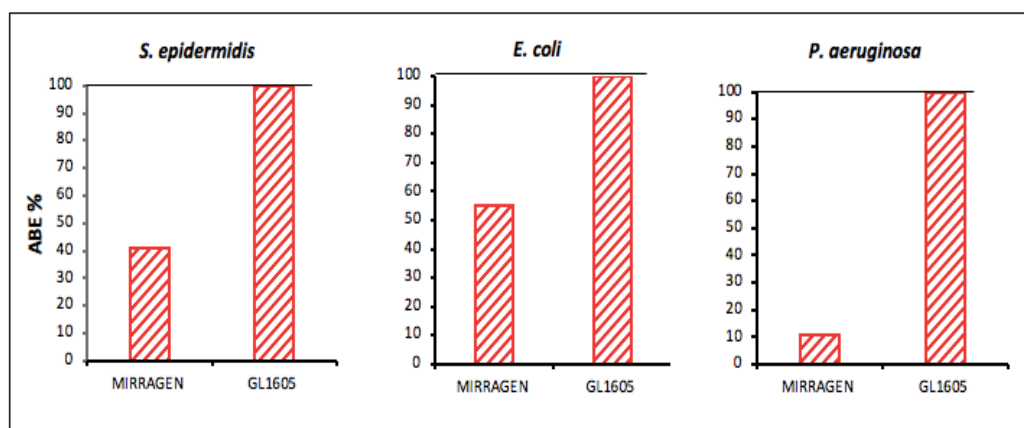


Figure 9. Antiseptic's Biofilm eradication% values of Mirragen and GL1605 on *S. epidermidis*, *E. coli*, and *P. aeruginosa* biofilms.

### 3. DISCUSSION

The strategic use of processed microscopic images to analyze biofilms represents the importance of integrating cutting-edge imaging technologies with novel antimicrobial materials to address the challenges posed by biofilm-associated nosocomial infections. This multidisciplinary approach not only enhances our understanding of biofilm dynamics but also opens new avenues for the development of effective strategies to combat HAIs, ultimately contributing to improved patient outcomes and reduced

healthcare costs. Through this research, the potential of Cu/Zn-BBGs as an innovative solution to a critical global health issue is vividly demonstrated, highlighting the significance of advancing biomaterials in the fight against infectious diseases.

The high-resolution images acquired from SEM provide a valuable qualitative assessment of the bioactive glasses' antibiofilm activity. When these images are considered alongside quantitative data such as CFU and CLSM a comprehensive picture of the Cu/Zn-BBGs' antibiofilm potential is highlighted. Moreover, the incorporation of manual machine learning algorithms in the assessment of biofilms treated with Cu/Zn-BBGs significantly enhances the quantitative analysis of SEM images. Machine learning and image processing techniques have the potential to significantly improve the accuracy and efficiency of biofilm analysis in SEM images. While traditional manual thresholding techniques have provided basic insights by allowing for the differentiation between biofilm and non-biofilm areas based on contrast, they lack precision and can be subject to user bias. In contrast, machine learning algorithms that involve segmentation techniques offer a more sophisticated and reproducible approach to image analysis. Through this segmentation, the algorithms can effectively quantify the area covered by biofilms, providing semiquantitative data that is less prone to subjective interpretation. This method was particularly useful when evaluating the efficacy of the Cu/Zn-BBGs, as it enabled the measurement of biofilm reduction in a more standardized manner.

The SEM analyses showed that Mirragen's impact on biofilms is relatively superficial, causing only minor disruptions to the biofilm structure. This observation aligned with the quantitative data which showed that Mirragen removed a minor portion of the biofilm. The slight damages observed in SEM images could correspond to the

localized disruptions rather than a complete breakdown of the biofilm matrix, accounting for the low percentage of biofilm removal. In stark contrast, GL1605 exhibited a robust antibiofilm activity, not only disrupting the biofilm structure, as evidenced by the homogenous damage seen in SEM images but also removing over 90% of the biofilm mass. This high level of efficacy suggests that GL1605 is not merely causing surface-level damage but is likely penetrating the biofilm matrix and dismantling the biofilm's architecture. The extensive biofilm reduction indicates that GL1605 is altering the biofilm's physical properties, such as its density, thickness, and adherence, which are crucial for its resilience and persistence. A previous study compared the sensitivity and specificity of manual and automatic SEM image segmentation and demonstrated the accuracy of automatic segmentation and its reproducibility. By generating a ROC curve, the study also displayed the effectiveness of automatic segmentation in analyzing biofilms on irregular surfaces (28).

Compared to traditional imaging techniques, CLSM offers several distinct advantages for biofilm research. Fluorescence-based staining methods used in conjunction with CLSM allow for the specific labeling of live and dead cells within the biofilm, enabling the dynamic assessment of biofilm viability in response to antimicrobial treatments. This contrasts with methods that provide only end-point or bulk measurements, lacking the resolution to discern the spatial distribution of viable and non-viable cells within biofilms. Additionally, CLSM's ability to perform longitudinal studies on the same biofilm sample over time without necessitating its destruction enables the real-time monitoring of biofilm development and the evaluation of antimicrobial interventions. This advantage is particularly valuable for assessing the kinetics of biofilm



formation and disassembly under various experimental conditions. Furthermore, CLSM's ability to visualize the three-dimensional structure of treated biofilms contributes to a deeper understanding of how copper and zinc ions influence biofilm integrity and viability. Changes in biofilm thickness, density, and the distribution of dead cells can be directly observed and quantified, offering insights into the mechanisms of action of the doped glasses.

By employing CLSM, this research seeks to provide a detailed analysis of the impact of Cu/Zn-BBGs on biofilm viability and structure, offering novel insights into the potential of these materials in preventing biofilm-associated HAIs. The novelty of this approach lies in the integration of advanced materials science with cutting-edge imaging techniques to address a critical issue in infection control, potentially paving the way for the development of more effective strategies to combat HAIs in healthcare settings.

The observed results across the *S. epidermidis*, *E. coli*, and *P. aeruginosa* biofilms provide significant insights into the antibiofilm properties of Mirragen and GL1605. The comparative analysis of these compounds reveals crucial differences in their mechanisms of action and efficacy, underpinning their potential applications in clinical microbiology and antibiofilm strategies.

In *S. epidermidis*, Mirragen did not significantly impact cell viability. This outcome suggests that Mirragen's mode of action may not be potent enough to disrupt the robust biofilm matrix. In contrast, GL1605 demonstrated a significant reduction in viable cells, indicative of a more potent antibiofilm activity that may involve disruption of biofilm integrity, inhibition of essential metabolic pathways, or direct damage to cellular structures.

For the gram-negative bacteria, *E. coli* and *P. aeruginosa*, which are characterized by their outer membrane barriers and diverse efflux mechanisms, similar trends were observed. Mirragen's slight reduction in viable cells could be attributed to its inability to effectively penetrate the cell envelope or its possible neutralization by the bacterial defense systems. On the other hand, the substantial decrease in cell viability caused by GL1605 suggests that the Cu/Zn-BBGs possess a broad-spectrum antibacterial activity capable of overcoming the protective barriers of gram-negative bacteria.

Moreover, the high efficiency of GL1605 in reducing viable cells suggests that it could be disrupting the outer membrane, thus facilitating the penetration of the PI stain and leading to increased fluorescence indicative of cell death. A high SYTO/PI ratio in Mirragen-treated and control biofilms suggests that most cells retain intact membranes and, hence are likely to be metabolically active. Conversely, the low SYTO/PI ratio in GL1605-treated biofilms indicates extensive cell membrane damage and cell death, which could be due to direct membrane disruption, interference with membrane synthesis, or induction of apoptotic-like pathways leading to cell lysis.

The observed decrease in biofilm volume and thickness suggests that GL1605 may interfere with biofilm formation at multiple levels. It may inhibit the initial adhesion of bacterial cells to surfaces, disrupt the production or structural integrity of the extracellular polymeric substance (EPS) matrix, or promote the detachment of cells from the biofilm. The removal of dead cells within the biofilms also implies that GL1605 has a post-formation disruptive effect, not only inhibiting growth but also actively disassembling the biofilm architecture.

The efficacy of GL1605 against both gram-positive and gram-negative organisms demonstrates its potential as a broad-spectrum antibiofilm agent. In clinical settings, the formation of biofilms on medical devices and tissues can lead to persistent infections that are resistant to conventional antibiotics. The ability of Cu/Zn-BBGs to penetrate and disrupt biofilms may offer a therapeutic advantage in treating these recalcitrant infections. Moreover, the application of such antibiofilm agents could be crucial in the development of coatings for medical devices to prevent biofilm formation and reduce the incidence of device-related infections. A study performed by Jung et al. (29) reported findings that aligned with previous observations, demonstrating the efficacy of Cu/Zn-BBGs in inhibiting *P. aeruginosa*, *S. aureus*, and *A. baumannii*. Compared to undoped BBG, the doped variants showed a significant antimicrobial effect. It was noted that the planktonic form of the bacteria was suppressed within 24 hours of exposure to the Cu/Zn-BBGs, and biofilms were effectively inhibited after 48 hours of treatment, using similar quantities of BBGs.

The difference in fluorescence intensity can be attributed to the distinct properties of the fluorescent stains used. The fluorescence intensity of SYTO and PI serves as a proxy for cellular viability within biofilms. SYTO dyes generally exhibit strong fluorescence upon binding to the nucleic acids within live cells, which possess intact cell membranes that prevent the entry of PI. PI, conversely, only penetrates cells with damaged membranes, which are typically nonviable, and upon binding to nucleic acids, emits fluorescence. Therefore, a high SYTO to PI fluorescence ratio is indicative of a larger population of live cells, whereas a low ratio suggests elevated cell mortality. The dramatic reduction in SYTO fluorescence in the presence of GL1605 implies that this

compound significantly disrupts cell membrane integrity, leading to cell death and subsequent PI staining.

Mirrugen, while showing some capacity for biofilm reduction, did not demonstrate high levels of eradication across the tested species. GL1605 achieved a remarkable 100% eradication rate across all species, highlighting its potential as a highly effective biofilm-eradicating agent. This level of efficacy suggests that GL1605 may possess a multifaceted mechanism of action capable of targeting and dismantling the biofilm matrix, penetrating the EPS, and killing the cells within. Such a broad-spectrum activity could revolutionize the treatment of biofilm-related infections, particularly in medical device-related infections where biofilms are a frequent cause of chronic infections and treatment failures.

The assessment of biofilm structural parameters is essential for evaluating the effectiveness of the materials. The structural complexity and physical parameters of biofilms are key factors in their mechanical stability and resistance to treatment. An antibiofilm agents that can reduce these parameters are likely to compromise the structural integrity of the biofilm, making it more amenable to physical removal or clearance by physiological processes. Moreover, assessing the viability of bacteria within the biofilm is equally important. Viable bacteria are the drivers of biofilm persistence and the spread of infection. They are responsible for the production of EPS, which fortifies the biofilm and facilitates the attachment and accumulation of more bacterial cells. Therefore, an antibiofilm agent that effectively reduces the viability of these cells will not only inhibit biofilm growth but may also facilitate the disruption of established biofilms. Assessing the structural parameters of biofilm volume and thickness alongside the

proportions of viable and dead bacteria within the biofilm offers a holistic view of an antibiofilm agent's efficacy. This comprehensive analysis is crucial for the development of more effective treatments against biofilm-associated infections, which are among the most challenging to treat due to their inherent resistance and resilience.

The significant antibiofilm effects observed with the GL1605 treatment across various bacterial species can be ascribed to its copper and zinc dopants. Copper and zinc are transition metals known for their antimicrobial properties, and their inclusion in BGG offers a multifaceted approach to combating biofilm formation and persistence. Copper ions possess potent biocidal properties and have been shown to induce oxidative stress in bacterial cells, leading to the generation of reactive oxygen species (ROS) which can cause widespread damage to nucleic acids, proteins, and lipids (30). The high affinity of copper for thiol groups in proteins can disrupt enzyme function and impair cellular metabolism. This oxidative damage to essential biomolecules can culminate in cell death, thus explaining the substantial reduction in viable cells within biofilms treated with GL1605 (31). One study indicated that mesoporous bioactive glass (MBG) with a 2 mol % copper composition was successful in curbing the proliferation of bacteria. Additionally, this copper-enhanced MBG hindered the establishment of biofilms by *S. epidermidis* and promoted their disintegration (32). These observations align with similar research, which corroborates the antimicrobial effectiveness of copper in preventing both bacterial propagation and biofilm formation, making it a viable substitute for traditional antibiotic-based systemic treatments (33, 34).

Zinc also exhibits antimicrobial activity, potentially through a variety of mechanisms. One such mechanism is the ability of zinc ions to disrupt bacterial

membrane integrity, leading to increased permeability and eventual cell lysis. Zinc may also bind to and interfere with the function of vital bacterial proteins, including enzymes involved in DNA replication and repair (35). Furthermore, zinc has been implicated in the inhibition of quorum sensing, the communication system that bacteria use to coordinate gene expression, including genes responsible for biofilm formation and maintenance (36). A recent study noted that zinc-enhanced BBGs compositions demonstrated a consistent ability to inhibit both gram-positive and gram-negative bacterial strains. The initial hours of testing exhibited significant inhibition for both types of bacteria, with the effect intensifying over time. Specifically, within the first 4 hours, the BBG with 1 mol % zinc doping exhibited a more potent inhibitory effect (37).

Moreover, the copper and zinc dopants could be altering the local pH or metal ion concentrations within the biofilm environment, further stressing the bacterial cells and impairing their ability to adapt or survive. The transition metals might also compete with essential metal ions like magnesium and calcium that are critical for biofilm structure, thereby destabilizing the biofilm architecture. The synergy between copper and zinc dopants in GL1605 could be crucial for its enhanced antibiofilm activity. This combination may lead to a dual mode of action where copper induces oxidative stress and zinc disrupts membrane and protein function. Additionally, both metals could be interfering with biofilm matrix components, such as extracellular polymeric substances (EPS), which provide structural integrity and protection to the biofilm. Disruption of the EPS matrix would expose bacterial cells to antimicrobial agents and the host immune system.

It is also important to consider the potential for resistance development against metal-based antimicrobials. While bacteria can evolve resistance to organic antibiotics through relatively simple genetic mutations, developing resistance to metal ions is often more complex and energetically costly, as it may require multiple genetic and metabolic changes. This complexity can render the development of resistance to metal-based antimicrobials like GL1605 more challenging for bacteria, potentially leading to a longer-lasting efficacy of such treatments. Exploring the potential resistance development against GL1605 will be essential for its sustainable use as an anti-biofilm agent in clinical settings

Given these observations, a detailed molecular analysis is also needed to further elucidate the mechanisms by which these materials exert their antibiofilm effects. Such an analysis could involve examining the interaction between the metal ions and bacterial cells, characterizing the ion release profiles, and understanding how these ions affect bacterial viability and biofilm architecture at the molecular level. Additionally, it would be beneficial to investigate the potential synergistic effects of the material matrix with the metal ions, which could provide insights into how to enhance the antibacterial properties of enhanced BBGs. This knowledge could drive the development of more effective treatments for wound infections, particularly those complicated by the presence of resilient biofilms.

#### 4. MATERIALS AND METHODS

**Bacterial strains:** Bacterial strains were obtained from the American Type Culture Collection (ATCC) and included *Staphylococcus epidermidis* ATCC 6538, *Pseudomonas aeruginosa* ATCC 27853, *Escherichia coli* ATCC 9637. Bacteria were grown on TSA plates for 24 h at 37 C under agitation in a 120 rpm orbital shaker. Each bacterial strain was grown in TSB at 37 C for 24 h. Overnight cultures were in TSB to maintain approximately  $10^8$  cells/mL.

**Biofilm formation:** Polycarbonate coupons with a 6mm diameter were used as substrates for biofilm formation. Overnight bacterial cultures were suspended in TSB to obtain a final density of  $10^8$  CFU/mL. Each bacterial suspension was added to a 24-well polystyrene plate containing the polycarbonate coupons which were then rinsed three times with PBS to remove planktonic bacteria. Prior to testing, all bacterial strains were assessed for their biofilm formation ability with the crystal violet assay using a GENESYS 103 UV-Vis spectrophotometer.

**Bioactive glass treatment:** Polycarbonate coupons with pre-formed biofilms were placed in a new, sterile well plate containing stimulated body fluid (SBF). Bioactive glass -3 punches of 6mm diameter- was added to the plates, and glass wool was added for the negative controls. The biofilm amount was evaluated after 48 h and 72 h of incubation for BBG direct and indirect treatment respectively.

**Scanning electron microscopy (SEM):** A Helios 4 Hydra CX DualBeam SEM was used to visualize biofilm morphological changes after treatment. Polycarbonate coupons were fixed, dehydrated, and gold sputter coated. The coupons were mounted on pin stubs



and placed on the SEM sample holder, and the same orientation was used for all samples. Images were taken at x2500 magnification for analysis. Fiji (distribution of the ImageJ software, US National Institutes of Health, Bethesda, Maryland, USA) was used to the images rendered into 250 nm pixel size. Biofilm surfaces were segmented using a collection of machine-learning algorithms for segmentation. For post-processing, noisy objects were removed from the segmented images, and the remaining percentage of the surface was calculated using the following formula (28):

$$\text{Biofilm remaining} = \frac{\text{area of biofilm after removal}}{\text{area of biofilm before removal}} \times 100$$

Confocal laser scanning microscopy (CLSM): Biofilms were stained with a fluorescent stain (L13152 LIVE/DEAD *BacLight*<sup>TM</sup> Bacterial Viability Kit; Invitrogen) according to the instructions of the manufacturer. This kit contains a mixture of two dyes: SYTO9 (green stain) for staining live bacteria and propidium iodide (red stain) for staining dead bacteria. Stained discs were incubated for 15 min at room temperature in the dark, and coverslips were placed on the specimens to minimize air contact. Biofilms were gently washed to remove dyes. Stained biofilms were examined using a confocal microscope. Confocal imaging was performed using 20X long working distance objective magnification on a Nikon A1R-HD Confocal Microscope (Eclipse Ti2). Images from 9 random fields were acquired from a sequential optical section of 2µm along the z-axis over the entire biofilm thickness. The resulting image stacks were rendered into 3D modes using image analysis software (Imaris 7.2.3, Bitplane, Zurich, Switzerland) as well as Image J. The Biofilm-covered Area % (BCA%) was calculated by differentiating areas

that are covered and uncovered by biofilms. Then, the antiseptic biofilm eradication percentage (ABE%) was calculated using the following formula (38):

$$\text{ABE \%} = \text{BCA}_{\text{non-treated biofilm}} - \frac{\text{FI of treated biofilm}}{\text{FI of non-treated biofilm}} \times \text{BCA}_{\text{treated biofilm}}$$

Statistical analysis: Experiments were performed in three replicates, and all results are expressed as the mean $\pm$ SD. A standard two-way ANOVA with post-hoc testing was used to examine the differences in pairwise comparisons for biofilm inhibition. FDR-adjusted alpha levels were used to assess significant p-values.

## REFERENCES

1. Stewart S, Robertson C, Pan J, Kennedy S, Haahr L, Manoukian S, Mason H, Kavanagh K, Graves N, Dancer SJ, Cook B, Reilly J. 2021. Impact of healthcare-associated infection on length of stay. *Journal of Hospital Infection* 114:23–31.
2. Al-Tawfiq JA, Tambyah PA. 2014. Healthcare associated infections (HAI) perspectives. *Journal of Infection and Public Health* 7:339–344.
3. HAI and Antibiotic Use Prevalence Survey | HAIC Activities | HAI | CDC. <https://www.cdc.gov/hai/eip/antibiotic-use.html>.
4. World Health Organization: WHO. 2022. WHO launches first ever global report on infection prevention and control. World Health Organization [Accessed: 24 Feb-2024].
5. Sharma SJ, Mohler JL, Mahajan SD, Schwartz SA, Bruggemann L, Aalinkeel R. 2023. Microbial Biofilm: a review on formation, infection, antibiotic resistance, control measures, and innovative treatment. *Microorganisms* 11:1614.
6. Watters C, Fleming D, Bishop DK, Rumbaugh KP. 2016. Host responses to biofilm, p. 193–239. *In* Progress in Molecular Biology and Translational Science.

7. Sun F, Qu F, Yan L, Mao P, Xia P, Chen H, Zhou D. 2013. Biofilm-associated infections: antibiotic resistance and novel therapeutic strategies. *Future Microbiology* 8:877–886.
8. Gritsch L, Conoscenti G, La Carrubba V, Nooeaid P, Boccaccini AR. 2019. Polylactide-based materials science strategies to improve tissue-material interface without the use of growth factors or other biological molecules. *Materials Science and Engineering: C* 94:1083–1101.
9. Rahmati M, Mozafari M. 2019. Selective contribution of bioactive glasses to molecular and cellular pathways. *ACS Biomaterials Science & Engineering* 6:4–20.
10. Ege D, Zheng K, Boccaccini AR. 2022. Borate Bioactive Glasses (BBG): bone regeneration, wound healing applications, and future directions. *ACS Applied Bio Materials* 5:3608–3622.
11. Westenberg DJ, Viswanathan R, Kadyk DL, Hibbs S, Kopel J, Day DE. 2021. Evaluation of three Borate-Bioactive Glass compositions for antibacterial applications. *Advances in Microbiology* 11:646–656.
12. Schuhladen K, Stich L, Schmidt J, Steinkasserer A, Boccaccini AR, Zinser E. 2020. Cu, Zn doped borate bioactive glasses: antibacterial efficacy and dose-dependent in vitro modulation of murine dendritic cells. *Biomaterials Science* 8:2143–2155.
13. Santos VRD, Campos TMB, Anselmi C, Thim GP, Bottino MC, Borges ALS, De Sousa Trichês E. 2023. Effect of Co, Cu, and Zn ions on the bioactivity and antibacterial properties of a borate bioactive glass. *Journal of Non-Crystalline Solids* 622:122643.
14. Arendsen L, Thakar R, Sultan AH. 2019. The use of copper as an antimicrobial agent in health care, including obstetrics and gynecology. *Clinical Microbiology Reviews* 32.
15. Mahamuni-Badiger P, Patil P, Badiger MV, Patel PR, Thorat-Gadgil BS, Pandit A, Bohara RA. 2020. Biofilm formation to inhibition: Role of zinc oxide-based nanoparticles. *Materials Science and Engineering: C* 108:110319.
16. McCann MT, Gilmore B, Gorman S. 2008. Staphylococcus epidermidis device-related infections: pathogenesis and clinical management. *Journal of Pharmacy and Pharmacology* 60:1551–1571.
17. Rohde H, Frankenberger S, Zähringer U, Mack D. 2010. Structure, function and contribution of polysaccharide intercellular adhesin (PIA) to Staphylococcus epidermidis biofilm formation and pathogenesis of biomaterial-associated infections. *European Journal of Cell Biology* 89:103–111.

18. Lebeaux D, Chauhan A, Rendueles O, Beloin C. 2013. From in vitro to in vivo Models of Bacterial Biofilm-Related Infections. *Pathogens* 2:288–356.
19. Wagner VE, Iglewski BH. 2008. *P. aeruginosa* Biofilms in CF Infection. *Clinical Reviews in Allergy & Immunology* 35:124–134.
20. Sen S, Johnston CG, Greenhalgh DG, Palmieri TL. 2016. Ventilator-Associated Pneumonia Prevention Bundle significantly reduces the risk of Ventilator-Associated Pneumonia in critically ill burn patients. *Journal of Burn Care & Research* 37:166–171.
21. Relucenti M, Familiari G, Donfrancesco O, Taurino M, Li X, Chen R, Artini M, Papa R, Selan L. 2021. Microscopy Methods for Biofilm Imaging: Focus on SEM and VP-SEM pros and cons. *Biology* 10:51.
22. Rao H, Choo S, Mahalingam SRR, Adisuri DS, Madhavan P, Akim AM, Chong PP. 2021. Approaches for Mitigating Microbial Biofilm-Related Drug Resistance: A focus on micro- and nanotechnologies. *Molecules* 26:1870.
23. Chan TF, Esedoğlu S, Nikolova M. 2006. Algorithms for finding global minimizers of image segmentation and denoising models. *Siam Journal on Applied Mathematics* 66:1632–1648.
24. Franklin MJ, Chang CJ, Akiyama T, Bothner B. 2015. New technologies for studying biofilms. *Microbiology Spectrum* 3.
25. Azeredo J, Azevedo NF, Briandet R, Cerca N, Coenye T, Costa AR, Desvaux M, Di Bonaventura G, Hébraud M, Jaglič Z, Kačániová M, Knöchel S, Lourenço A, Mergulhão F, Meyer RL, Nychas GE, Simões M, Tresse O, Sternberg C. 2016. Critical review on biofilm methods. *Critical Reviews in Microbiology* 43:313–351.
26. Van Hoogstraten SWG, Kuik C, Arts JJ, Cillero-Pastor B. 2023. Molecular imaging of bacterial biofilms—a systematic review. *Critical Reviews in Microbiology* 1–22.
27. Achinas S, Yska SK, Charalampogiannis N, Krooneman J, Euverink G-J. 2020. A Technological Understanding of Biofilm Detection Techniques: A review. *Materials* 13:3147.
28. Vyas N, Sammons R, Addison O, Dehghani H, Walmsley AD. 2016. A quantitative method to measure biofilm removal efficiency from complex biomaterial surfaces using SEM and image analysis. *Scientific Reports* 6.
29. Jung SB, Day T, Boone T, Buziak B, Omar A. 2019. Anti-biofilm activity of two novel, borate based, bioactive glass wound dressings. *Biomedical Glasses* 5:67–75.
30. Chaturvedi KS, Henderson JP. 2014. Pathogenic adaptations to host-derived antibacterial copper. *Frontiers in Cellular and Infection Microbiology* 4.

31. Saporito-Magriñá C, Musacco-Sebio R, Andrieux G, Kook L, Orrego MT, Tuttolomondo MV, Desimone MF, Boerries M, Borner C, Repetto MG. 2018. Copper-induced cell death and the protective role of glutathione: the implication of impaired protein folding rather than oxidative stress. *Metallomics* 10:1743–1754.
32. Bari A, Bloise N, Fiorilli S, Novajra G, Vallet-Regí M, Bruni G, Torres-Pardo A, González-Calbet JM, Visai L, Vitale-Brovarone C. 2017. Copper-containing mesoporous bioactive glass nanoparticles as multifunctional agent for bone regeneration. *Acta Biomaterialia* 55:493–504.
33. Sbarra MS, Arciola CR, Di Poto A, Saino E, Rohde H, Speziale P, Visai L. 2009. The Photodynamic Effect of Tetra-Substituted N-Methyl-Pyridyl-Porphine Combined with the Action of Vancomycin or Host Defense Mechanisms Disrupts *Staphylococcus Epidermidis* Biofilms. *The International Journal of Artificial Organs* 32:574–583.
34. Villanueva ME, Del Rosario Diez AM, González J, Pérez CJ, Orrego MT, Piehl LL, Teves S. 2016. Antimicrobial Activity of Starch Hydrogel Incorporated with Copper Nanoparticles. *ACS Applied Materials & Interfaces* 8:16280–16288.
35. Sirelkhatim A, Mahmud S, Seeni A, Kaus NHM, Ann LC, Bakhori SKM, Hasan H, Mohamad D. 2015. Review on Zinc oxide nanoparticles: antibacterial activity and toxicity Mechanism. *Nano-Micro Letters* 7:219–242.
36. Khan MohdF, Husain FM, Zia Q, Ahmad E, Jamal A, Alaidarous M, Banawas S, Alam MdM, Alshehri B, Jameel M, Alam P, Ahamed MI, Ansari AH, Ahmad I. 2020. Anti-quorum sensing and anti-biofilm activity of Zinc oxide nanopikes. *ACS Omega* 5:32203–32215.
37. Mutlu N, Kurtuldu F, Ünalán I, Neščáková Z, Kaňková H, Galusková D, Michálek M, Liverani L, Galusek D, Boccaccini AR. 2022. Effect of Zn and Ga doping on bioactivity, degradation, and antibacterial properties of borate 1393-B3 bioactive glass. *Ceramics International* 48:16404–16417.
38. Krasowski G, Migdał P, Woroszyło M, Fijałkowski K, Chodaczek G, Czajkowska J, Dudek B, Nowicka J, Oleksy-Wawrzyniak M, Kwiek B, Paleczny J, Brożyna M, Junka A. 2022. The Assessment of Activity of Antiseptic Agents against Biofilm of *Staphylococcus aureus* Measured with the Use of Processed Microscopic Images. *International Journal of Molecular Sciences* 23:13524.

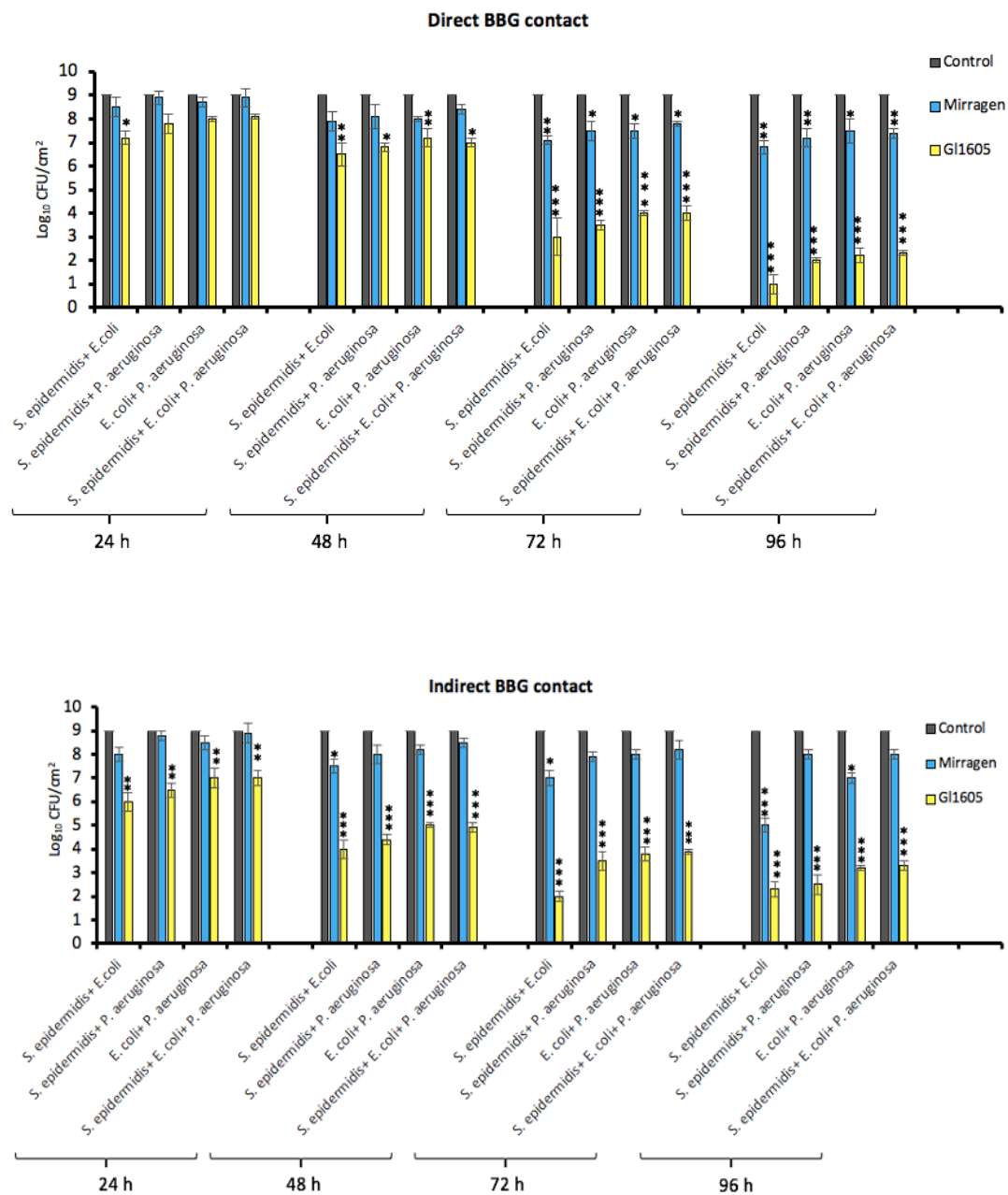
## SECTION

### 2. MULTI-SPECIES BIOFILMS

Bacteria within biofilms exhibit a high degree of genomic plasticity and diversity, often facilitated by horizontal gene transfer [21, 22]. This genetic exchange is optimized within biofilms due to their close spatial arrangement and sophisticated quorum sensing systems. The result is a rich gene pool from which bacteria can draw, allowing individual members to expend less energy maintaining their genomic repertoire while ensuring collective access to a comprehensive set of genetic tools for survival and virulence. Polymicrobial biofilms benefit from numerous synergistic interactions, such as passive resistance, where resistant strains can shield sensitive ones, and metabolic cooperation, where the waste products of one organism can serve as nutrients for another [23, 24]. These synergies not only enhance the survival of the biofilm but also contribute to its pathogenicity. Therefore, this study also displayed the effectiveness of direct and indirect application of copper and zinc-enhanced BBGs on polymicrobial biofilms grown statically and dynamically. Results demonstrated the effectiveness of the enhanced BBGs after 48 hours and 72 hours when applied directly and indirectly respectively. Dynamic biofilms were more persistent compared to static biofilms, requiring more time in contact with the enhanced BBG to achieve a bactericidal effect.

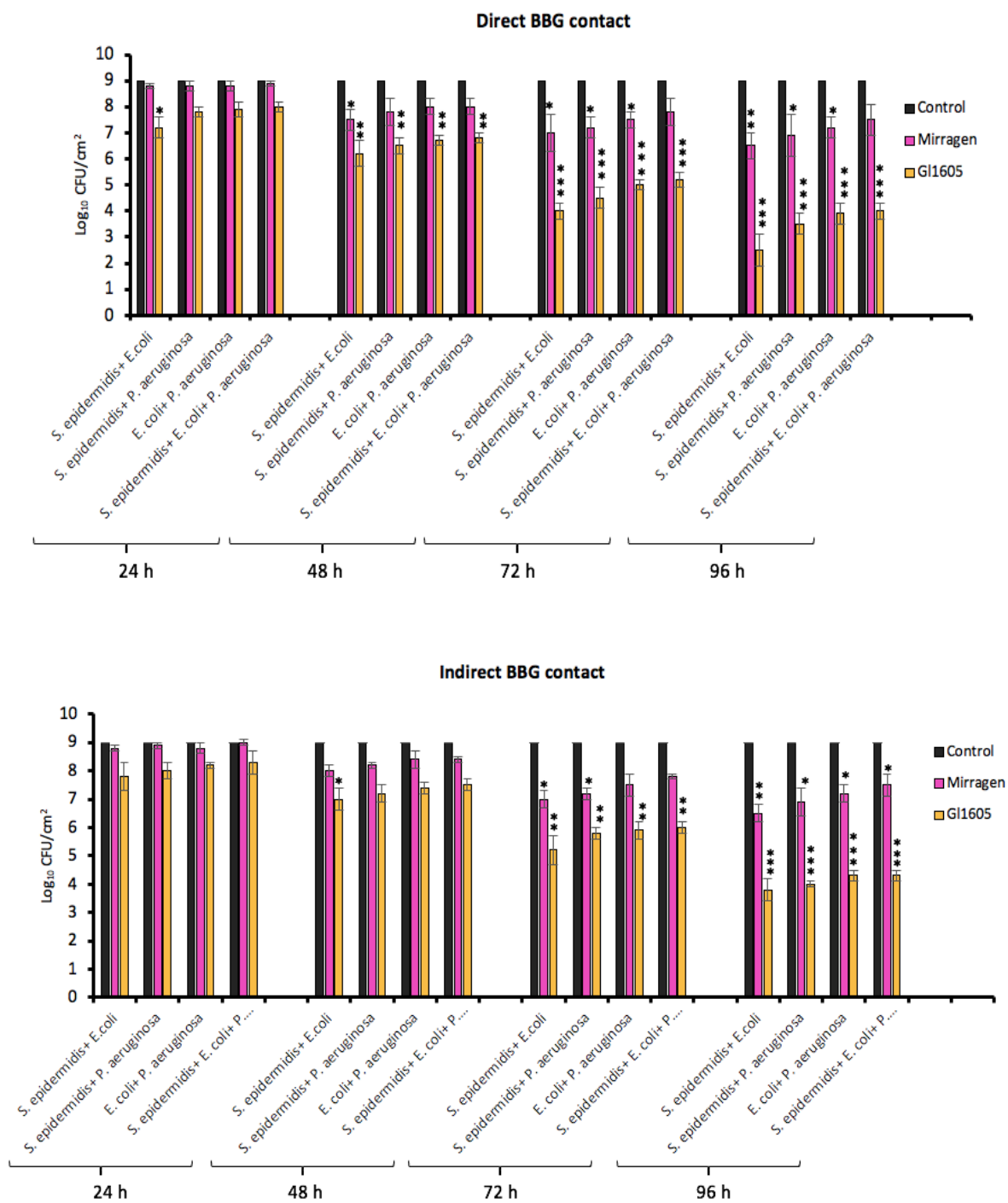
## 2.1. STATIC BIOFILMS

The anti-biofilm effectiveness of BBGs on polymicrobial biofilms.



## 2.2. DYNAMIC BIOFILMS

The anti-biofilm effectiveness of BBGs on polymicrobial biofilms.





### 3. CONCLUSIONS

The antibacterial/antibiofilm efficacy of the copper and zinc-doped BBG (GL1605) has provided substantial evidence of its potent activity against clinically relevant bacterial species: *S. epidermidis*, *E. coli*, and *P. aeruginosa*. The bactericidal properties of GL1605 were systematically evaluated against severe preformed static and dynamic. Direct application of the GL1605 on Static biofilms exhibited a bactericidal effect within 48 hours, while indirect application achieved a similar effect after 72 hours. In the dynamic preformed biofilms, the direct application resulted in a bactericidal effect at 72 hours, extending to 96 hours for indirect application. SEM and CLSM analyses were employed to corroborate these findings, indicating disrupted biofilm integrity and decreased bacterial density. The antibiofilm effectiveness of the GL1605 was further investigated against polymicrobial biofilms. Biofilms where *P. aeruginosa* was present, some persistence was observed. However, a bactericidal effect was achieved after 96 hours, suggesting a species-specific interaction that may affect the kinetics of biofilm eradication. In contrast, the undoped BBG variant (Mirragen) exhibited only limited bacteriostatic effects after an extended period, which suggests that the doped ions of copper and zinc are instrumental in mediating the observed antibiofilm action in GL1605. The pH modulation effects of the BBGs were also examined. Although shifts in pH were observed, they do not appear to be the principal mechanism behind the observed antibiofilm properties. However, it can possibly have some effects. A crucial finding of this study is the apparent linear relationship between the dissolution kinetics of the copper and zinc ions and the antibiofilm effectiveness of the GL1605. Future studies

should aim to delineate the genetic and molecular mechanisms through which copper and zinc ions exert their antibiofilm effects. A deeper understanding of these pathways will be pivotal in the optimization of BBG formulations and may reveal new strategies for managing nosocomial infections.

**BIBLIOGRAHY**

1. E. Caselli *et al.*, “An Innovative Strategy for the Effective Reduction of MDR Pathogens from the Nosocomial Environment,” in *Advances in Experimental Medicine and Biology*, 2019, pp. 79–91. doi: 10.1007/5584\_2019\_399.
2. E. Cerceo, S. Deitelzweig, B. M. Sherman, and A. Amin, “Multidrug-Resistant Gram-Negative Bacterial Infections in the hospital setting: overview, implications for clinical practice, and emerging treatment options,” *Microbial Drug Resistance*, vol. 22, no. 5, pp. 412–431, Jul. 2016, doi: 10.1089/mdr.2015.0220.
3. H. Khan, F. K. Baig, and R. Mehboob, “Nosocomial infections: Epidemiology, prevention, control and surveillance,” *Asian Pacific Journal of Tropical Biomedicine*, vol. 7, no. 5, pp. 478–482, May 2017, doi: 10.1016/j.apjtb.2017.01.019.
4. M. Haque, M. Sartelli, J. McKimm, and M. A. Bakar, “Health care-associated infections &ndash; an overview,” *Infection and Drug Resistance*, vol. Volume 11, pp. 2321–2333, Nov. 2018, doi: 10.2147/idr.s177247.
5. P. Gilbert, T. Maira-Litrán, A. J. McBain, A. H. Rickard, and F. W. Whyte, “The physiology and collective recalcitrance of microbial biofilm communities,” in *Advances in Microbial Physiology*, 2002, pp. 203–256. doi: 10.1016/s0065-2911(02)46005-5.
6. F. Baino, “Bioactive glasses – When glass science and technology meet regenerative medicine,” *Ceramics International*, vol. 44, no. 13, pp. 14953–14966, Sep. 2018, doi: 10.1016/j.ceramint.2018.05.180.
7. O. D. Abodunrin, K. E. Mabrouk, and M. Bricha, “A review on borate bioactive glasses (BBG): effect of doping elements, degradation, and applications,” *Journal of Materials Chemistry B*, vol. 11, no. 5, pp. 955–973, Jan. 2023, doi: 10.1039/d2tb02505a.
8. J. S. Fernandes, M. I. B. C. Martins, N. M. Neves, M. H. Fernandes, R. L. Reis, and R. A. Pires, “Intrinsic Antibacterial borosilicate glasses for bone tissue engineering applications,” *ACS Biomaterials Science & Engineering*, vol. 2, no. 7, pp. 1143–1150, Jun. 2016, doi: 10.1021/acsbiomaterials.6b00162.
9. D. Ege, K. Zheng, and A. R. Boccaccini, “Borate Bioactive Glasses (BBG): bone regeneration, wound healing applications, and future directions,” *ACS Applied Bio Materials*, vol. 5, no. 8, pp. 3608–3622, Jul. 2022, doi: 10.1021/acsabm.2c00384.

10. P. A. Dash, S. Mohanty, and S. K. Nayak, "A review on bioactive glass, its modifications and applications in healthcare sectors," *Journal of Non-Crystalline Solids*, vol. 614, p. 122404, Aug. 2023, doi: 10.1016/j.jnoncrysol.2023.122404.
11. M. B. Taye, H. S. Ningsih, and S. Shih, "Exploring the advancements in surface-modified bioactive glass: enhancing antibacterial activity, promoting angiogenesis, and modulating bioactivity," *Journal of Nanoparticle Research*, vol. 26, no. 2, Feb. 2024, doi: 10.1007/s11051-024-05935-2.
12. Z. Azari *et al.*, "Fabrication and characterization of cobalt- and copper-doped mesoporous borate bioactive glasses for potential applications in tissue engineering," *Ceramics International*, vol. 49, no. 23, pp. 38773–38788, Dec. 2023, doi: 10.1016/j.ceramint.2023.09.214.
13. N. Alasvand, A. Behnamghader, P. B. Milan, and M. Mozafari, "Synthesis and characterization of novel copper-doped modified bioactive glasses as advanced blood-contacting biomaterials," *Materials Today Chemistry*, vol. 29, p. 101465, Apr. 2023, doi: 10.1016/j.mtchem.2023.101465.
14. R. Hong, T. Kang, C. A. Michels, and N. Gadura, "Membrane Lipid Peroxidation in Copper Alloy-Mediated Contact Killing of *Escherichia coli*," *Applied and Environmental Microbiology*, vol. 78, no. 6, pp. 1776–1784, Mar. 2012, doi: 10.1128/aem.07068-11.
15. A. C. F. Harrop, K. R. Tupally, P. Pandey, and H. S. Parekh, "Opportunities for bioactive glass in Gastrointestinal Conditions: A review of production methodologies, morphology, composition, and performance," *Molecular Pharmaceutics*, vol. 20, no. 12, pp. 5954–5980, Nov. 2023, doi: 10.1021/acs.molpharmaceut.3c00188.
16. N. Alasvand, A. Behnamghader, P. B. Milan, S. Simorgh, A. Mobasheri, and M. Mozafari, "Tissue-engineered small-diameter vascular grafts containing novel copper-doped bioactive glass biomaterials to promote angiogenic activity and endothelial regeneration," *Materials Today Bio*, vol. 20, p. 100647, Jun. 2023, doi: 10.1016/j.mtbio.2023.100647.
17. H. Khan, A. Ahmad, and R. Mehboob, "Nosocomial infections and their control strategies," *Asian Pacific Journal of Tropical Biomedicine*, vol. 5, no. 7, pp. 509–514, Jul. 2015, doi: 10.1016/j.apjtb.2015.05.001.
18. I. Francolini, L. Hall-Stoodley, and P. Stoodley, "Biofilms, biomaterials, and Device-Related infections," in *Elsevier eBooks*, 2020, pp. 823–840. doi: 10.1016/b978-0-12-816137-1.00054-
19. Z. Peng, X. Wang, J. Huang, and B. Li, "Pathogenic *Escherichia coli*," in *Elsevier eBooks*, 2024, pp. 1065–1096. doi: 10.1016/b978-0-12-818619-0.00069-1.

20. P. Pachori, R. Gothalwal, and P. Gandhi, “Emergence of antibiotic resistance *Pseudomonas aeruginosa* in intensive care unit; a critical review,” *Genes and Diseases*, vol. 6, no. 2, pp. 109–119, Jun. 2019, doi: 10.1016/j.gendis.2019.04.001.
21. W. Song, B. Wemheuer, P. D. Steinberg, E. M. Marzinelli, and T. Thomas, “Contribution of horizontal gene transfer to the functionality of microbial biofilm on a macroalgae,” *The ISME Journal*, vol. 15, no. 3, pp. 807–817, Feb. 2021, doi: 10.1038/s41396-020-00815-8.
22. L. L. Nesse and R. Simm, “Biofilm: a hotspot for emerging bacterial genotypes,” in *Advances in Applied Microbiology*, 2018, pp. 223–246. doi: 10.1016/bs.aambs.2018.01.003.
23. G. Orazi and G. A. O’Toole, “‘It takes a Village’: Mechanisms underlying antimicrobial recalcitrance of polymicrobial biofilms,” *Journal of Bacteriology*, vol. 202, no. 1, Dec. 2019, doi: 10.1128/jb.00530-19.
24. A. Luo, F. Wang, S. DeGang, X. Liu, and B. Xin, “Formation, Development, and Cross-Species interactions in biofilms,” *Frontiers in Microbiology*, vol. 12, Jan. 2022, doi: 10.3389/fmicb.2021.757327.

## VITA

Sarah Fakher earned her Bachelor of Science Degree in 2020 and completed her Master of Science Degree in Applied and Environmental Biology in 2024 from Missouri University of Science and Technology. While pursuing her master's degrees, Sarah was the GTA for the Physiology, General Biology, and Microbiology Labs.

Sarah has been engaged in several leadership and representative roles. Sarah was the Biological Sciences Department representative in 2022-2023 on several of the university committees. In addition, she was the head of public relations and the vice president for the Graduate Women in Science in 2022-2024. Sarah was also the Director of Communication for the Council of Graduate Students in 2023-2024, where she was the conduit of graduate students matters with the S&T community and the Provosts.

Sarah is very passionate about Microbiology, Bioengineering, and Materials Science; she is placed on the Bio Sci Phi Sigma Honor Society for Academic Excellence, won the Claypool Award for Medical Research and Innovation in 2023, and earned Best Research First Place Winner in the Missouri S&T Graduate Research Showcase in 2024.